

MIRL REPORT NO. 86

CHEMICAL CHARACTERIZATION OF LIQUEFACTION  
PRODUCTS OF AN INERTINITE ENRICHED NORTHERN ALASKA  
COAL

A  
THESIS

Presented to the Faculty of the University of Alaska  
in Partial Fulfillment of the Requirements  
for the Degree of

Master of Science

By  
Venugopal Mayasandra, M.B.A., M.S.

Fairbanks, Alaska

December 1989

*Library of Congress Cataloging in Publication Data*

Library of Congress Catalog Card Number 90-61083  
ISBN 0-911043-10-1

December 1989

Published by

Mineral Industry Research Laboratory  
210 O'Neill Research Laboratory  
University of Alaska Fairbanks  
Fairbanks, Alaska 99775-1180

## ABSTRACT

A Northern Alaskan coal rich in inertinites was further enriched by density gradient separations. The degree of condensation of the enriched coal was estimated to be low, mainly 3 ring. The reactivity of the inertinite enriched coal was determined by comparing yields from direct liquefaction with H<sub>2</sub> at 0 and 30 minute residence times, 425°C, using an H-donor solvent in one case and moly-catalyst in the other with H<sub>2</sub> pressures of 500 and 1000 psig respectively. Solid products were analyzed by Fourier Transform Infrared Spectroscopy while the hexane solubles were separated into various chemical classes, viz. alkanes, neutral polycyclic aromatic compounds, hydroxy polycyclic aromatic oxygen heterocycles, and secondary, tertiary amino polycyclic aromatic compounds. The chemical compounds in these fractions were further analyzed by gas chromatography - mass spectrometry (GC-MS) and capillary gas chromatography. This work confirmed earlier data showing that inertinites are not as detrimental to liquefaction as previously thought.

## TABLE OF CONTENTS

Abstract .....	i
Table of Contents .....	ii
List of Appendices .....	iii
List of Figures .....	iv
List of Tables .....	vi
Acknowledgments .....	vii
Dedication .....	viii
<b>Chapter 1</b> .....	<b>1</b>
1. Introduction .....	1
2. Sample Selection .....	4
3. Sample Preparation .....	4
4. Specific Gravity Fractionation .....	4
5. Petrological Analysis .....	5
<b>Chapter 2</b> .....	<b>7</b>
1. Liquefaction - General Considerations .....	7
a. Indirect Liquefaction .....	7
b. Direct Liquefaction .....	7
2. Pyrolysis .....	7
3. Solvent Extraction .....	7
4. Solvent Extraction Procedure .....	10
5. Product Generation .....	10
6. Hydroliquefaction .....	10
7. Hydroliquefaction Product Recovery and Fractionation .....	10
8. Catalytic Liquefaction .....	13
9. Catalyst Impregnation of Coal .....	13
10. Determination of Liquefaction Products .....	13
a. Total Conversion .....	13
b. Gas Analysis .....	14
c. Asphaltenes and Preasphaltenes .....	14
11. H <sub>2</sub> O Production During Liquefaction .....	14
12. Method of H <sub>2</sub> O Estimation .....	15
<b>Chapter 3</b> .....	<b>16</b>
1. Infrared and X-ray Diffraction Studies of the Enriched Coal, Its Liquefaction Products and Low Temperature Ash .....	16
2. Low Temperature Ashing .....	18
3. Preparation of KBr Pellets for FTIR .....	18
4. Cronauer and Ruberto's Kinetic Model .....	23
<b>Chapter 4</b> .....	<b>28</b>
1. Chemical Class Separation and Characterization of Organic Compounds in Oil/Tar .....	28
2. Column Chromatography Procedure .....	28
3. Results and Discussion .....	30
4. Hexane Eluate (A-1), Aliphatic Hydrocarbons .....	30
5. Benzene Eluate (A-2), Neutral PAC .....	33

## TABLE OF CONTENTS (Continued)

6. Chloroform Ethanol-Eluate (A-3), N-PAC .....	33
7. Ethanol-THF Eluate (A-4), HPAH .....	33
8. Nitric Acid Oxidation .....	39
9. HNO <sub>3</sub> Oxidation Procedure .....	39
<b>Chapter 5</b> .....	<b>43</b>
1. Summary and Conclusion .....	43
2. Recommendations for Additional Work .....	44
<b>Bibliography</b> .....	<b>45</b>

## LIST OF APPENDICES

<b>Appendix A: Tables</b> .....	<b>51</b>
Table I Weight fractions obtained at different specific gravities .....	51
Table II Petrographic Analysis of Original Coal and Enriched Fractions .....	51
Table III A Summary of the Major Characteristics of the Three Maceral Groups in Hard Coal .....	52
Table IV Parametric conditions of the Gas Chromatograph during gas analysis .....	53
Table V Concentration of cations in the combined washings of ammonium acetate and HCl (% wt in enriched DAF coal) .....	53
Table VI % wt concentration of major elements in the ash of enriched coal .....	54
Table VII Concentration of trace elements, ppm in the ash of enriched coal .....	54
Table VIII Analysis of residues .....	54
<b>Appendix B: Calculation involving the impregnation of coal with the catalyst</b> .....	<b>55</b>
<b>Appendix C: A. Calculation of carbon preference index (CPI)</b> B. Calculation of pristane/phytane ratio (r) .....	<b>56</b>

## LIST OF FIGURES

Figure 1a.	Alaska's coal resources in terms of world resources.....	1
Figure 1b.	Percentages of Alaska's coal resources by rank .....	1
Figure 2.	Alaska's coal basins, fields, and isolated occurrences .....	3
Figure 3.	Flow diagram for wet sieving .....	4
Figure 4.	Flow diagram for feed coal preparation .....	5
Figure 5.	Flow diagram for specific gravity separation to enrich inertinite macerals .....	5
Figure 6.	MIRL design of round bottom centrifuge bottle .....	6
Figure 7a.	Simplified flow diagram for SRC-I process .....	8
Figure 7b.	Simplified flow diagram for SRC-II process .....	8
Figure 8a.	Simplified flow diagram of H-Coal process .....	9
Figure 8b.	Simplified flow diagram of Exxon Donor Solvent process.....	9
Figure 9a.	Flow diagram of product work up after hydroliquefaction .....	11
Figure 9b.	Flow diagram of product work up after catalytic liquefaction .....	12
Figure 10.	Catalyst preparation .....	13
Figure 11.	FTIR Spectrograms: a) inertinite enriched coal, b) residue after solvent extraction .....	19
Figure 12.	FTIR Spectrograms: a) inertinite enriched coal, b) 0 minute residue, c) 30 minute residue .....	21
Figure 13.	FTIR Spectrograms: a) inertinite enriched coal, b) 0 min. asphaltene, c) 30 min. asphaltene .....	22
Figure 14.	FTIR Spectrograms: a) inertinite enriched coal, b) 0 min. preasphaltene, c) 30 min. preasphaltene .....	24
Figure 15.	FTIR Spectrograms: a) inertinite enriched coal, b) 30 minute residue, c) 30 minute preasphaltene, d) 30 minute asphaltene .....	25
Figure 16.	FTIR Spectrograms: a) inertinite enriched coal, b) Low temperature ash (LTA) .....	26

## LIST OF FIGURES (Continued).

Figure 17.	X-ray diffraction spectrum of Low temperature ash .....	27
Figure 18.	Flow diagram for chemical class separation .....	29
Figure 19a.	Capillary GC profile of aliphatic hydrocarbons of fraction A-1 .....	31
Figure 19b.	Capillary GC profile of aliphatic hydrocarbons of fraction A-1 at higher attenuation .....	32
Figure 20.	Capillary GC profile of neutral polycyclic aromatic compounds of fraction A-2 .....	34
Figure 21.	Capillary GC profile of secondary nitrogen polycyclic aromatic heterocycles of fraction S-1 .....	36
Figure 22.	Capillary GC profile of amino polycyclic aromatic hydrocarbons of fraction S-2 .....	37
Figure 23.	Capillary GC profile of tertiary nitrogen polycyclic aromatic heterocycles of fraction S-3 .....	38
Figure 24.	Capillary GC profile of hydroxypolycyclic aromatic hydrocarbons of fraction A-4 .....	40
Figure 25.	GC-MS total ion profile of esterified HNO <sub>3</sub> oxidation product .....	42

## LIST OF TABLES

Table 1	Identified coal resources of Alaska by province . . . . .	2
Table 2	Maceral Composition . . . . .	2
Table 3	Proximate and Ultimate Analyses . . . . .	2
Table 4	Solvent Extraction: yield of products from enriched coal . . . . .	10
Table 5	Gas Analyses . . . . .	14
Table 6	Hydroliquefaction (product yields) . . . . .	15
Table 7	Catalytic liquefaction (product yields) . . . . .	15
Table 8	Water Produced During Liquefaction (% Wt) . . . . .	16
Table 9	Corrected % Wt Total Conversion of Coal . . . . .	16
Table 10a	Band Assignments for FTIR Spectra of Coals and Coal Products . . . . .	17
Table 10b	Infrared Absorption Bands for Kaolinite and Quartz. . . . .	18
Table 10c	Principal x-Ray Diffraction Spacings of Kaolinite and Quartz . . . . .	18
Table 11	Percent wt of neutral alumina fractions of hexane solubles (oils/tar) . . . . .	30
Table 12	Fractions from silicic acid (% wt) . . . . .	30
Table 13	n-Aliphatic hydrocarbons in fraction A-1 . . . . .	33
Table 14	Polycyclic aromatic compounds in fraction A-2 . . . . .	35
Table 15	Secondary nitrogen polycyclic aromatic heterocycles (2 <sup>0</sup> PANH) in fraction S-1 . . . . .	35
Table 16	Amino polycyclic aromatic hydrocarbons (APAH) in fraction S-2 . . . . .	35
Table 17	Tertiary nitrogen polycyclic aromatic heterocycles (3 <sup>0</sup> PANH) in fraction S-3 . . . . .	35
Table 18	Hydroxyl polycyclic aromatic hydrocarbons in fraction A-4 . . . . .	41



## ACKNOWLEDGMENTS

It is my great pleasure to present the people who made this work possible. I sincerely thank my advisor and thesis committee chairman, Dr. Warrack G. Willson, for his help and direction. My appreciation and thanks to the members of my thesis committee, Dr. David R. Maneval and Dr. John W. Keller, for their encouragement and suggestions. I am indebted to Dr. P.D. Rao who lent me his strong support as my advisor. Also a million thanks to Ms. Jane E. Smith for her technical assistance.

During my tenure of Assistantship/Fellowship at MIRL I had the good fortune to meet and work with some marvelous people. Mr. Daniel E. Walsh is one of those ever affable people; I thank him immensely.

If it was not for Dr. Milton L. Lee (Brigham Young University, Provo, Utah) this work would not have been completed and I thank him and members of his group, Dr. H-C. K. Chang and Dr. K.E. Markides. I also want to thank Ms. Annette Oyler and Ms. LaVoy C. Hill for their help while I was at BYU, and Dr. D.W. Later for referring me to Dr. Milton Lee.

I gratefully acknowledge the help of Mr. Dennis Finseth of Pittsburgh Energy Technology Center, Dr. C.L. Knudson of EMRC, North Dakota, Dr. Susan M. Henrichs and Mr. Doug McIntosh of the Marine Science Department, Dr. Thomas Clausen and Ms. Marlys Schneider of the Chemistry Department, and Dr. Frank Letowski and Dr. H. K. Lin of the Mineral Industry Research Laboratory, University of Alaska. I take this opportunity to thank my colleagues Mr. G.C. Rutt, Mr. M. Belowich, Mr. W.H. Yuen, Mr. Z.F. Wang, Mr. Fang Guor Cheng and Mr. Li Yufu, and especially my deep appreciation to Mr. Ye Kang Chuang for his help and friendship. Further, my thanks are due to the Farmer family, Cathy and Hugh, and the Gillis family, Jim and Karin, for their good friendship. Finally, I thank Cathy Farmer, Carol Leakey for typing this thesis and the United States Dept. of Interior, Bureau of Mines (Grant number G.1174102) and MIRL for the financial assistance.

*Dedicated  
To  
Dr. Milton L. Lee*

# CHAPTER 1

## 1. Introduction

The extensive coal reserves of Alaska have been estimated at 4 trillion tons<sup>(1)</sup> and about 1/6 of the total resource of this planet<sup>(2)</sup> (Figure 1-a). Because of the variation in environments and ages, different types of coal occur. The pie chart<sup>(3)</sup> (Figure 1-b) and Table 1<sup>(2)</sup> show the percent distribution of Alaska's coal, geographic regions (Figure 2) and its resources in 10<sup>6</sup> short tons by rank, respectively.

The conversion of Northern Alaska's vast deposits of coal into clean burning liquid fuels can be justified on several factors. The most important of these are: 1) Alaska is a nearly inexhaustible source of coal. 2) Alaska has great resources of natural gas (estimated at 34 trillion cubic feet) that could be steam reformed to produce hydrogen which is an essential ingredient in the liquefaction of coal. 3) Catalysts, like molybdenum and tin, occur in Alaska. These could be used as inexpensive disposable catalysts in the hydrogenation or liquefaction of coal. 4) There is the possibility of transporting the liquefied fuels through the trans-Alaska pipeline spanning a distance of 800 miles from Prudhoe Bay to Valdez, which is an ice free port. When Alaska's oil reserves become depleted, this pipeline, constructed at a cost of around 8 billion dollars, could be the ideal mode of transportation of liquefied coal from Northern Alaskan fields. Unfortunately, most Northern Alaskan coals are found to be rich in inertinite maceral group.

Of the three maceral groups (Table III, Appendix A) found in coal, viz. vitrinite, exinite and inertinite, the inertinite group is found to be least reactive in combustion reactions; i.e., ignition and combustion of inertinite is comparatively slower than vitrinite (the viscous coking and caking component) and exinite (the tar and hydrogen producer) groups. The macerals of the inertinite group are rich in carbon and poor in hydrogen. However, it has been shown that the semifusinite and macrinite of the inertinite group in Gondwana coals are quite reactive<sup>(4,5,6)</sup>. They constitute a major portion of the inertinite present in Gondwana coals (coals of the Southern hemisphere, viz. Australia, India and South Africa). The optical property (low reflectivity) of semifusinite and macrinite of the Gondwana coals are found to be similar to those found in Northern Alaskan coals<sup>(7)</sup>. Further, they both have high mineral matter (ash) content. Table 2 shows the maceral composition, R<sub>o</sub> max, and ASTM rank of the UA-139 coal and the inertinite enriched coal. The proximate and ultimate analyses of the coals are shown in Table 3.

The purpose of this work is not only to compare the direct liquefaction behavior of the inertinite enriched coal by hydrol liquefaction using tetralin and catalytic liquefaction with molybdenum as catalyst, but also to chemically characterize the products. Characterization of liquefaction products are desirable for the following reasons:

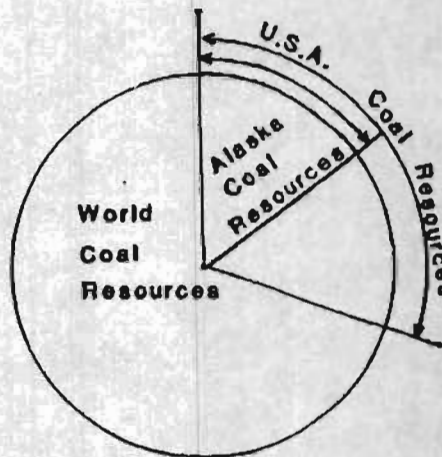


Figure 1a. Alaska's coal resources in terms of world resources.

Source: Public disclosure file 86-90

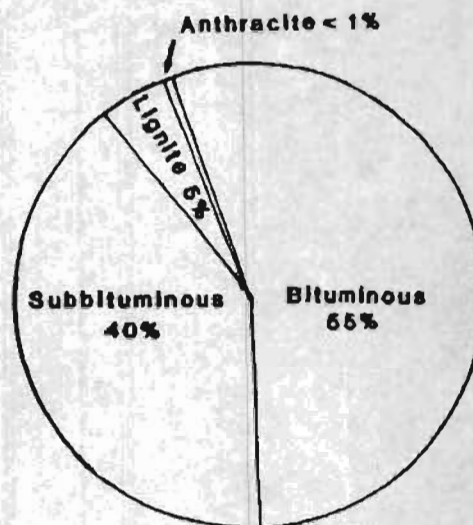


Figure 1b. Percentage of Alaska's coal resources by rank.

Source: Public disclosure file 88-15.

a) Identification and hence elimination of certain toxic and carcinogenic compounds would decrease the occupational and environmental health hazards involved with the production and combustion of synthetic fuels<sup>(8,9,10)</sup>.

**Table 1**  
**Identified coal resources of Alaska by province.**

	10 <sup>6</sup> Short tons	Rank
Northern Alaska province	150,000	High volatile bituminous and subbituminous; extensive lignite and minor anthracitic coals are not identified resources.
Cook Inlet-Susitna province		
Beluga and Yentna fields	10,000	Subbituminous
Kenai field (onshore only)	320	Subbituminous
Matanuska field	150	High volatile bituminous to anthracite
Broad Pass field	50	Lignite
Susitna field	100	Subbituminous
Nenana province		
Nenana basin proper	7,000	Subbituminous
Little Tonzona field	1,500	Subbituminous
Jarvis Creek field	75	Subbituminous
Alaska Peninsula province Chignik and Herendeen Bay fields, Unga I.	430	High volatile bituminous
Gulf of Alaska province Bering River field	160	Low volatile bituminous to anthracite
Yukon-Koyukuk province Tramway Bar field	15	High volatile bituminous
Upper Yukon province Eagle field	10	Subbituminous and lignite
Seward Peninsula province Chicago Creek field	4.7	Lignite

Source: PDF 86-90

**Table 3**  
**Proximate and Ultimate Analyses**

			Wt%	
			UA-139#	Enriched Coal
<b>Table 2</b>				
<b>Maceral Composition</b>				
	UA-139 <sup>a</sup>	Enriched Coal		
<b>Macerals</b>	<b>% Composition</b>			
Vitrinite	66.6	36.4	Moisture	11.25
Exinite	2.2	0.2	Ash (Moisture Free)	23.88
Inertinite	31.2	63.4	Volatile Matter <sup>*</sup>	36.62
R <sub>g</sub> max	0.55	0.56	Fixed Carbon <sup>*</sup>	63.38
ASTM Rank hvCb			BTU/lb (Heating Value <sup>†</sup> )	12,215
			% C <sup>*</sup> (Uncorrected for CO <sub>2</sub> )	74.92
			% H <sup>*</sup>	4.10
			% N <sup>*</sup>	1.22
			% S <sup>*</sup> (Total)	0.37
			% O (diff)	19.39
			# Adapted from Fossil Energy (USDOE) P.D. Rao & E.N. Wolff, Nov. 1982, Report No. 63.	
			Note: * Dry ash free (DAF) basis	

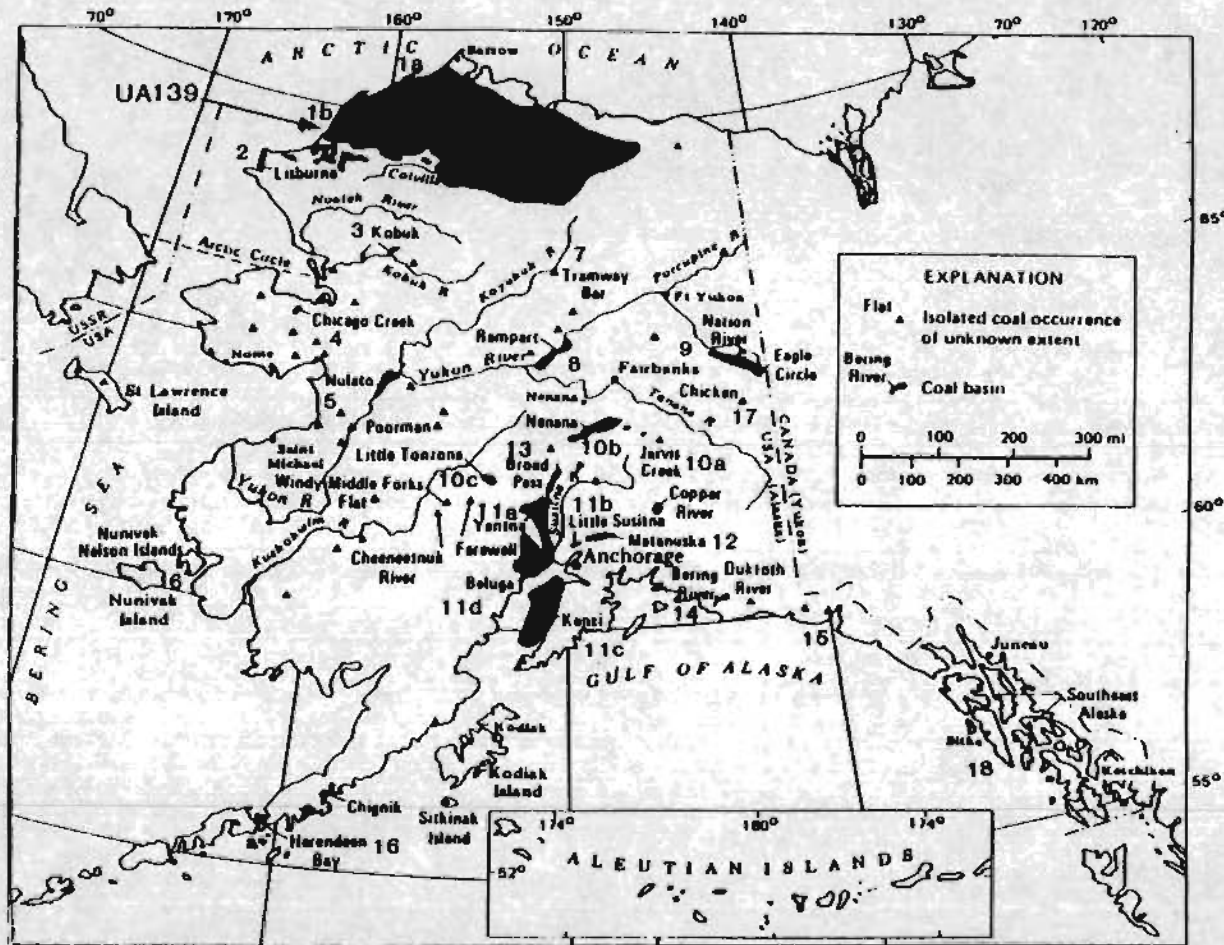


Figure 2. Alaska's coal basins, fields and isolated occurrences.

b) It has been shown that certain heterocyclic compounds like carbazoles, phenazines, pyrrole derivatives and dibenzofurans, reduce the stability of liquid fuels through gum formation, discoloration and odor<sup>(11)</sup> during storage<sup>(12,13,14,15,16)</sup>. They also hinder catalytic cracking<sup>(17)</sup>. Also, basic nitrogen compounds are known to poison catalysts and deactivate them by forming coke deposits<sup>(18)</sup>. Thus their removal is critical in producing a saleable product;

c) Many commercially important chemicals that are used in the manufacture of pharmaceuticals, pesticides, herbicides, fertilizer and dyes occur as components of synthetic fuel or by-products during its production<sup>(9,19)</sup>; and

d) Data obtained from this research work could be applied in the conversion of Alaskan inertinite rich coals into liquid fuel products.

## 2. Sample Selection

The sample selected for this study is an inertinite rich coal, UA-139, from number 7 coal bed from the Cape Beaufort mine, situated in the Northern Alaska coal field<sup>(20,21)</sup>. The location of the coal field is shown in Figure 2. The proximate and ultimate analyses of UA 139 and the enriched coal are listed in Table 3.

As an on-going project in this laboratory, the Mineral Industry Research Laboratory (MIRL), Rutt and Youtcheff<sup>(22)</sup> and Lee and Youtcheff<sup>(23)</sup> have studied catalytic liquefaction using Mo and hydroliquefaction with tetralin respectively. Although UA-139, the same coal that was employed in the above two studies, was used in this study, the inertinite content of the coal was increased to more than 100% of its original concentration by specific gravity fractionation. Before the coal was subjected to inertinite concentration, it was pulverized, riffled and wet sieved to obtain a mesh size of -65 X 400. Figure 3 shows the flow diagram of the wet sieving procedure.

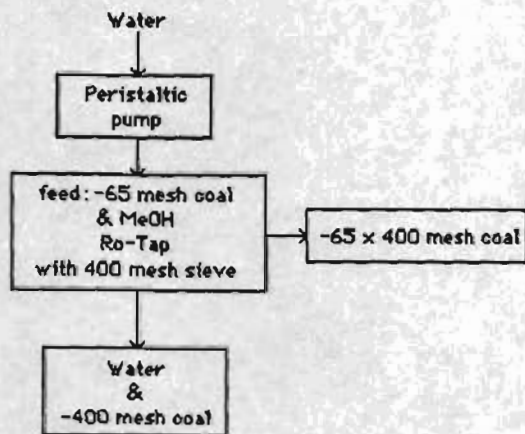


Figure 3. Flow diagram for wet sieving.

## 3. Sample Preparation

**Wet Sieving:** A 5 kg sample of UA-139 coal was dried at 38°C until a constant weight was obtained. The dried coal was pulverized to 65 mesh, riffled and dry sieved to obtain -65 mesh product which was wet sieved using a Ro-tap sieve shaker fitted with a 400 mesh sieve. During the wet sieving the coal (-65 mesh) was treated with a small quantity of methanol to wet the coal. The -65 x 400 mesh fraction remaining on the sieve was dried at 38°C overnight and 110°C until the weight was constant (Flow diagram, Figure 4).

## 4. Specific Gravity Fractionation (Float-Sink Analysis)

When pulverized coal is placed in a liquid that has a specific gravity which is in between the range of specific gravities of the different maceral rich particulate groups, a separation will occur. The particles with lower specific gravities with reference to the liquid will float while those with higher specific gravities will sink. This principle was applied to increase the inertinite concentration of UA-139 coal.

In this procedure an organic medium was prepared at different specific gravities varying from 1.4 to 1.6 using perchloroethylene and adding naphtha to control the variation in specific gravities. A few drops of non-ionic surfactant (Aerosol OT 75%, American Cyanamid Co.) was added to help in the dispersion of fine coal particles in the organic medium. A specific gravity meter was used in monitoring the specific gravities. Although aqueous salt solutions of zinc chloride, calcium chloride or cesium chloride are generally used as media in density gradient separations (specific gravity fractionation), chlorinated or brominated hydrocarbons are usually preferred since they offer a wider range of specific gravities (1.0 to 2.9 g/cm<sup>3</sup>). They are also preferred when fine coal (<75mm) is involved in the separation<sup>(24)</sup>. However, organic liquids are more expensive and proper precautions should be taken to avoid their toxicity. Recently a new method using density gradient centrifugation (DGC)<sup>(25,26)</sup> has been developed at Argonne National Laboratory. It is reported to be more efficient in producing maceral concentrates of high purity.

The flow chart (Figure 5) shows the sequence of the procedure used in the enrichment of inertinite of UA-139 coal. First, a 1.4 specific gravity medium was prepared. About 20g of the -65 x 400 mesh coal was taken in each of the four centrifuge bottles (Figure 6). They were filled with the 1.4 specific gravity medium up to 3/4 full, balanced and centrifuged for 15 minutes at about 1500 RPM. After allowing the particles to settle, the floats and sinks were separated by decantation using the decantation stopper (Figure 6). The floats were discarded and the sinks were separated by filtration. The filter paper containing the sinks was allowed to dry in the hood. The dried sinks thus obtained

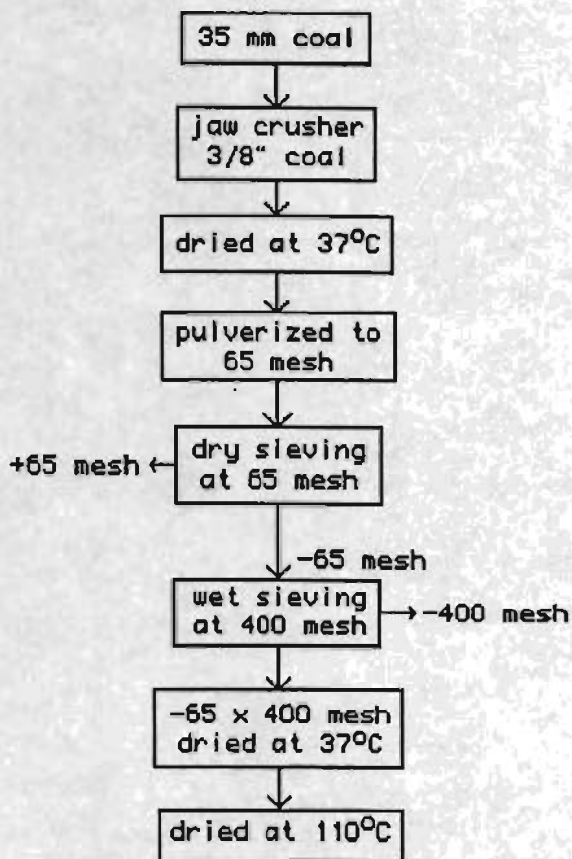


Figure 4. Flow diagram for feed coal preparation.

were used at 1.45 SPG and the sinks from 1.45 SPG were taken through 1.50. The above procedure was repeated with 1.55 and 1.60 SPG. The weight fractions obtained at different specific gravities are shown in Table I (Appendix A).

## 5. Petrological Analysis

The various specific gravity fractions were made into pellets and polished according to ASTM procedure D2797-85. The petrological analyses of these pellets showed that the inertinites were concentrated in the 1.50 to 1.55 and 1.55 to 1.60 specific gravity fractions. Table II (Appendix A) shows the percent composition of the different macerals in the raw coal (UA-139), 1.50 to 1.55 and 1.55 to 1.60 specific gravity fractions and their composite. Since the yields of these fractions were low, a decision was made to combine the two fractions. Thus, applying specific gravity fractionation, the inertinite concentration was increased from 31.2% in the raw coal to 63.4% in the composite 1.50 - 1.60 specific gravity fraction (Table 2).

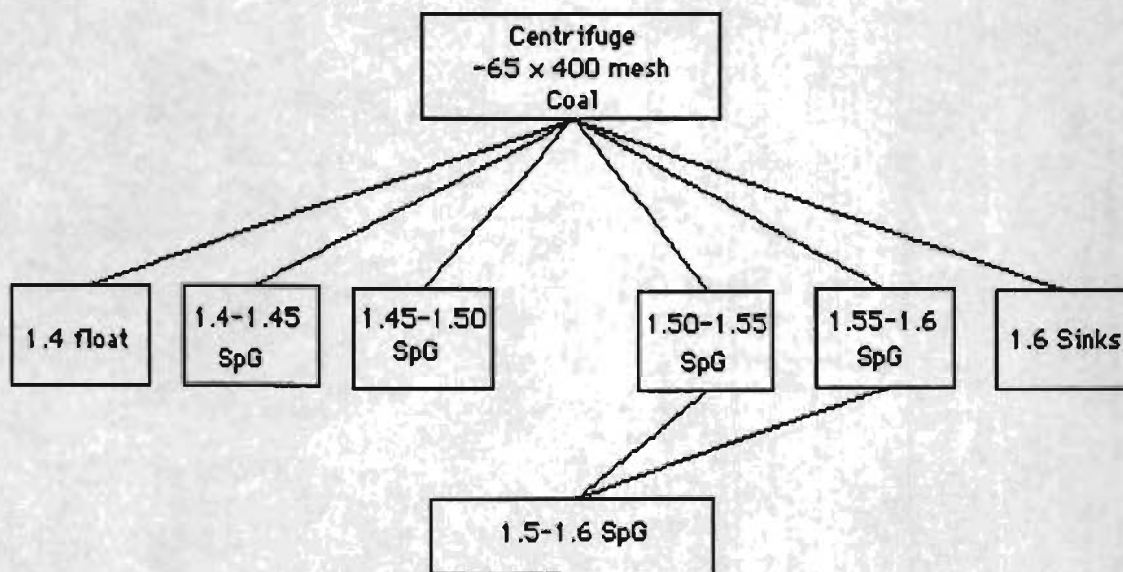
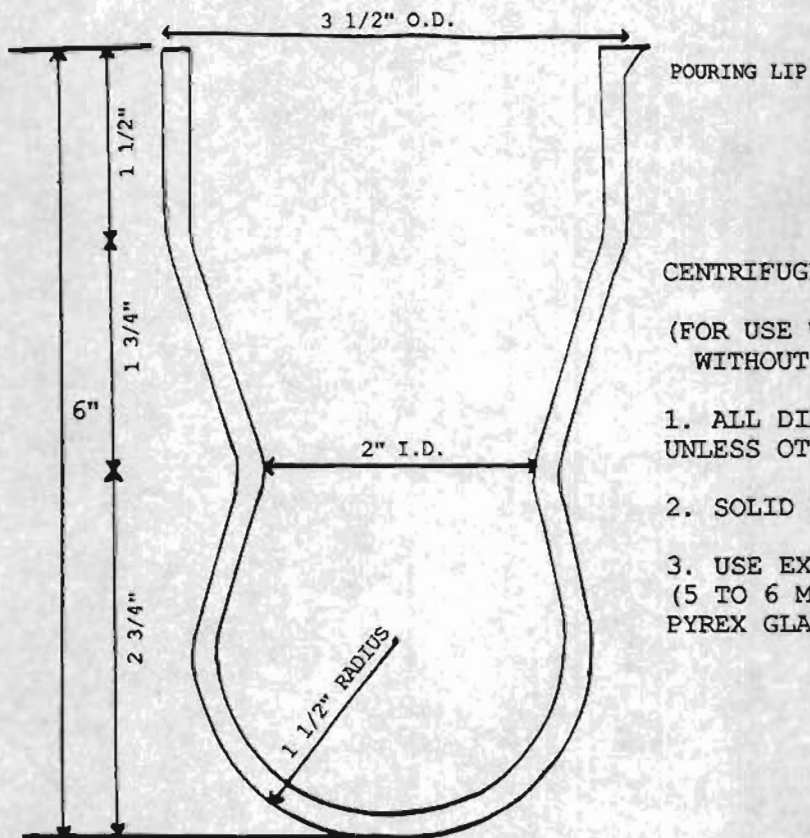


Figure 5. Flow diagram for specific gravity separation to enrich inertinite macerals.



**CENTRIFUGE BOTTLE**

(FOR USE WITH ICE-353S  
WITHOUT DOME)

1. ALL DIMENSIONS ARE O.D. UNLESS OTHERWISE NOTED.
2. SOLID BOTTOM, OPEN TOP
3. USE EXTRA HEAVY WALL (5 TO 6 MM) THICKNESS PYREX GLASS.

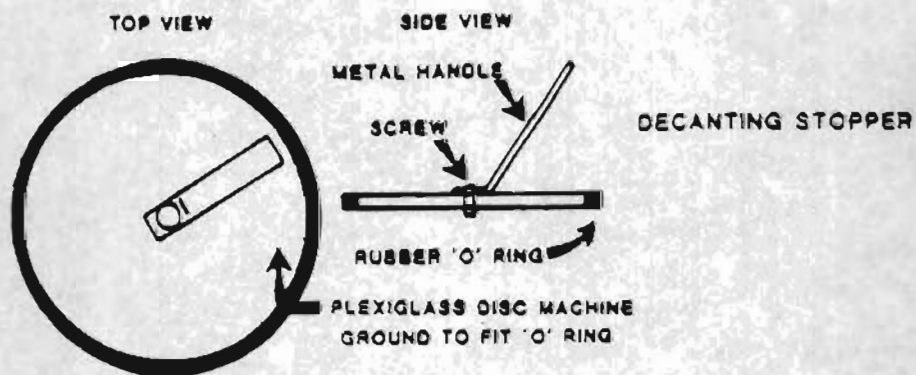


Figure 6. MIRL design of round bottom centrifuge bottle.



## CHAPTER 2

### 1. Liquefaction - General Considerations

#### a. Indirect Liquefaction

Coal can be liquefied in two distinctly different processes. The indirect method of liquefaction involves converting solid coal into synthesis gas which is a mixture of carbon monoxide and hydrogen. Synthesis gas is reacted with iron, a Fisher-Tropsch catalyst<sup>(27,28)</sup>, to produce a whole spectrum of hydrocarbon products, including chemical feedstocks, motor fuels, waxes and oils. The advantage of this indirect process is that it is somewhat flexible and can alter product distribution according to market demands as better and more selective catalysts are developed<sup>(29,30)</sup>. Fisher and Tropsch discovered this method of synthesizing hydrocarbons in 1920<sup>(27,28)</sup>. Since then the technology has become well established<sup>(31)</sup>. Presently, South Africa is producing most of its liquid fuels and chemical feedstocks from coal based on Fisher-Tropsch synthesis (SASOL I, II and III). The newer plants, SASOL II and III, can produce 100 times more than the original commercial units that were operating in Germany during World War II<sup>(29)</sup>.

#### b. Direct Liquefaction

Direct liquefaction involves the addition of hydrogen to coal during its thermal decomposition. This process is generally known as hydrogenation or hydrogenolysis of coal. Liquid fuels by hydrogenation of coal are usually obtained at comparatively lower temperatures in the presence of a donor solvent (hydrogen shuttle) like tetralin or a catalyst. Research work done between 1912 and 1926 led Bergius and Pott-Borche<sup>(27)</sup> of Germany to the development of direct liquefaction of coal, and in 1931 Bergius was awarded the Nobel Prize in chemistry.

During the early 1970's when OPEC imposed an oil embargo, some advances were made in obtaining clean-burning fuels from coals containing high mineral matter (i.e., high ash content) and high sulfur. Thus, solvent refined coals SRCI, SRCII<sup>(32)</sup> were produced on a pilot plant scale at lower severity and with lower hydrogen consumption than the German technology. H-coal<sup>(33,34)</sup> and Exxon Donor Solvent (EDS)<sup>(35,36,37,38)</sup> were the other two competing direct liquefaction processes that were developed to pilot plant scale. Block flow diagrams of the above mentioned processes are shown in Figures 7a, 7b and 8a, 8b.

More recently a two stage process has been developed<sup>(39,40,41)</sup> that shows promise for reducing direct liquefaction costs. During the first stage, a heavy but soluble liquid was produced through thermal non-catalytic dissolution in a donor solvent. After removal of mineral matter and heavy ends, the upgraded product was obtained using a catalyst. In such a two stage process, which is known as an integrated two stage liquefaction (ITSL) process<sup>(42,43)</sup>, hydrogen consumption was reduced, the useful life of the catalyst was extended, and a better quality product was made. Other

benefits were a better rate of reaction (short residence time), lower severity, reduced hydrocarbon gas make<sup>(44)</sup>, and lower waste production.

Currently, the direct liquefaction process is still in the pilot plant stage and technologically it is not as advanced and established as indirect liquefaction processes. Research work needs to address these deficiencies, because direct liquefaction offers a more efficient route to liquid products than does indirect liquefaction.

### 2. Pyrolysis

Liquid hydrocarbons can also be produced from pyrolysis or carbonization processes. Although liquids from both pyrolysis and direct processes are naphthenic and aromatic, the liquids from the latter are more amenable to reforming into high octane fuels at better yields. Both liquids must be hydrotreated to remove sulfur and nitrogen species which are catalyst poisons<sup>(29)</sup>. Hydrotreatment can also remove toxic components (carcinogens) in the high boiling fractions<sup>(45,46)</sup>.

### 3. Solvent Extraction

Early work involving coal extraction was mainly directed towards isolating the "coking principle" and adding it to poor coking coals to enhance their coking properties<sup>(47)</sup>. Elaborate schemes of extraction of coal were developed during the early part of this century. Pyridine<sup>(48)</sup> and benzene under pressure<sup>(49)</sup> were generally used as solvents. Since 1950, extraction studies<sup>(50,51,52,53,54)</sup> have taken a new turn and four important distinctions have been made<sup>(55)</sup>.

- Non-specific extraction: When coal is extracted below 100°C, only a few percent of the coal, waxes and resins are extracted. Therefore, the extract is not considered to be typical of the constitution of the original coal. Solvents like benzene, toluene and benzene-ethanol mixtures (3:1) are usually used.
- Specific extraction: Usually 20-40% of the coal is extracted and the nature of the extract is believed to be similar to the original coal. Solvents like pyridine are usually employed and the temperature is generally below 200°C.
- Extractive disintegration: Yields as high as 90% have been reported<sup>(58)</sup> with solvents like anthracene oil and/or B-naphthol at temperatures ranging from 300-350°C. However, the high temperature will contribute to the breakdown of the coal matrix and hence the higher yield.
- Extractive chemical disintegration: This is carried out with solvents like cresols and other phenols in the presence of hydrogen shuttlers, like tetralin or diphenylamine at temperatures above 300°C<sup>(57)</sup>.

In this work, benzene-ethanol (azeotropic) mixture and tetrahydrofuran were used as solvents.

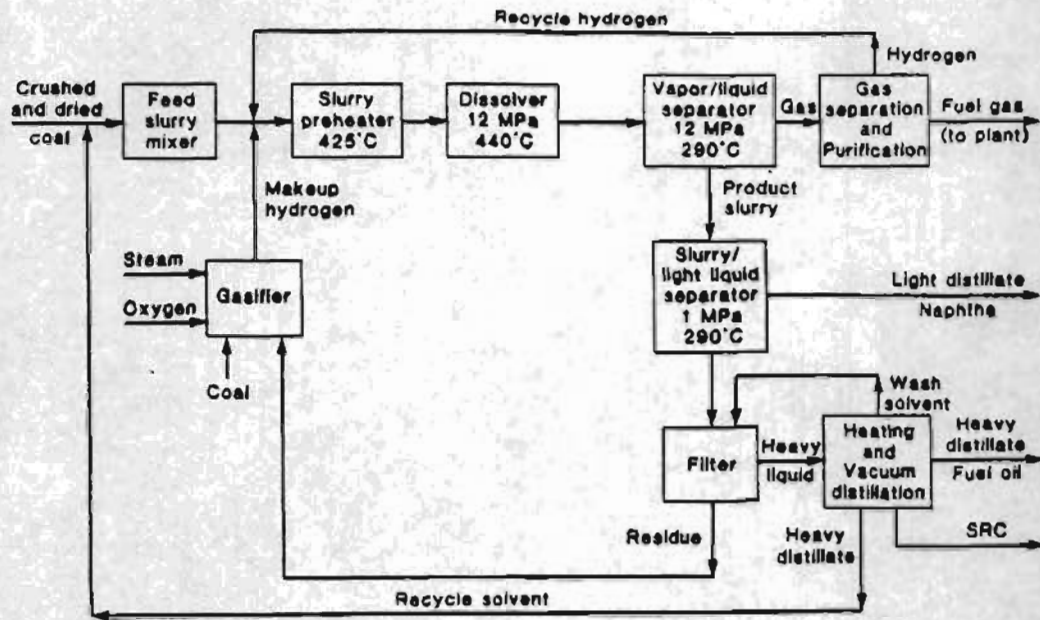


Figure 7a. Simplified flow diagram of SRC-I process for a commercial scale design with H<sub>2</sub> production by gasification.

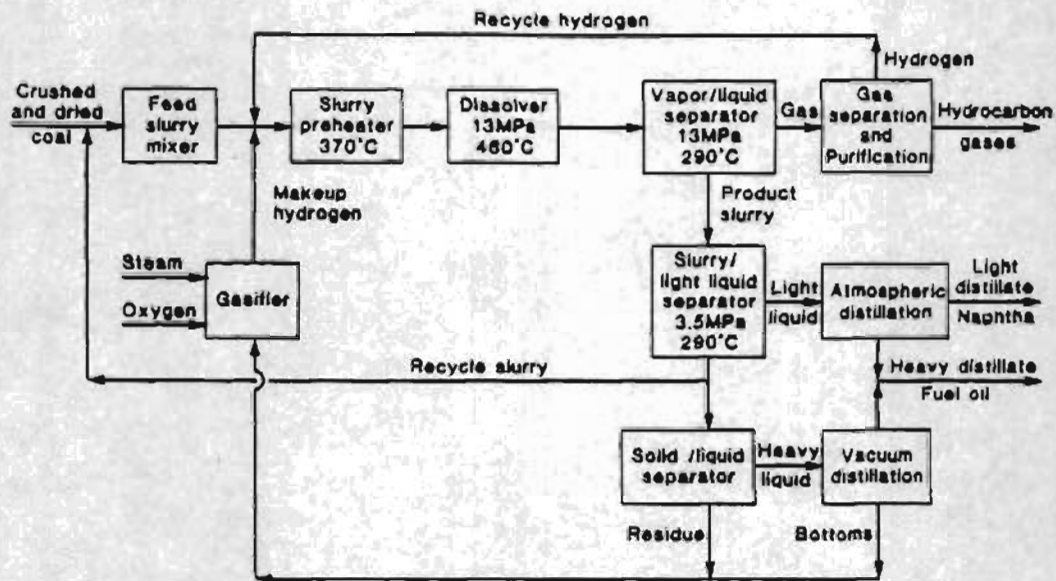


Figure 7b. Simplified flow diagram of SRC-II process for a commercial scale design with H<sub>2</sub> production by gasification.

Source: R.F. Probstein & R.E. Hicks.(29)

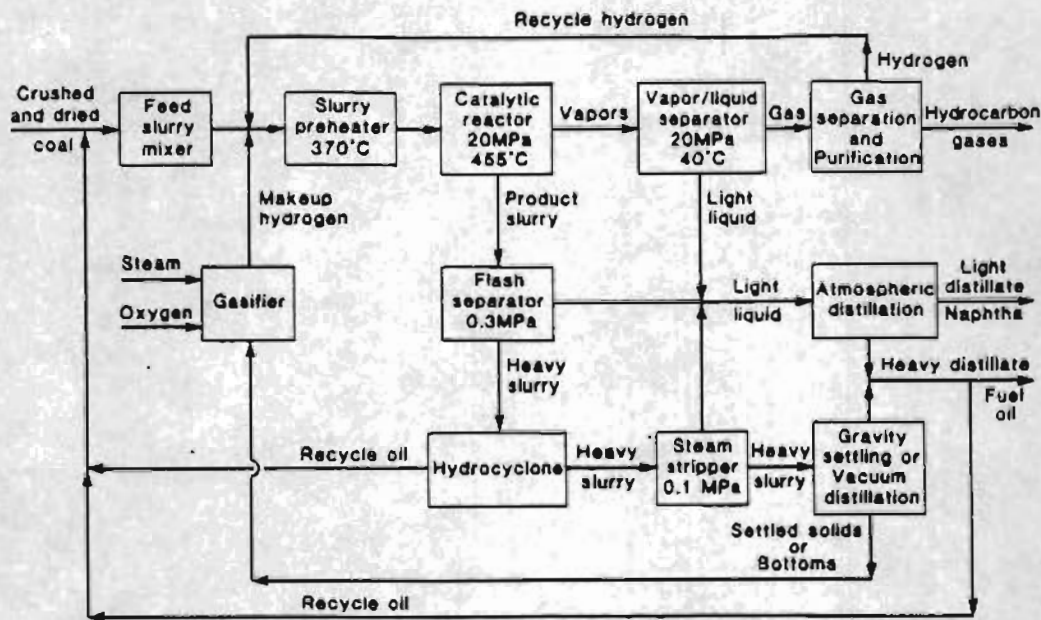


Figure 8a. Simplified flow diagram of H-coal process for a commercial scale design with H<sub>2</sub> production by gasification.

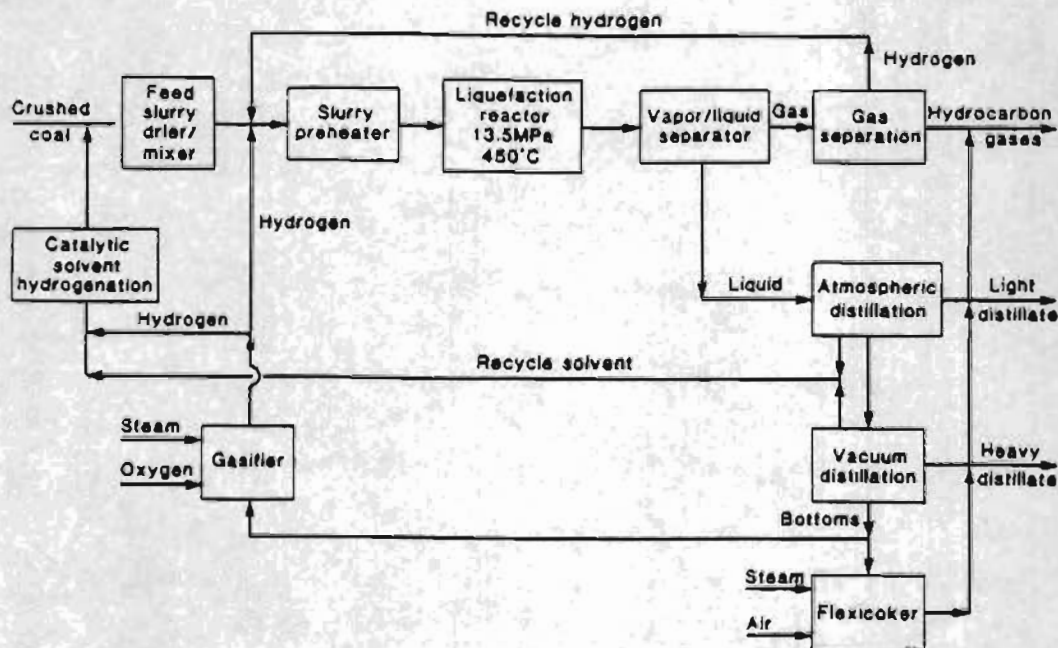


Figure 8b. Simplified flow diagram of Exxon Donor Solvent process for a commercial scale design with H<sub>2</sub> production by gasification.

Source: R.F. Probstein & R.E. Hicks.<sup>(29)</sup>

#### 4. Solvent Extraction Procedure

Five grams of enriched coal were taken in a tared, porous ceramic thimble, and extracted with a 3:1 mixture of benzene and ethanol in a soxhlet apparatus under nitrogen atmosphere at the solvent's boiling point. The extraction was continued until solvent in the soxhlet jacket became colorless (usually 2-3 days, depending on the coal). The extract was concentrated to about 10-15 ml below 60°C in a rotary evaporator. About 30 ml of hexane was added to the concentrated extract and the precipitate allowed to settle overnight. The precipitated asphaltene was separated using a 0.45  $\mu$  millipore filter and washed with 25 ml of hexane. The residue (asphaltene) was dried overnight in a vacuum oven at 100°C. The filtrate containing hexane solubles was evaporated below 60°C in a rotary evaporator to obtain oils. The thimble containing the residue was also dried in a vacuum oven for 24 hours at about 100°C, cooled and weighed to obtain consistent weight.

Similar extraction procedures were repeated with tetrahydrofuran (THF) at its boiling point (67°C). The precipitate separating from THF on addition of 30 ml of hexane was preasphaltene. The residue (THF insoluble) in the thimble was dried overnight at 70°C in a vacuum oven, as THF is more volatile. All the products were stored in vials under nitrogen.

Table 4 shows weight percent yield of the products obtained by extraction.

Table 4  
Solvent Extraction: yield of products from enriched coal

Product	Wt % Yield*
a. Asphaltene (Benzene-ethanol soluble)	1.34
b. Oil (Hexane solubles)	0.18
c. Residue	98.48 (100-(a+b))
d. Preasphaltene (THF soluble)	1.50
e. THF Residue	96.98 (100-(a+b+d))

Note: The low yield of products a, b, and d is probably due to high inertinite and low vitrinite and exinite concentrations.

\* DAF basis

#### 5. Product Generation

In this study products were generated by catalytic liquefaction, hydroliquefaction and solvent extraction, not only to compare the yields but also to chemically characterize the products obtained by catalytic liquefaction. Figures 9a and 9b are flowsheets showing workup and product generation in the above mentioned liquefaction methods.

#### 6. Hydroliquefaction

Both hydroliquefaction and catalytic liquefaction were carried out in a microreactor "tubing bomb"<sup>(58,59)</sup>. The equipment for liquefaction has been described elsewhere<sup>(60,61,23)</sup>. Three grams of enriched coal and 7.2 ml of tetralin (hydrogen donor) solvent were placed in each of the two bombs. The bombs were sealed and tested for leaks using nitrogen at a pressure of 1500 psig. If no leaks were detected, the nitrogen under pressure was released, the system purged and pressurized with hydrogen to 500 psig., Figure 9a. The two microreactors were set on a holder and attached to a vertically oscillating system. The coal and the donor solvent were shaken for a couple of minutes for good mixing. The fluidized sand bath was heated to 436°C, which is 11°C higher than the required reaction temperature of 425°C. Immediately after the bombs were depressed into the fluidized sand bath, the thermostat of the sand bath was set at 425°C, which was the desired liquefaction temperature. The microreactors (bombs) attained a constant temperature of 425°C in two minutes.

Liquefaction experiments were conducted in duplicate at the above temperature and residence times of 0 and 30 minutes, respectively. At the end of the residence time, the bombs were quenched in a water bath at room temperature for 30 minutes. The gases were collected in a sample bag for analysis by gas chromatography and volumetric measurement using a wet test meter.

#### 7. Hydroliquefaction Product Recovery and Fractionation

The contents of each bomb was quantitatively washed into a 500 ml beaker using 400 ml of hexane and the product recovery/fractionation scheme in Figure 9b was begun. The hexane insolubles, asphaltenes and preasphaltenes were allowed to settle overnight and separated on a 0.45  $\mu$  filter paper, washed with about 100 ml of hexane. The residue was dried in a vacuum oven for 24 hours at 100°C.

A couple of grams of dry hexane insolubles were saved and the rest was weighed in a tared ceramic thimble and extracted with toluene under nitrogen in a soxhlet apparatus until solvent in the jacket became colorless (about 50 hours). The thimble containing the residue, preasphaltene, was dried in a vacuum oven at 110°C for 24 hours, cooled and reweighed. The toluene extract was concentrated to 15-20 ml in a rotary evaporator. About 200 ml of hexane was added, the precipitated asphaltene was allowed to settle overnight, separated with a tared 0.45  $\mu$  filter paper and dried in a vacuum oven overnight at 100°C.

A similar extraction procedure with THF was repeated with the residue in the thimble after it was cooled and weighed to obtain consistent weight. Thus, asphaltene, preasphaltene and residue (THF insoluble) were generated as illustrated in Figure 9a. All these products were stored in vials under nitrogen.

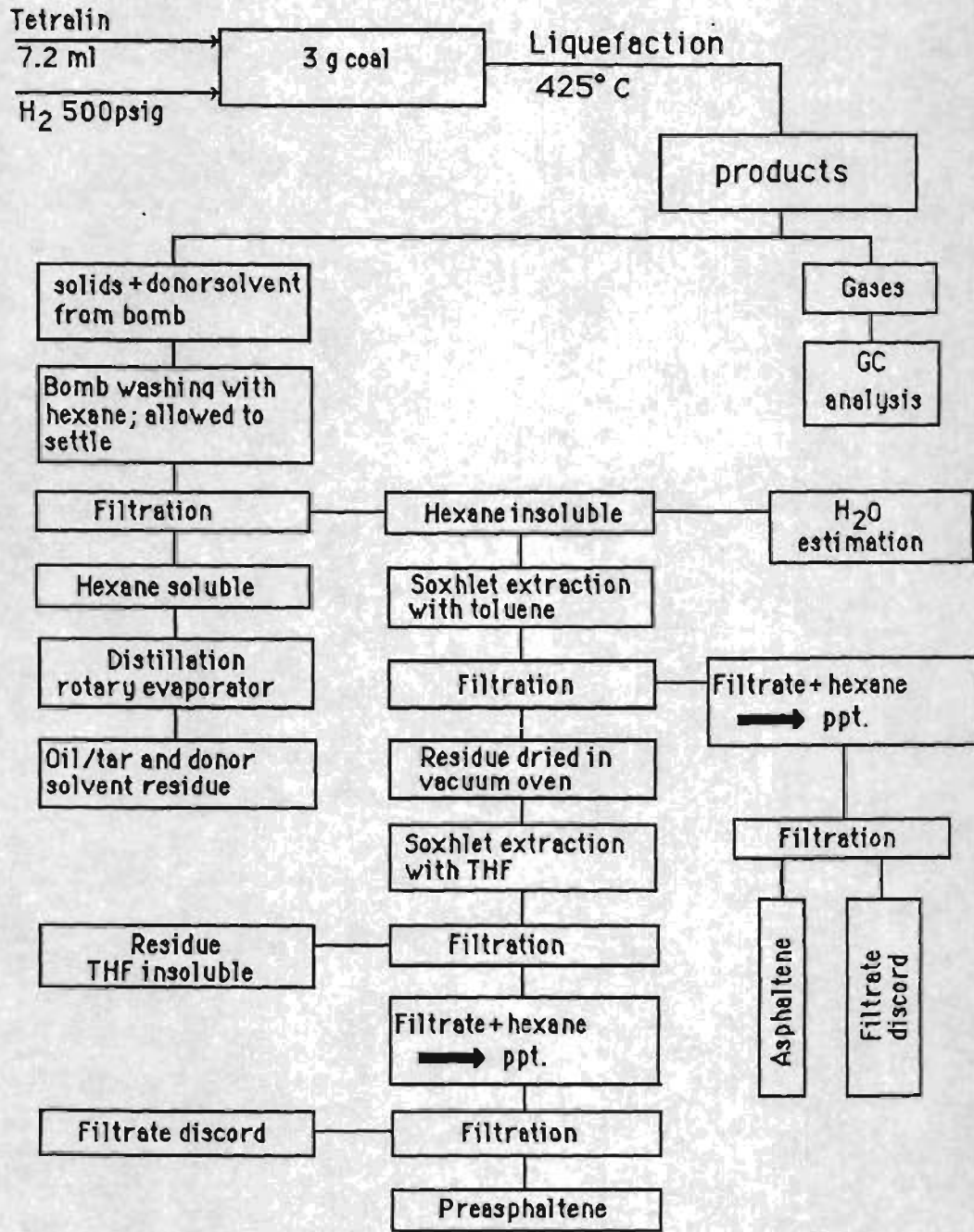


Figure 9a. Flow diagram of product work up after Hydroliquefaction.

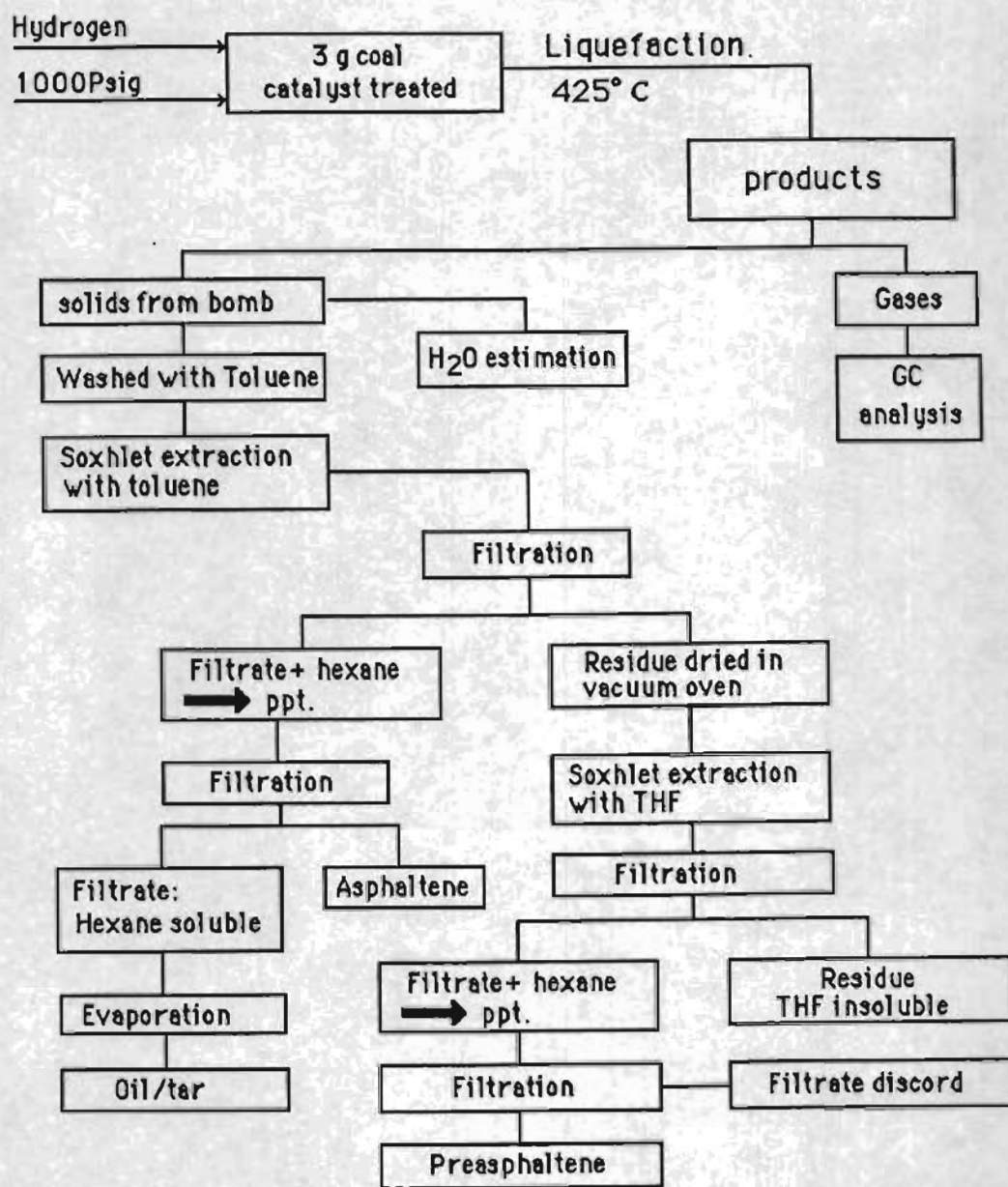


Figure 9b. Flow diagram of product work up after Catalytic liquefaction.

The filtrate containing the hexane solubles, tetralin and its derivatives was evaporated below 60°C in a rotary evaporator to remove hexane. The liquid residue was stored in vials.

## 8. Catalytic Liquefaction

Catalytic liquefaction was conducted at the same conditions of temperature (425°C), residence times (0 and 30 minutes), and coal charge as that of hydroliquefaction. The main differences are shown in Figure 9b. 1) The coal was impregnated with the MoS<sub>2</sub> catalyst prior to liquefaction. 2) No donor solvent was present. 3) The micro reactor was pressurized to 1000 psig of H<sub>2</sub>. 4) After the liquefaction, the solid content in the bomb was washed with 300-350 ml of toluene and quantitatively transferred into a tared ceramic thimble for extraction in a soxhlet apparatus. 5) After filtering out the precipitated asphaltene obtained from the concentrated toluene extract by adding hexane, the filtrate was evaporated to dryness in a rotary evaporator below 60°C. The residue, oils/tars, were separated into chemical classes and analyzed by column chromatography, GC-MS and capillary GC according to the procedure developed by Later et al.<sup>(62)</sup> The preasphaltene and THF insolubles were generated exactly as mentioned under hydroliquefaction, Figure 9b.

## 9. Catalyst Impregnation of Coal

The aqueous impregnation procedure to load the coal with molybdenum sulfide (MoS<sub>2</sub>) is due to Given and Derbyshire<sup>(63)</sup>. 5 N HCl was added dropwise to a three fold excess of Na<sub>2</sub>S in a flat bottom flask (A) with a side tube (Figure 10). The H<sub>2</sub>S generated was bubbled through a weighed quantity of ammonium heptamolybdate, (NH<sub>4</sub>)<sub>6</sub>Mo<sub>7</sub>O<sub>24</sub>·4H<sub>2</sub>O (AHM), dissolved in 50 to 60 ml of deionized water in flask (B) to produce the thio salt of ammonium molybdate, (NH<sub>4</sub>)<sub>2</sub>MoS<sub>4</sub>. This salt decomposes to give MoS<sub>2</sub>, the active form of the catalyst in the hydrogenation of coal.<sup>(64)</sup> The colorless solution of AHM turns red during the early part of the reaction and becomes dark at the end of the reaction.

The unreacted H<sub>2</sub>S was absorbed in the scrubber containing 1:1 acetone and 1M NaOH solution in flask (C). A weighed amount of coal was treated with an exact volume of the dark solution such that each gram of coal was impregnated with 1% wt molybdenum. The resulting slurry was initially allowed to dry at 50°C in a vacuum oven and subsequently at 100°C until a constant mass was obtained. During drying, the slurry was stirred several times to insure uniform impregnation of catalyst. The dry mass is usually a cake which is broken up, sieved using a 48 mesh screen and riffled to obtain a homogeneous mix of the sample. The sample was stored under nitrogen before using it for liquefaction.

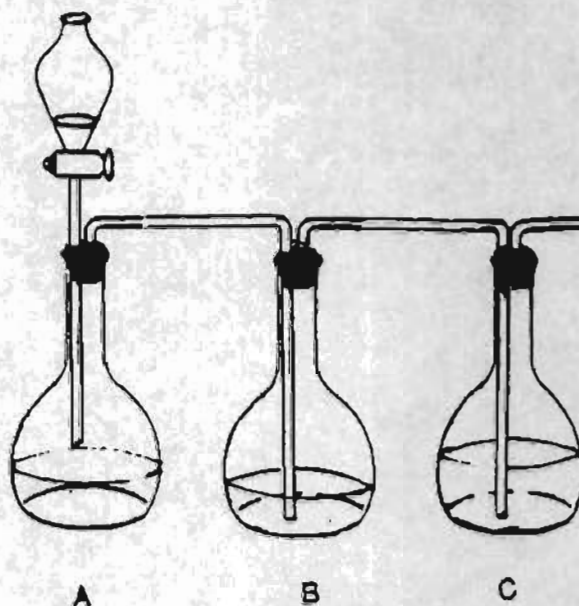
## 10. Determination of Liquefaction Products

### a. Total Conversion

The total percent conversion and the yields of the products were calculated on dry ash free (DAF) basis. The values were obtained by using the following formula:

$$\% \text{ conversion} = \frac{\text{wt coal} - \text{wt insoluble residue}}{\text{wt coal}} \times 100$$

Note: The weight of catalyst (1% coal) was included in case of catalytic liquefaction.



A : Na<sub>2</sub>S + 5N HCl

B : Ammonium hepta molybdate solution

C : 1:1 Acetone + 1M NaOH solution

Figure 10. Catalyst preparation

Note: 4g (approximately a 3 fold excess) of Na<sub>2</sub>S was placed in flask A. 5N HCl was dropped slowly to generate H<sub>2</sub>S which reacts with 0.7190g of AHM to produce a dark liquid in flask B. Excess H<sub>2</sub>S was absorbed in 1:1 acetone-NaOH solution. Since the acetone-NaOH solution does not absorb all the escaping H<sub>2</sub>S, the preparation should be done in the hood. See Appendix B for calculations involving the generation and impregnation of the catalyst.

### b. Gas Analysis

Gases produced during liquefaction were determined by analyzing the composition of the gas mixture by gas chromatography (GC). The volume of the mixture of gases was determined by a wet test meter. Using these two data the total amount of the gas was calculated. The gas mixture was analyzed on a Varian Model 3700 gas chromatograph (Varian, Associates, Palo Alto, Ca.) equipped with both flame ionization (FID) and thermal conductivity (TCD) detectors capable of monitoring gases from two different columns at the same time. The carrier gas was helium and the data were obtained on two strip chart recorders. CH<sub>4</sub>, CO, and CO<sub>2</sub> were detected by TCD and hydrocarbon gases (C<sub>1</sub>, C<sub>2</sub>, C<sub>3</sub>... etc.) were detected by FID.

Standard gas mixtures (Supelco, Inc., Bellefonte, Pa.) were used to calibrate the GC to quantify the gases in the above analysis. The instrument was calibrated each week. The parametric conditions set up on the GC during the analysis are given in Table IV, Appendix A.

After the completion of the GC analysis, the volume remaining in the sampling bag was forced through a wet test meter using a short piece (2-4 cm) of tygon tube to connect the sampling bag and meter. The amount of gases dissolving in the water contained in the wet test meter was assumed to be negligible. The volume obtained from the wet test meter was added to the volume that was used up in the GC analysis. Thus, the total volume of the gases (V<sub>i</sub>) generated during liquefaction was determined.

If V<sub>i</sub> represents the amount of each gas produced, and X<sub>i</sub> represents the percent each gas, then the total volume of gas collected was equal to V<sub>i</sub> (corrected to STP), and:

$$V_i = X_i/100 (V_t)$$

### c. Asphaltenes and Preasphaltenes

The amount of asphaltene and preasphaltenes was determined using the formulas given below:

wt% of asphaltene\* =

$$\frac{\text{wt coal} - (\text{wt gas} + \text{wt oil} + \text{wt preasphaltene} + \text{wt residue})}{\text{wt of coal}} \times 100$$

wt% of preasphaltene\* =

$$\frac{\text{wt coal} - (\text{wt gas} + \text{wt oil} + \text{wt asphaltene} + \text{wt residue})}{\text{wt of coal}} \times 100$$

\* DAF basis

Tables 5, 6 and 7 show the various product yields of liquefaction. The product yields are found to be consistent with the trend of the earlier studies of hydroliquefaction and catalytic liquefaction with UA-139 coal, conducted in this laboratory<sup>(22,23)</sup>.

## 11. H<sub>2</sub>O Production During Liquefaction

Water is produced as a byproduct during liquefaction<sup>(65)</sup> mainly due to the presence of organic oxygen functional groups like hydroxyl (OH), carboxyl (COOH), carbonyl (C=O) and ether (C-O-C) in coal<sup>(66,67)</sup>.

Some inorganics (mineral matter) also contribute to the formation of water. During hydrogenolysis of coal, the production of water occurs at the expense of hydrogen and is an ineluctable outcome. Thus some hydrogen is wasted in the formation of water instead of being used to cap the free radicals formed during liquefaction and retard retrograde reactions. Removal of oxygen as CO<sub>2</sub> and CO is more desirable than the production of water.

It has been shown that the carboxylic (COOH), carbonylic (C=O) and etheric (C-O-C) oxygen functionalities are greatly reduced while hydroxylic oxygen functionality is increased during the liquefaction of coal<sup>(68)</sup>. The increased

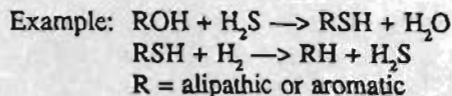
Table 5  
Gas Analyses

Gases	(% Weights)			
	Hydroliquefaction		Catalytic liquefaction	
	Residence Time			
	0 Min.	30 Min.	0 Min.	30 Min.
CO	0.21	0.53	0.36	0.98
CO <sub>2</sub>	3.68	6.25	3.95	7.46
CH <sub>4</sub>	0.06	0.46	0.10	0.71
C <sub>2</sub> H <sub>4</sub>	0.01	0.20	0.03	0.42
C <sub>3</sub> H <sub>8</sub>	0.01	0.10	0.02	0.21
C <sub>4</sub> H <sub>10</sub>	0	0.03	0.01	0.13
C <sub>5</sub> H <sub>12</sub>	0	0.01	0.01	0.08
Total % Wt	3.97	7.58	4.48	9.99

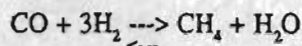
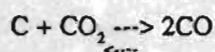
Note: Average value of two runs  
DAF basis



-OH along with the original OH groups of the coal react with  $H_2S$  (generated either by the pyritic sulfur<sup>(68,69)</sup> and/or organic sulfur<sup>(70,71)</sup> present in coal) to produce aliphatic and aromatic mercaptans and water. The mercaptans are then reduced to regenerate  $H_2S$  and the appropriate hydrocarbon.

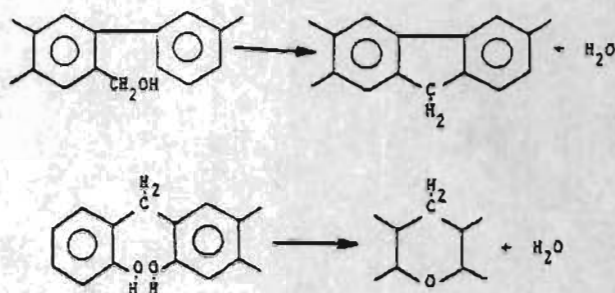


This is why the presence of sulfur (organic and pyritic) in small quantities is desirable in feed coals used for liquefaction. In catalytic liquefaction with Mo as catalyst, the active form  $MoS_2$ <sup>(64)</sup> supplies the  $H_2S$  required for the above process to occur. Another pair of reactions that produce water during liquefaction are:



Also, during conversion the loss of aromatic hydrogen and decrease in aliphatic structures is evident from Fourier Transform Infrared (FTIR) studies. This is observed in the decrease of intensity in the band at  $1600\text{ cm}^{-1}$ , part of which is attributed to aromatic structure and the decrease in intensity of the two bands at  $2920$  and  $2850\text{ cm}^{-1}$  of the aliphatic

structure in the 30 minute residue. Whitehurst et al.<sup>(65)</sup> has shown that the H/C ratio and the oxygen content decreases with the increase in the conversion of coal. The following is their proposed mechanism in which water occurs as a by-product.



Further, release of water held by clay minerals starts at about  $200^\circ\text{C}$  and is complete around  $300^\circ\text{C}$ <sup>(74)</sup>. Therefore, the  $H_2O$  produced during liquefaction should be accounted for by subtracting the amount (% wt) formed from the % wt conversion reported in Tables 6 and 7.

## 12. Method of $H_2O$ Estimation

In this work the Dean-Stark method was employed to determine the % wt of water in the reaction products. The contents of the bomb after liquefaction was quantitatively transferred to a 250 ml round bottom flask along with its toluene washings. About 100 ml of toluene was used to wash and scrape the bomb. The mixture was refluxed for 24 hours

**Table 6**  
Hydroliquefaction  
(Product yield)

Product	Average % Wt Yields Residence Time	
	0 Minutes	30 Minutes
1. Gases	3.97	7.58
2. Oil	7.30	21.02
3. Asphaltene	5.02	13.48
4. Preasphaltene	1.01	3.51
Total Conversion	17.30	45.59

**Table 7**  
Catalytic liquefaction  
(Product yield)

Product	Average % Wt Yields Residence Time	
	0 Minutes	30 Minutes
1. Gases	4.48	9.99
2. Oil	10.18	27.70
3. Asphaltene	8.99	22.02
4. Preasphaltene	2.02	5.50
Total Conversion	25.67	65.21

Note: Average of two runs  
DAF basis

using a Dean-Stark condenser. The mixture of water and toluene collected in the graduated condenser tube was cooled and allowed to settle for a few hours at room temperature. Since the phase separation was not well defined, a minute crystal (<1mg) of  $\text{KMnO}_4$  was added to the mixture. After about an hour, the well separated junction of the two phases was measured in ml to obtain the volume of  $\text{H}_2\text{O}$ . The change in the volume of water due to the addition of  $\text{KMnO}_4$  was negligible. Table 8 shows the % wt of water formed during hydro and catalytic liquefactions at 0 and 30 minutes of residence time. Table 9 shows the corrected % wt total conversion.

**Table 8**  
Water Produced During Liquefaction (% Wt)

Liquefaction	% wt $\text{H}_2\text{O}$	
	Residence time: 0'      30'	
Hydro	2.52	3.37
Catalytic	3.88	5.18

Note: Average of two runs  
DAF basis

**Table 9**  
Corrected % Wt Total Conversion of Coal  
(from Tables 6 & 7)

Liquefaction	% Wt conversion before $\text{H}_2\text{O}$ correction		% Wt conversion after $\text{H}_2\text{O}$ correction	
	Residence time			
	Minutes 0	30	Minutes 0	30
Hydro	17.30	45.59	14.78	42.22
Catalytic	25.67	65.21	21.79	60.03

Note: DAF basis

## CHAPTER 3

### 1. Infrared and X-ray Diffraction Studies of the Enriched Coal, Its Liquefaction Products and Low Temperature Ash

Infrared spectroscopy is one of the well established methods for analyses of chemical compounds in coal derived materials. Application of IR spectroscopy to coal began in the 1950's<sup>(72,73)</sup> with the advent of Fourier Transform Infrared (FTIR) analysis. Painter et al.<sup>(74)</sup> and Solomon et al.<sup>(75)</sup> have applied the technique to study the functional groups in coal and its products. IR spectroscopy is based on the rate of change of molecular vibrations when infrared radiation is absorbed by a molecule. IR active molecules meet the two absorption requirements: 1) A state of resonance between the frequency of radiation and the natural frequency of vibration of the molecule; 2) a resonance vibration that changes the dipole moment ( $\mu$ ) of the molecule. The larger the change in the dipole moment, the stronger the absorption; i.e. the stronger the intensity of the IR band and vice versa. Compounds containing polar groups like C=O show strong IR absorption due to large dipole moment displacements, while non-polar groups show weak or no absorption.

Mathematically,

$$I = C (d/dt) \mu^2$$

where,

I = intensity of absorption

C = proportionality constant

$\mu$  = dipole moment

Certain molecules like  $\text{O}_2$ ,  $\text{H}_2$ , and C=C in ethylene are symmetrical and a change in dipole moment in such molecules are not possible. Hence, they are IR inactive.

The FTIR instrument has many advantages over the older dispersive type, including: 1) The use of interferometer instead of slits and gratings produces a higher energy throughput that helps in the analysis of highly absorbent materials similar to coal. 2) Spectral data are recorded and stored in digital form which allows for scale expansion and the diffused features of the spectra can be studied through spectral subtraction to obtain a difference spectrum yielding bands obscured by other absorption bands<sup>(76)</sup>. 3) Also, better curve resolution can be obtained through Fourier transform analysis.

Although the assignment of most absorption bands to the different functional groups is well established in the literature, certain controversies still exist. For example, Solomon<sup>(76,77)</sup> has assigned several bands between the 1000 and 1350  $\text{cm}^{-1}$  to ethers. But, Painter et al.<sup>(74)</sup> disagree, stating that such assignments cannot be precise due to closely

**Table 10a**  
**Band Assignments for FTIR Spectra of Coals and Coal Products**

Aliphatic and Aromatic Groups		Oxygen-Containing Functional Groups	
Wave Number cm <sup>-1</sup>	Assignment	Wave Number cm <sup>-1</sup>	Assignment
3030	Aromatic C-H	3300	Hydrogen-bonded
2950 sh	CH <sub>3</sub>		
2920	Aliphatic C-H		
2850	CH <sub>2</sub> and CH <sub>3</sub>		
		1720-1690	C=O, ketone, aldehyde and -COOH
		1650-1630	C=O, highly conjugated
			O 
1600	Aromatic ring stretch	Approx. 1600	e.g., Ar-C-Ar Highly conjugated Hydrogen-bonded C=O
		1590-1560	Carboxyl group in salt form, -COO <sup>-</sup>
1490 sh	Aromatic ring stretch		
1450	CH <sub>2</sub> and CH <sub>3</sub> bend; possibility of some aromatic ring nodes		
1375	CH <sub>3</sub> groups		
		1330-1110	C-O stretch and O-H bend in phenoxy structures, ethers
		1100-1000	Aliphatic ethers, alcohols
900-700	Aromatic C-H out- of-plane bending modes		
860	Isolated aromatic H		
833(weak)	1,4 substituted aromatic groups		
815	Isolated H and/or 2 neighboring H		
750	1,2 substituted; 4 neighboring H		

Source: Painter et al., 1981

occurring vibrational energy levels or intramolecular mechanical coupling between adjacent C-C and C-O stretching vibrations in ethers or C-O stretching and OH bending in phenols. Further, the band occurring near 1600  $\text{cm}^{-1}$  has been given several assignments. One of the assignments is the aromatic ring stretching vibration while the other is the chelated carboxyl type structure similar to that found in acetyl acetone. Another by Painter et al.<sup>(74)</sup> suggests that the band be assigned to aromatic ring stretching vibration reinforced by phenolic -OH group or by  $\text{CH}_2$  group linking aromatic units and/or ether bridges. Table 10a shows the band assignment used in this report to assign the various functional groups usually observed in coals.

FTIR is also very useful in identifying the mineral matter present in coals<sup>(78,79)</sup>. Table 10b shows the band assignment to the various minerals present in the coals and Table 10c shows the principal x-ray diffraction (XRD) spacings of kaolinite and quartz.

Table 10b

Infrared Absorption Bands for Kaolinite and Quartz

Mineral	Absorption bands ( $\text{cm}^{-1}$ )
Kaolinite	3695, 3665, 3650, 3620, 1180, 1025, 1000, 910, 782, 749, 690, 530, 460, 422, 360, 340, 268
Quartz	1160, 1065, 790, 770, 687, 500, 450, 388, 362, 256

Source: Analytical Methods for Coal and Coal Products Vol. II, page 278, Ed: C. Karr, Jr.

Table 10c

Principal x-Ray Diffraction Spacings of Kaolinite and Quartz

Mineral	Diffraction Spacing ( $\text{Å}$ )
Kaolinite	7.15(100), 3.57(80), 2.38(25)
Quartz	4.26(35), 3.34(100), 1.82(17)

Source: Analytical Methods for Coal and Coal Products Vol. II, page 278, Ed: C. Karr, Jr.

Note: Relative intensities in the parantheses.

This study is essentially the qualitative analysis of the functional groups and their fate as the coal was converted into the various products, viz. asphaltenes, preasphaltenes and residues during catalytic liquefaction. FTIR spectra that follow were all derived from the solid products and residues from catalytic liquefaction. Hexane solubles (oil/tar) were not studied by FTIR, but their analyses will be covered in detail in Chapter 4. Mineral matter content of the coal was studied using the low temperature ash (LTA). Both FTIR and XRD methods were employed in the LTA analysis.

## 2. Low Temperature Ashing

A good literature review on low temperature ashing is found in the second volume of Analytical Methods for Coal and Coal Products<sup>(80)</sup>. The procedure followed in this work is due to Miller<sup>(81)</sup>. A sample of 2.5g of inertinite enriched coal was stirred with 100 ml of 1N ammonium acetate solution for three hours at 25°C and filtered. An additional 50 ml of ammonium acetate was used to wash the residue. The volume of the filtrate was made up to mark with ammonium acetate in a 200 ml volumetric flask. This procedure was repeated four times to obtain a total of five washings with ammonium acetate. After the fifth washing with ammonium acetate, the residue was treated in exactly the same manner using 1N HCl. The filtrate was made up to the mark with HCl in a 200 ml volumetric flask. The solutions in the six volumetric flasks were analyzed for cations using a DC plasma emission spectrometer (Beckman, Spectraspan V). Table V, Appendix A, shows the cation concentrations in the six washings. The stripping of the cations is necessary as it hastens the process of low temperature ashing. The residue from the above washings was dried in a vacuum oven at 100°C, until a constant weight was achieved.

The low temperature ash was obtained using an instrument manufactured by LFE, Model LTA-302, equipped with a double chambered oxygen plasma unit. A dried sample of the coal in two tared petrie dishes containing 1.0g each was treated at 100 watts/channel RF and a flow rate of 50 cc/min of oxygen. The chamber was maintained at a pressure of 1 mm of mercury. The samples were stirred two times in the first eight hours and once every three or four hours until there was hardly any weight loss.

## 3. Preparation of KBr Pellets for FTIR

A (1%) mixture 1:99 mg of KBr was taken in a stainless steel vial containing a pestle ball (1/4" diameter). It was mixed and well ground to obtain uniform particle size using a shaking apparatus (made by Vevadent Inc. for Perkin & Elmer) for 20 seconds. The mixture was loaded to a dies press and subjected to a pressure of 10 tons/square inch for 30 sec, under vacuum. The pressure was released to zero and reapplied again to 10 tons/square inch for 1 minute. The KBr pellets thus prepared were stored in a desiccator before

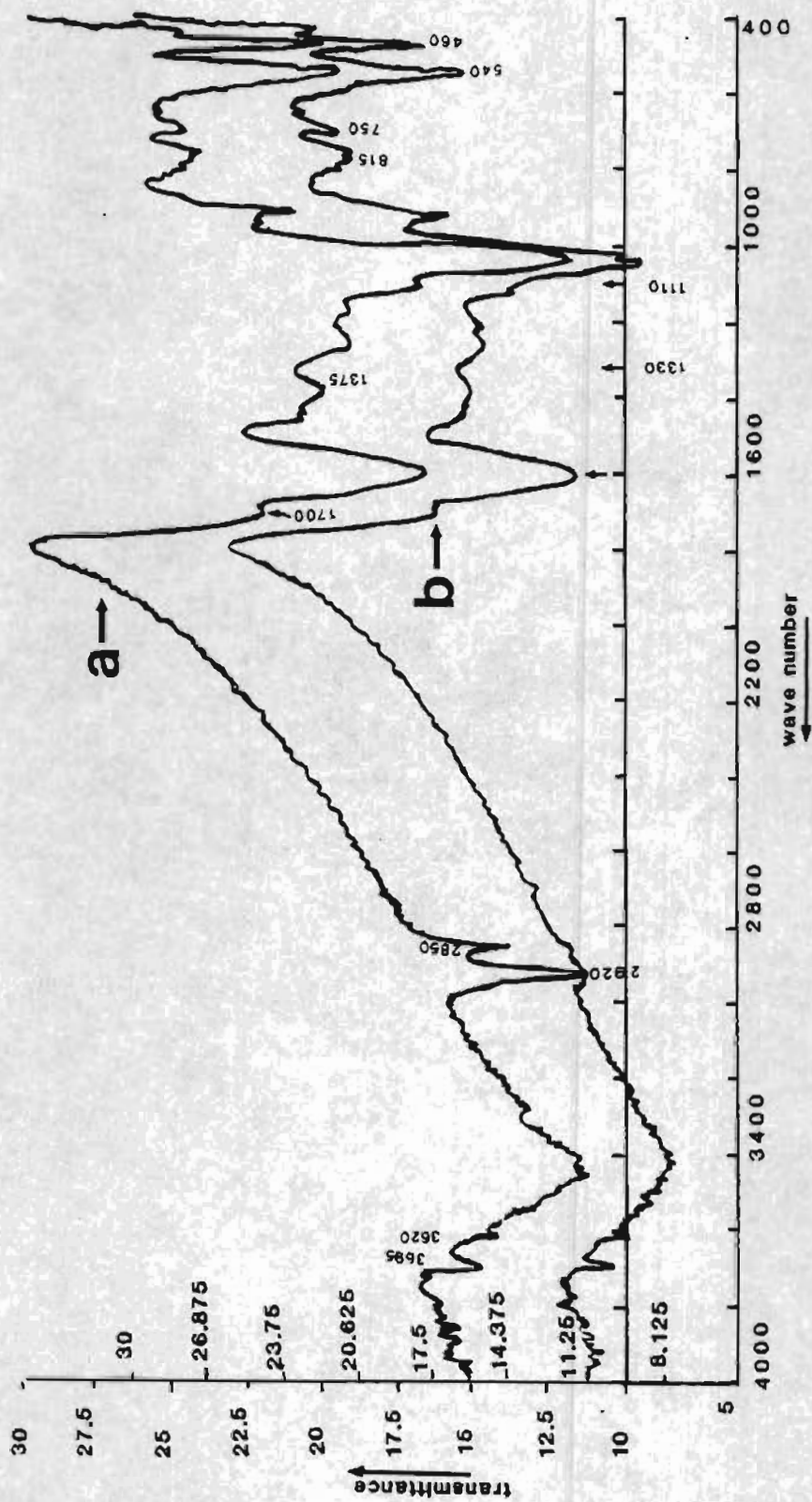
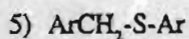
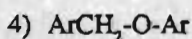
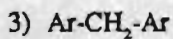
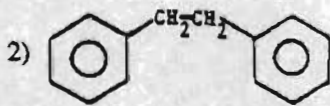
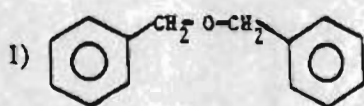


Figure 11. FTIR spectrograms: a. Inertinite enriched coal.  
 b. Residue after solvent extraction.

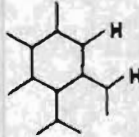
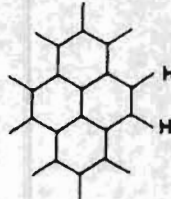
they were used to obtain the FTIR spectra. The KBr pellets and FTIR spectra were produced by D. Finseth of the Pittsburgh Energy Technology Center, Pittsburgh, Pennsylvania on a Digilab FTS-20 instrument by co-adding 16 scans at a spectral resolution of 8 cm<sup>-1</sup>.

The IR spectrum, Figure 11, is that of the inertinite enriched coal, which is typical of a high ash coal. The bands at 2950 (shoulder), 2920 and 2850 cm<sup>-1</sup> indicate the presence of aliphatic CH<sub>3</sub>, CH, CH<sub>2</sub> and CH<sub>3</sub> respectively. The band at 1450 cm<sup>-1</sup> further reaffirms the presence of aliphatic CH<sub>2</sub> and CH<sub>3</sub> bending. The absorption band at 3030 cm<sup>-1</sup> (aromatic C-H) is not prominent since the carbon content of this coal is only about 71%. According to Fujii et al.<sup>(82)</sup>, the band at 3030 cm<sup>-1</sup> becomes more prominent when the carbon content of the coal is over 81% and more intense with increasing coal rank. So, too, the intensity of the band at 2920 cm<sup>-1</sup> has been found to attain a maximum as the carbon reaches 86% and with increase in rank and then decreases in intensity sharply thereafter. Wen<sup>(83)</sup> demonstrated the useful application of FTIR to the SRCII process by monitoring bands at 3030 and between 2860 and 2960 cm<sup>-1</sup>. Based on the intensities of the above bands due to the aromatic hydrogen H<sub>ar</sub> and the aliphatic hydrogen H<sub>al</sub>, the degree of polymerization D<sub>p</sub> = H<sub>ar</sub>/(H<sub>ar</sub> + H<sub>al</sub>) of the various process streams were monitored for coke formation during the development of SRC II.

The main difference between the two spectra of the inertinite enriched coal a, and its solvent extraction residue b (Figure 11), is that the bands at 2920 and 2850 cm<sup>-1</sup> (aliphatic CH, CH<sub>2</sub> and CH<sub>3</sub>) are absent in the residue, b. This demonstrates the fact that the bonds involving the aliphatic moiety of the coal are more labile, i.e. they are easily broken during the early stages of liquefaction or pyrolysis<sup>(84)</sup>. Example of labile linkages in coal<sup>(85,86)</sup>:



The other prominent bands of the spectra in Figure 11 can be assigned as follows:

	Group	cm <sup>-1</sup>
1	C=O	1700 (shoulder)
2	a) Aromatic ring stretching b) Highly conjugated hydrogen bonded C=O	1600
3	CH <sub>3</sub>	1375
4	C-O stretch and OH bend in phenoxy-structures, ethers	1330-1110
5	Aliphatic ethers and Alcohols	1100-1000
6	 isolated CH group	750
	 two adjacent CH groups	815
7	Kaolinite	3695, 3620, 540, and 460

Note: Although quartz is one of the mineral matter components of this coal, it was not detectable by IR. However, its presence was confirmed by XRD (see Figure 17).

Figure 12, a, b and c, shows spectra of the enriched coal, its 0 min. and 30 min. liquefaction residues respectively. As expected, the aliphatic bands (CH, CH<sub>2</sub> and CH<sub>3</sub> stretchings) at 2920 and 2850 cm<sup>-1</sup> decrease as residence time increases while the shoulder at 1700 cm<sup>-1</sup> due to carbonyl is no longer discernable in either b or c. There is an attenuation in the intensity of the large band (representing aromatic ring stretching, etc.) at 1600 cm<sup>-1</sup> in the spectra b and c. However, there are noticeable increases in intensities in bands at 3695,

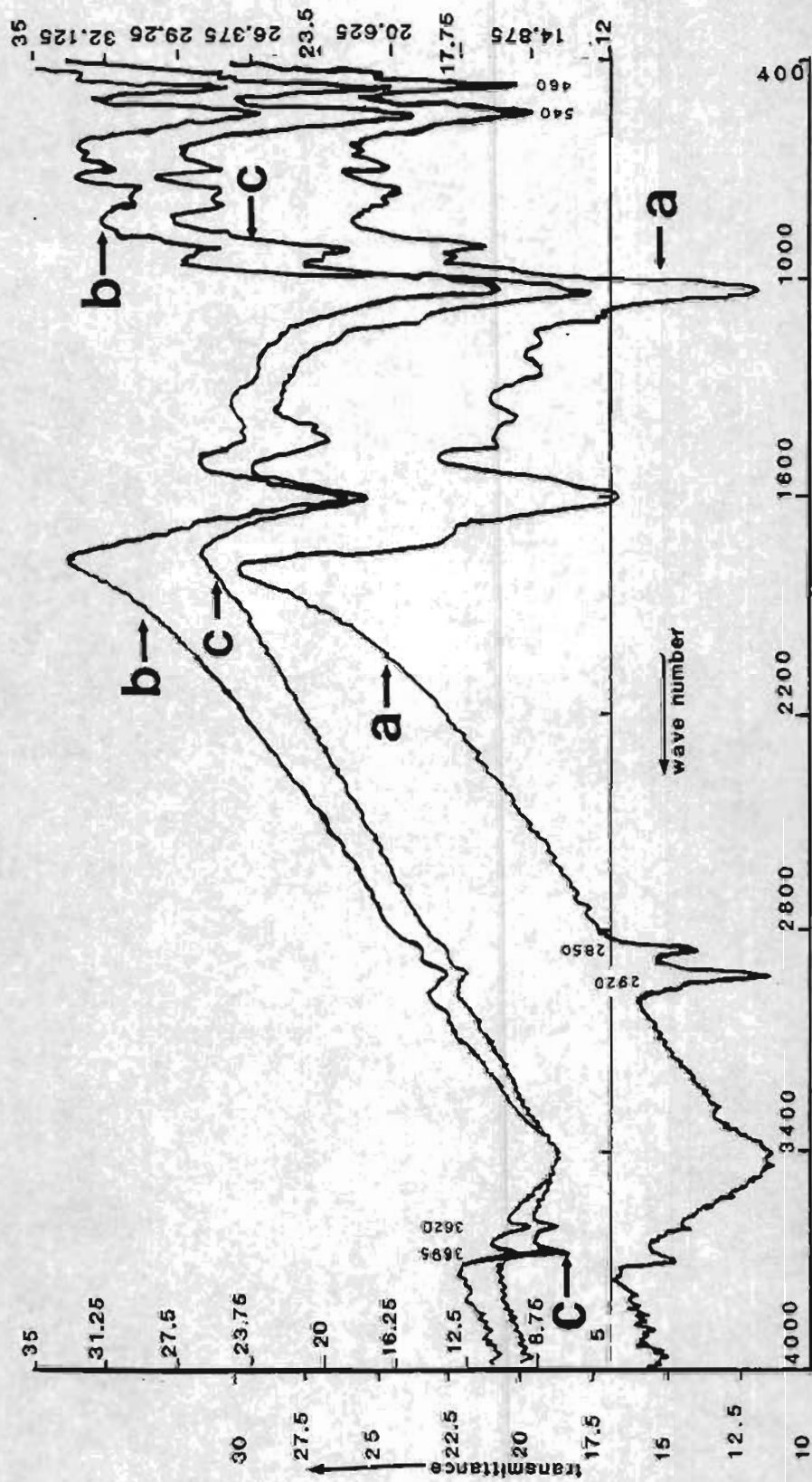


Figure 12. FTIR spectrogams: a. Inertinite enriched coal.  
 b. 0 minute residue.  
 c. 30 minute residue.

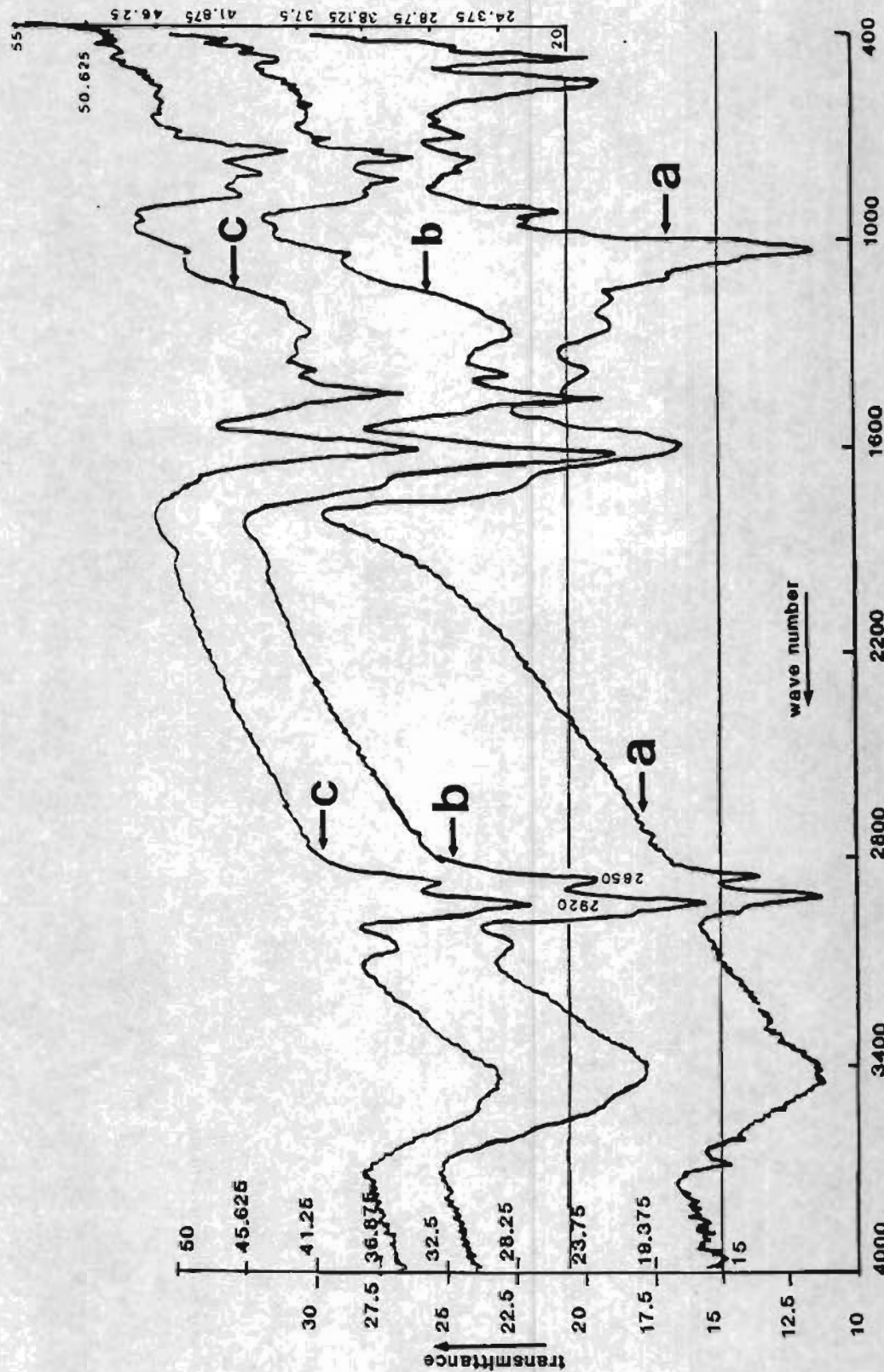


Figure 13. FTIR spectrograms: a. Inertinite enriched coal, b. 0 minute asphaltene, c. 30 minute asphaltene.

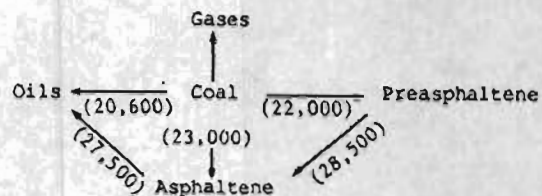


2620, 540 and 460 due to the increased concentration of kaolinite in the residues. Also, increasing in intensity is the strong band due partly to ether<sup>(84)</sup> occurring between 1100 and 1000  $\text{cm}^{-1}$ . Kaolinite may also contribute to the absorption of this band.

Figure 13 shows spectra of the enriched coal a and its 0 and 30 min. asphaltenes b and c respectively. Except for the variation in band intensities, the spectra b and c looks very similar. The prominent bands absent in the asphaltene spectra are obviously those due to kaolinite (at 3695, 540, and 460  $\text{cm}^{-1}$ ), alcohol and ethers (between 1100-1000  $\text{cm}^{-1}$ ). Further, the presence of stronger and narrower bands at 3030, 2920, 2850 and 1600  $\text{cm}^{-1}$  indicate that the asphaltenes, at least initially are enriched in species containing many aliphatic linkages. These absorptions mentioned above are noticeably stronger in the 0 min. asphaltene b than the 30 min. asphaltene c. It is probably because of the opportunity for Mo-initiated cracking reactions to occur at the longer residence time, converting asphaltene into oils<sup>(66)</sup> and yielding a lighter product.

Spectra in Figure 14 are those of enriched coal, its 0 min. and 30 min. preasphaltenes. Similar to the spectra of asphaltenes, the bands due to kaolinite (3695, 540 and 460  $\text{cm}^{-1}$ ) are absent. Other bands at 2920 and 2850  $\text{cm}^{-1}$  indicate the presence of aliphatic C-H,  $\text{CH}_2$  and  $\text{CH}_3$  groups. The strong absorbance at 1600  $\text{cm}^{-1}$  remains in all the three spectra with varying intensities due to polynuclear condensed aromatic nucleus containing  $\text{CH}_2$  groups in the rings<sup>(87)</sup> and/or donor-acceptor phenomena between the aromatic sheets of the molecule<sup>(88)</sup>. Further contributions to this band are from hydrocarbons, heteroatoms, aromatic structures, hydrogen bonded C=O, graphitic structures and water either bonded chemically or present physically<sup>(89)</sup>. It is a very commonly observed band in coal and exists in char even when the coal is pyrolysed to 800°C<sup>(90)</sup>. The broad band at 3400  $\text{cm}^{-1}$  is attributed to  $\text{H}_2\text{O}$  (hydrogen bonding) adsorbed by the KBr pellet. The bands due to the aliphatic and aromatic groups are stronger in the 30 min. preasphaltene c than in the 0 min. preasphaltene b indicating a greater concentration in the latter. This observation agrees with the yield profile given in Tables 6 and 7. The production of more asphaltenes and oils, as well as increased hydrogenation of preasphaltenes with residence time, supports the kinetic model proposed by Cronauer and Ruberto<sup>(66)</sup>.

#### 4. Cronauer and Roberto's Kinetic Model



The numbers in the parentheses are the activation energies (cal/g. mole) proposed by Cronauer et al. associated with each conversion. However, these numbers should be lower in our reactions since the cracking reactions are mediated by the Mo catalyst.

Figures 15a, b, c and d are the spectra of coal, its 30 min. residue, preasphaltene and asphaltene respectively. The spectra of the three primary heavy products for a single residence time are presented together to show clearly that the reaction data fits the Cronauer and Roberto's kinetic model.

Spectra a and b in Figure 16 are the enriched coal and low temperature ash (LTA). The main difference in the two spectra is the disappearance of the bands at 2920 and 2850  $\text{cm}^{-1}$  and the reduced intensities of the band at 1600  $\text{cm}^{-1}$ . The existence of this band in coal residues pyrolysed up to 800°C is well known and has been mentioned earlier. Although some organic groups like esters and alcohols may contribute to the strong absorption between 1100-1000  $\text{cm}^{-1}$ , its increased intensity in LTA is evidence that the absorption is mainly due to the increased concentration of mineral matter, especially kaolinite (1025 and 1000  $\text{cm}^{-1}$ ). Kaolinite also has characteristic bands at 3695 and 3620  $\text{cm}^{-1}$ , as shown in the increased intensity in the LTA. Mukherjee et al.<sup>(91)</sup> have reported that kaolinite acts as a catalyst in the liquefaction reaction.

Figure 17 is the x-ray diffraction spectrum of LTA. It confirms the presence of kaolinite since the peak at 7.16 Å (Table 10c) disappeared when the sample was heated to 550°C. Under these conditions kaolinite decomposes into amorphous meta kaolinite which is not detectable by XRD. The presence of quartz was also easily determined by XRD as an intense peak was observed at 3.3 Å (Figure 17).

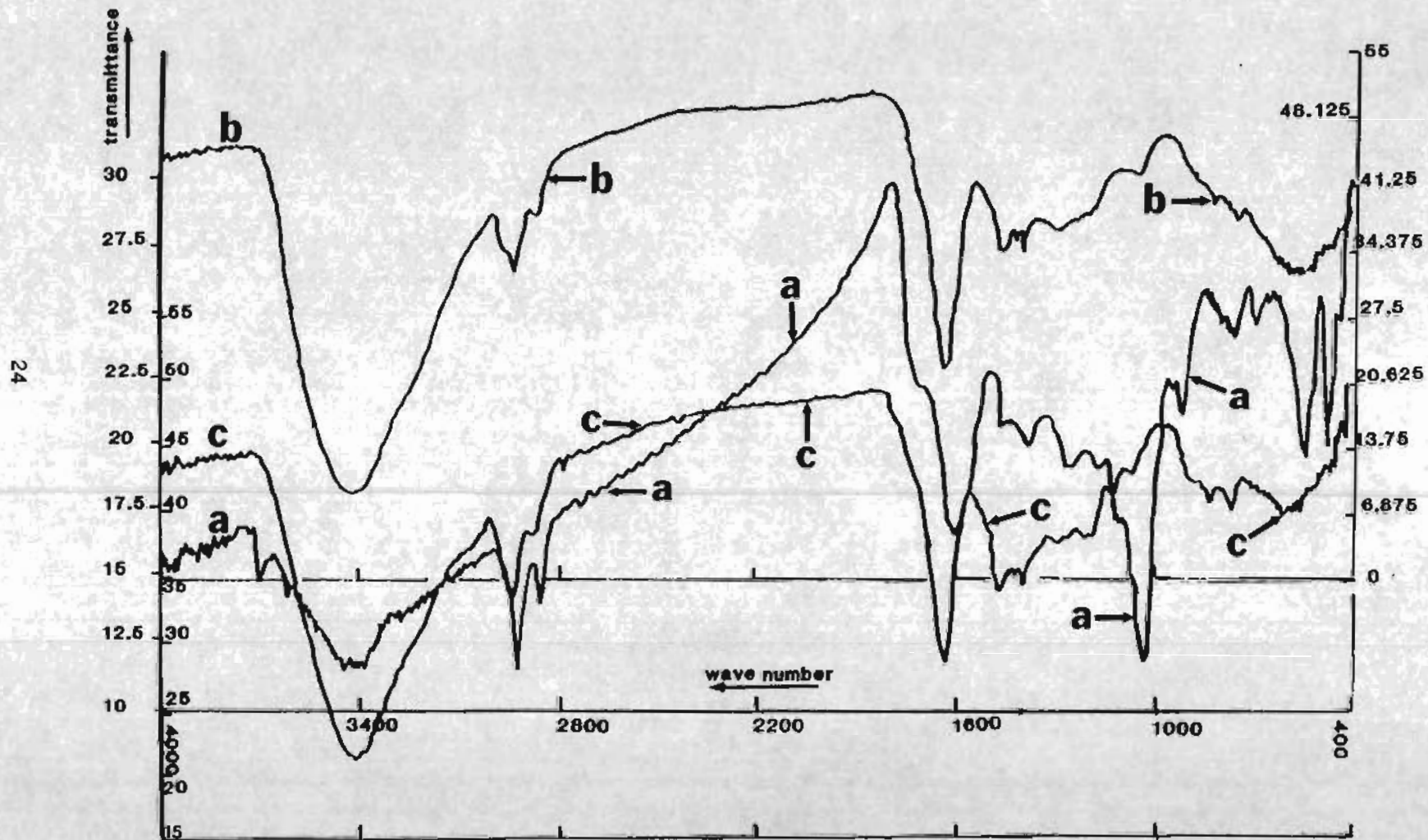


Figure 14. FTIR spectrograms: a. Inertinite enriched coal, b. 0 min. preasphaltene, c. 30 min. preasphaltene.

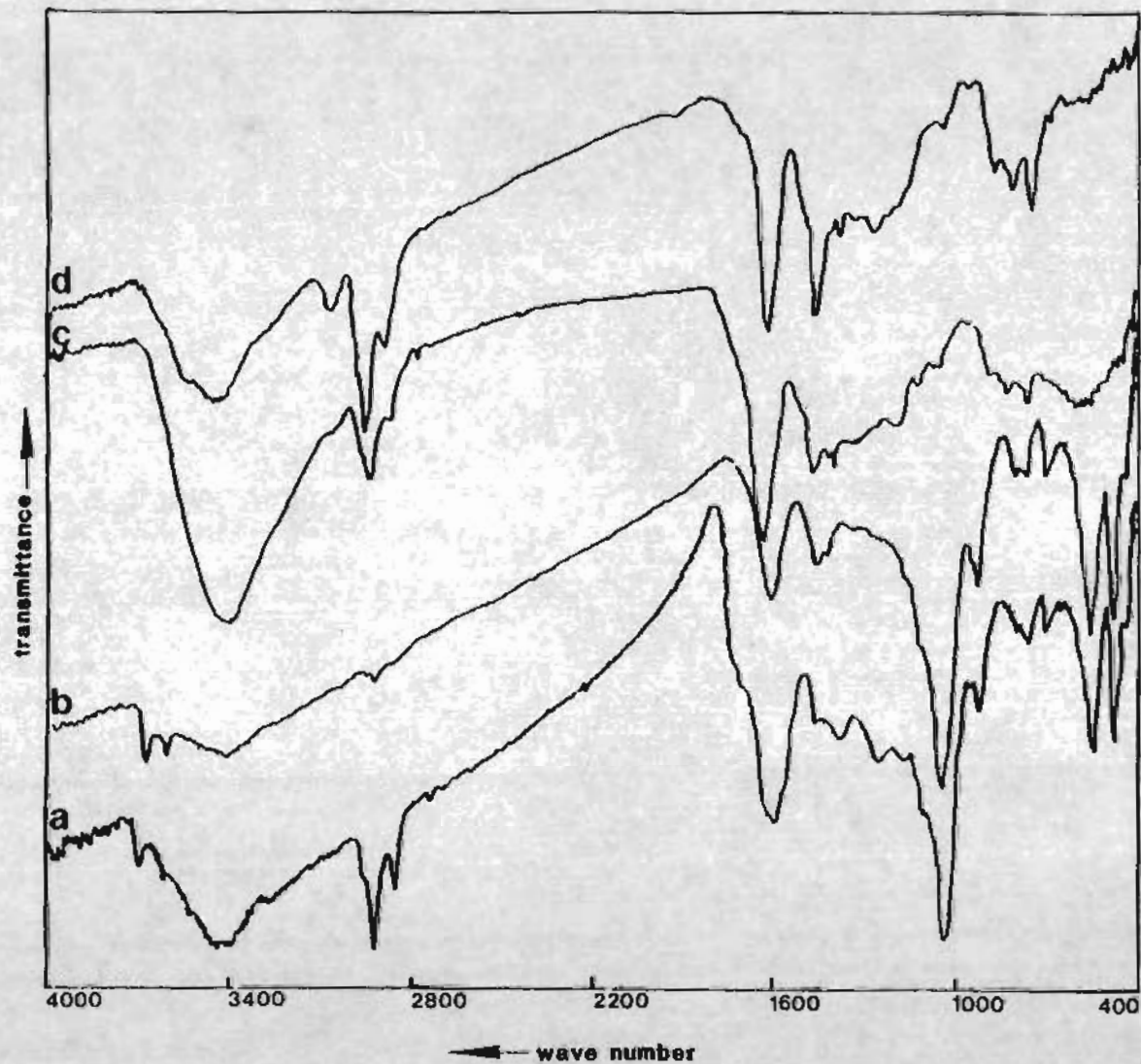


Figure 15.

FTIR spectrograms:

- a. Inertinite enriched coal.
- b. 30 minute residue.
- c. 30 minute pre-asphaltene.
- d. 30 minute asphaltene.

Note: A medium intensity peak at  $1383\text{ cm}^{-1}$  which is uncharacteristic of pre-asphaltenes (impurity) was subtracted from spectra c.

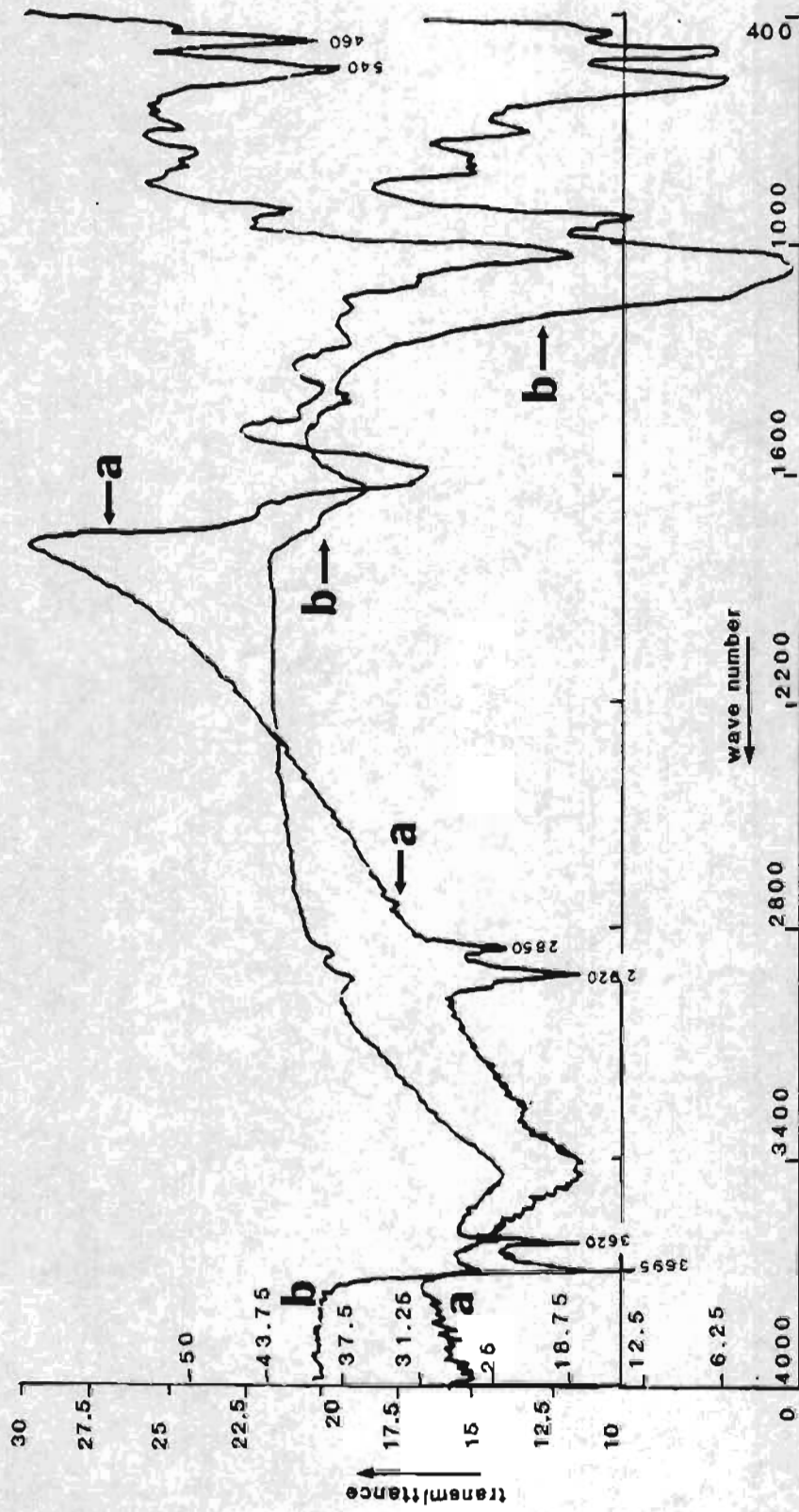


Figure 16. FTIR spectrograms: a. Inertinite enriched coal. b. Low temperature ash (LTA).

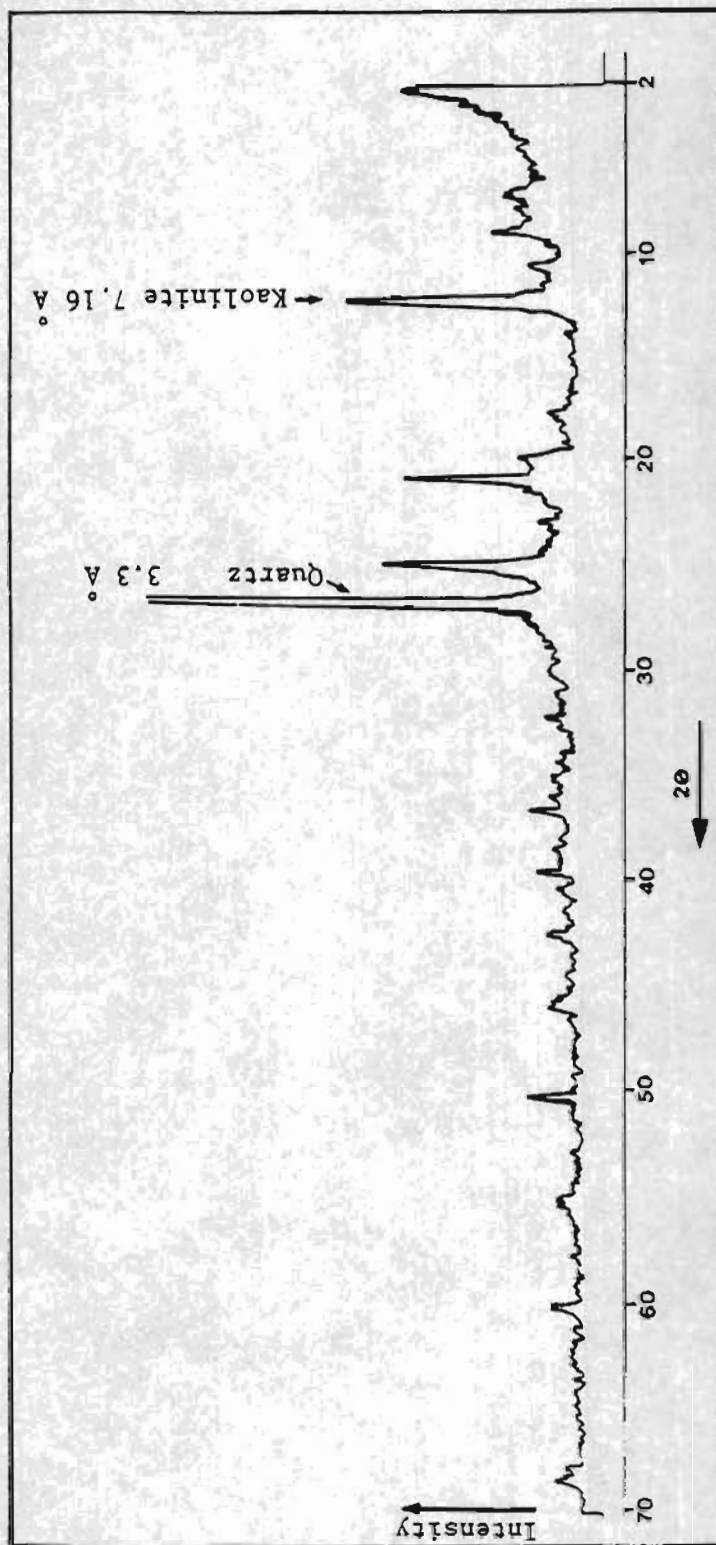


Figure 17. X-ray diffraction spectrum of Low temperature ash (LTA).

## CHAPTER 4

### 1. Chemical Class Separation and Characterization of Organic Compounds in Oil/Tar

Since the nature of the liquid fuels derived from coal is complex, several groups of research workers have developed different schemes to separate and identify their components. But in all these methods the common factor is the first step which involves the fractionation according to chemical class. The most common procedure adopted to obtain the different chemical classes is either solvent partitioning and/or column chromatography. The National Bureau of Standards<sup>(92)</sup> have developed a solvent extraction procedure in conjunction with high performance liquid chromatography (HPLC) and GC to separate neutral oils, acids and bases.

The method developed by Oak Ridge Laboratory<sup>(93,94,95)</sup> involved fractionation by an acid-base extraction and subsequent solid-liquid chromatography on Sephadex LH-20, silicic acid and basic alumina. By this method they were able to separate aliphatic and aromatic hydrocarbons along with heterocyclic and polar aromatic compounds. Wilson et al.<sup>(96)</sup> have used the above scheme in the analysis of coal liquefaction products, before and after hydrotreatment, to report neutral polycyclic aromatic hydrocarbons (PAH) and heterocyclic aromatic compounds.

Farcasiu<sup>(97)</sup> of the Mobil Research and Development Corporation has isolated nine fractions from solvent refined coal (SRC) using activated silica gel as the solid support. The order of the eluotropic series that she has followed is rather unusual in the sense that the more polar solvents are used in the middle of the series instead of at the end. However, she was able to characterize aliphatic, aromatic and heterocyclic components of SRC.

Mudamburi and Given<sup>(61)</sup>, using an elution series of 1) hexane, 2) toluene, 3) chloroform and 4) methanol with acidic alumina (solid support), have separated 1) alkanes, 2) aromatic hydrocarbons, 3) ethers, benzologs and bases and 4) phenols, respectively, from the hexane solubles (oils) obtained from hydroliquefaction of different coals. However, they had to distill off hexane, tetralin and naphthalene before obtaining the oils.

Schiller and Mathison<sup>(98)</sup>, using neutral alumina, have fractionated solids and liquids derived from coal. They employed mass spectroscopy with other methods to identify saturated and aromatic hydrocarbons, ethers, benzofurans, nitrogen and hydroxyl compounds. Another method known as SARA<sup>(99)</sup> technique has often been used to identify components in petroleum distillates and also in coal derived products.

In all the above mentioned methods the schemes are tedious, time consuming and complex, requiring highly

trained personnel. In some of the methods the materials used are expensive and require large quantities of high purity solvents. Tar emulsification can occur, components can be lost during solvent removal, and inefficient separation in the case of certain solvent extraction schemes and partitioning of polar compounds<sup>(100)</sup> can lead to overlapping of compound types.

The method developed by Later et al.<sup>(62)</sup> (Figure 18) seems to minimize the aforementioned problems. Their procedure can be performed in 6-8 hours and requires less than 1g of substrate and 500 ml of solvents. This procedure was demonstrated using an SRC II heavy distillate sample (BP range 260-450°C) derived from West Virginia coal of the Pittsburgh Seam<sup>(62)</sup>. The oil/tar obtained from direct catalytic liquefaction of inertinite rich Alaskan bituminous coal in this work was chemically characterized using the method developed by Later et al.<sup>(62)</sup>. However, since the enriched coal contained very small quantities of sulfur, the step involving the separation of sulfur compounds from the A-2 fraction was not followed.

### 2. Column Chromatography Procedure

Approximately 0.3 g of the oil/tar was dissolved in 3 ml of chloroform and adsorbed on to 3 g of alumina (neutral aluminum oxide, Brockman Activity I 20-200 mesh, Fisher No. A 950). The slurry was vigorously stirred under a steady stream of nitrogen. When all the chloroform was evaporated, a brownish yellow, powdery product was obtained. This sample was packed on top of a 11 mm internal diameter column containing 6 g of neutral alumina. Care was taken to eliminate any air bubbles when packing the column with the alumina hexane slurry. The sample was eluted with 40 ml of hexane (to obtain fraction A-1, aliphatic hydrocarbons) followed by 75 ml benzene (fraction A-2, neutral polycyclic aromatic compounds), 90 ml of chloroform preserved with 0.75% ethanol (fraction A-3, nitrogen polycyclic aromatic compounds). And, finally, 75 ml of THF (without any inhibitors) with 7.5 ml or 10% ethanol (fraction A-4, hydroxyl polycyclic aromatic hydrocarbons).

The benzene eluate, fraction A-2, was not subjected to the separation of polycyclic aromatic sulfur heterocycles (PASH) as the concentration of sulfur in the enriched coal was very low (0.24%). Further, in the amount of sample taken (0.3 g), the concentration of sulfur in the form of PASH becomes almost negligible. Therefore, fraction A-2 was analyzed for only neutral polyaromatic hydrocarbons (PAH) by GC-MS and capillary GC.

Fraction A-3, the chloroform-ethanol eluate containing nitrogen polycyclic aromatic hydrocarbons (N-PAC) was adsorbed on to 0.5 g silicic acid (100 mesh, Aldrich) and the solvent was removed by stirring the mixture under a steady stream of nitrogen. A light yellowish powdery product was obtained. This was packed on top of a 22 mm internal diameter column containing 2 g of silicic acid slurried with hexane. Again, care was taken to get rid of any air bubbles.

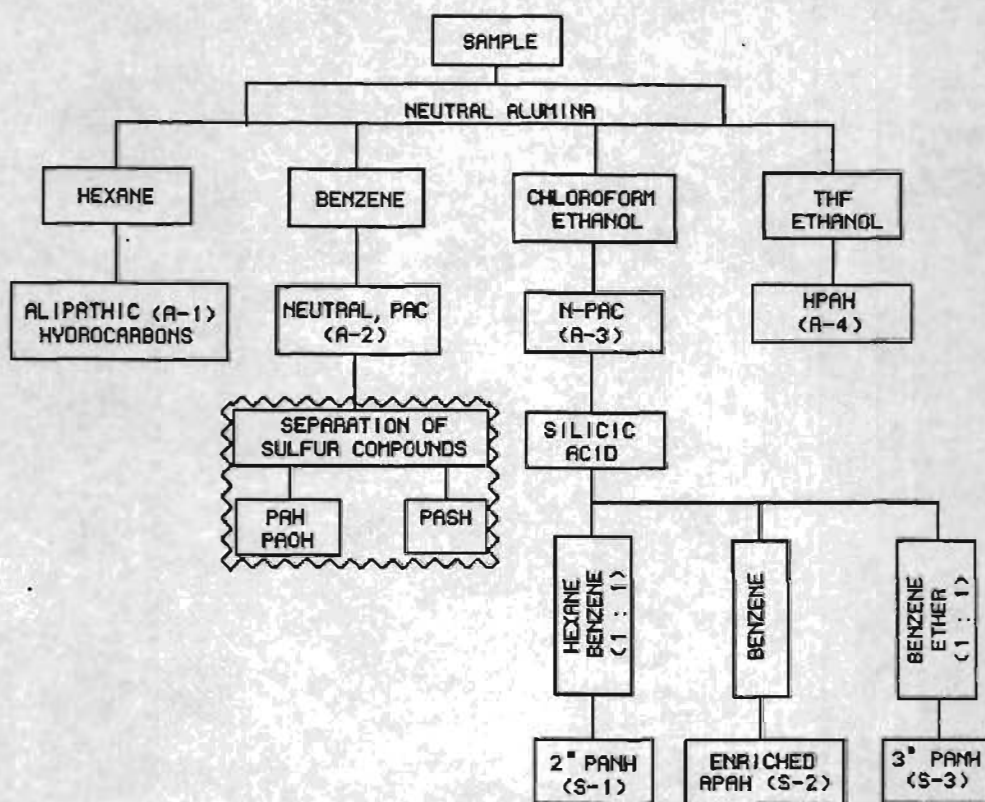


Figure 18. Flow diagram for chemical class separation of hexane solubles (oils/tar).

- PAC: Polycyclic Aromatic Compounds..
- N-PAC: Nitrogen Polycyclic Aromatic Compounds
- HPAH: Hydroxyl Polycyclic Aromatic Hydrocarbons.
- PAH: Poly Aromatic Hydrocarbons.
- PAOH: Polycyclic Aromatic Oxygen Heterocycles.
- PASH: Polycyclic Aromatic Sulfur Heterocycles.
- 2°PANH: Secondary Polycyclic Aromatic Nitrogen Heterocycles.
- 3°PANH: Tertiary Polycyclic Aromatic Nitrogen Heterocycles.
- APAH: Amino Polycyclic Aromatic Hydrocarbons.

Note: Separation of sulfur compounds from A-2 fractions was not followed because of the low concentration of sulfur in the inertinite enriched coal and also sulfur tends to concentrate in char (Table VIII, Appendix A).

The silicic acid column was eluted to obtain fractions S-1, S-2 and S-3 with 75 ml of 1:1 (V:V) hexane-benzene, 50 ml of benzene and 75 ml of 1:1 (V:V) benzene-anhydrous ether respectively. The S-1 fraction was analyzed for secondary nitrogen polycyclic aromatic compounds (2°-PAH), while S-2 and S-3 were analyzed for enriched amino polycyclic aromatic hydrocarbons (APAH) and tertiary nitrogen polycyclic aromatic heterocycles (3°-PAH) respectively. Before the GC-MS and capillary GC analyses, the various fractions (A-1, A-2, A-4 and S-1, S-2, S-3) were concentrated to about 2 ml with a rotary evaporator in a tared flask and finally dried under a steady stream of nitrogen. The weight of the dry mass was determined and dissolved in appropriate volumes of benzene. The solvents used were HPLC grade while the solid supports, neutral alumina and silicic acid were used as received from the supplier.

### 3. Results and Discussion

Tables 11 and 12 show the wt % composition of different compound types in the hexane solubles (oils/tars) resolved using neutral alumina and silicic acid respectively. Since Later et al.'s procedure yielded lower recovery (80-85% wt), two modifications were adopted. They were: 1) larger amounts of solvents were used; 2) the solid supports, neutral alumina and silicic acid, were refluxed with MeOH to recover the compounds that were not removed by the THF/MeOH mixture and benzene/ether mixture during the regular elution; 3) the step involving the benzene eluate (A-2) containing neutral PAC to separate PASH from PAH and PAOH was not followed due to reasons mentioned earlier.

### 4. Hexane Eluate (A-1), Aliphatic Hydrocarbons

As non-polar hydrocarbons, the n-aliphatics were easily stripped with hexane. Figure 19 shows the capillary GC profile of n-aliphatics present in the hexane eluate (A-1).

The chromatogram was obtained on a Hewlett-Packard gas chromatograph HP model 5890. The retention times corresponding to the different n-aliphatic carbons are labeled under each peak. These retention times were determined on the basis of retention times of standard n-hydrocarbon homologous ranging from C<sub>7</sub> to C<sub>25</sub>. The base line in Figure 19a is less ragged probably due to lower concentrations of olefins and branched isomers of the original (parent) straight chain alkanes. The chromatogram was attenuated to show pristane and phytane peaks, consequently the more abundant alkanes C<sub>14</sub> to C<sub>25</sub> were truncated. Another chromatogram of the hexane eluate A-1 was rerun at a later date at the Institute of Marine Science (IMS) hydrocarbon laboratory at UAF on a similar instrument with the same column packing (DB-5) but slightly shorter length and a higher attenuation to keep the alkane peaks on scale. As expected, a smooth envelope with a maximum at C<sub>18</sub> was obtained, Figure 19b. On the basis of peak heights, which are proportional to concentration, the carbon preference index (CPI)<sup>(101,102,103,104)</sup> between C<sub>16</sub>-C<sub>32</sub> is found to be approximately equal to unity, indicating an excellent grade of crude oil.

$$CPI^* = \frac{1}{2} \left( \frac{\sum(C_{17} \text{ to } C_{31})}{\sum(C_{16} \text{ to } C_{30})} + \frac{\sum(C_{17} \text{ to } C_{31})}{\sum(C_{18} \text{ to } C_{32})} \right) = 1.04$$

\*(see Appendix C)

The CPI yields information regarding the relative maturities of coals and crude oils. When the CPI of the n-alkane content in a given specimen such as bitumen from coal or shale is equal to unity, it approaches the characteristics of a typical crude oil. The CPI of the hexane solubles (oil/tar) obtained by catalytic hydrogenation in this work was found to be approximately equal to unity, hence its characteristics should be similar to crude oil in terms of alkane distribution.

Table 11  
Percent wt of neutral alumina fractions of hexane solubles (oils/tar)

Fraction	Compound Type	% wt'
A-1	Aliphatic hydrocarbons	10.21
A-2	Neutral PAC	32.02
A-3	N-PAC	7.03
A-4	HPAH	26.22
A-5	Column clean out (alumina) with MeOH	6.52
		82.00

Table 12  
Fractions from silicic acid

Fraction	Compound Type	% wt*	% wt of Hexane solubles
S-1	2° PANH	49.03	3.45
S-2	Enriched APAH	16.99	1.19
S-3	3° PANH	14.08	0.99
S-4	Column clean out (silicic acid) with MeOH	1.46	0.10
		81.56	5.73

\* Average of two runs



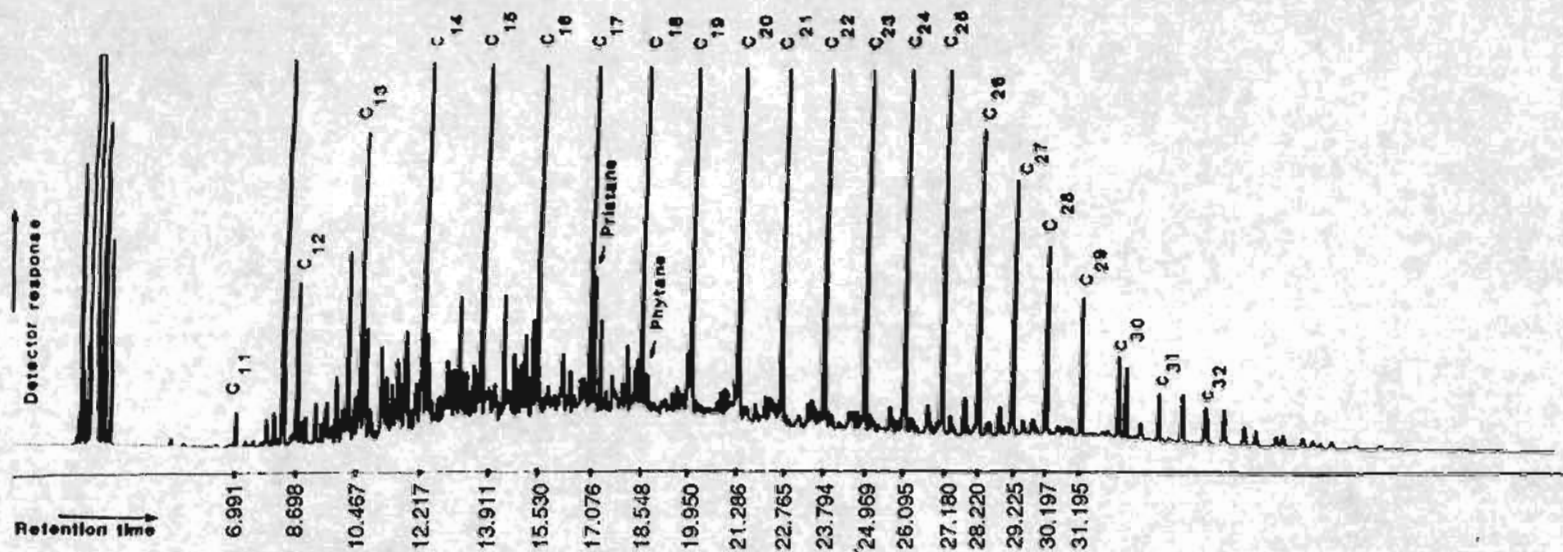


Figure 19a. Capillary GC profile of aliphatic hydrocarbons of fraction A-1. Compounds are listed in Table 13. The chromatogram was obtained using a 60m x 0.25mm fused silica capillary column DB-5 (25 micron film, 5% Me and 95% Phenyl silicone). Temperature program: 80°C to 320°C at 8°C/min. (FID). Note: To identify pristane and phytane, the attenuation was lowered. The lower attenuation truncated the peaks C<sub>14</sub> - C<sub>25</sub>. The chromatogram was obtained on a Hewlett-Packard instrument, HP model 5890.

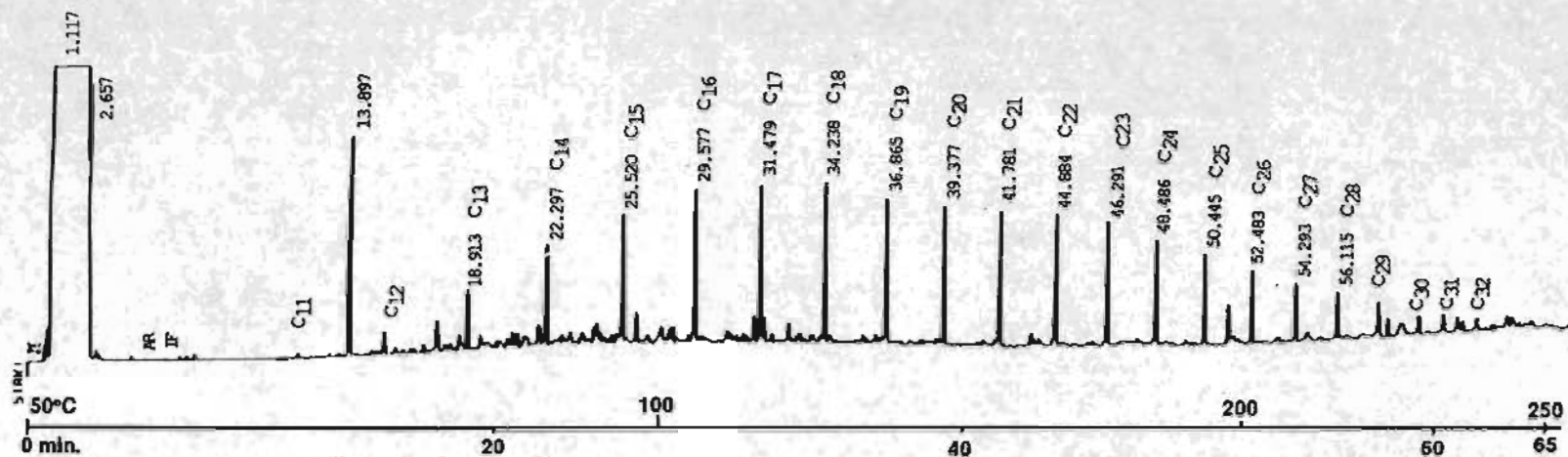


Figure 19b. Capillary GC profile of aliphatic hydrocarbons of fraction A-1 at higher attenuation. A smooth envelope maximizing at C<sub>18</sub>. The chromatogram was obtained on a similar instrument as in Figure 19, with the same column packing (DB-5) but shorter length. Temperature programmed from 50°C to 300°C at 4°C/min. after 2 min. isothermal period (FID).

The isoprenoid hydrocarbons  $C_{19}$  and  $C_{20}$  are pristane and phytane respectively. These are usually present in any coal's alkanes. Their precursor is phytol, which is a  $C_{20}$  side chain of chlorophylls. During coalification, depending upon the oxidation potential of the coal facies, phytol is either oxidized to phytanic acid, which decarboxylates to pristane, or is reduced to phytane<sup>(105)</sup>. Thus, by knowing  $r$ , the pristane to phytane ratio, it is possible to surmise the depositional environment of the coal. Since  $r$  was about 4.25 (see Appendix C), the oxidative potential of the coal facies must have been predominantly oxidizing.

The n-alkanes identified in the hexane eluate (A-1) are listed in Table 13. The other fractions, viz. A-2, A-4, S-1, S-2, and S-3, were analyzed using a Hewlett-Packard (HP) 5970 mass selective detector operated at 70 eV electron beam energy in conjunction with HP 5890 gas chromatograph fitted with a 12 m x 0.2 mm i.d. fused silica column coated with a 0.33 micron film of cross linked polymethyl siloxane stationary phase (SB-phenyl-5). The GC profiles of the above mentioned fractions were obtained by splitless injection into a HP 5880 gas chromatograph which was also fitted with the same kind of column as mentioned above.

Table 13  
n-Aliphatic hydrocarbons in fraction A-1

Peak No.	Mol. Wt.	Compound
$C_{11}$	156	n-Hendecane
$C_{12}$	170	n-Dodecane
$C_{13}$	184	n-Tridecane
$C_{14}$	198	n-Tetradecane
$C_{15}$	212	n-Pentadecane
$C_{16}$	226	n-Hexadecane
$C_{17}$	240	n-Heptadecane
$C_{18}$	254	n-Octadecane
$C_{19}$	268	n-Nonadecane
$C_{20}$	282	n-Eicosane
$C_{21}$	296	n-Heneicosane
$C_{22}$	310	n-Docosane
$C_{23}$	324	n-Tricosane
$C_{24}$	338	n-Tetracosane
$C_{25}$	352	n-Pentacosane
$C_{26}$	366	n-Hexacosane
$C_{27}$	380	n-Heptacosane
$C_{28}$	394	n-Octacosane
$C_{29}$	408	n-Nonacosane
$C_{30}$	422	n-Triacontane
$C_{31}$	436	n-Hentriacontane
$C_{32}$	450	n-Dotriacontane

## 5. Benzene Eluate (A-2), Neutral PAC

Figure 20 shows the capillary GC profile of A-2 and the chromatographic conditions. In an earlier attempt the peaks of four membered ring compounds like pyrene and fluoranthene were hard to identify in the chromatogram due to their low concentration. Concentration of the sample was required to obtain discernable peaks. This observation is consistent with the results obtained by  $HNO_3$  oxidation, which showed that the predominant part of the coal structure did not exceed a degree of condensation of three rings, and is concordant with the average structure of young, high volatile bituminous/subbituminous coal. Besides containing a comparatively high concentration of PAH compounds similar to SRC<sup>(62,106)</sup> and coal extracts<sup>(107)</sup>, the A-2 fraction of hexane solubles was also found to contain a large amount of alkylated PAH.

Although the sample used by Later et al.<sup>(62)</sup> was a solvent refined coal obtained from the Pittsburgh Seam of West Virginia Coal, almost all the compounds reported by them were identified in the hexane solubles (oils/tar) in this work. This is probably because both the feed coals were of the same rank (high volatile bituminous) despite their different origin. Table 14 lists the PAC compounds identified in the A-2 fraction. Because of the relatively polar nature of solvent benzene, heterocyclic oxygen compounds like dibenzofuran and its homologous were also eluted in the A-2 fraction.

## 6. Chloroform-Ethanol Eluate (A-3), N-PAC

The dark band eluted from alumina by chloroform-ethanol, A-3, was the smallest at 7.03% wt (Table 11). This A-3 fraction was further separated into S-1, S-2 and S-3 containing secondary ( $2^\circ$ PANH), primary (APAH) and tertiary ( $3^\circ$  PANH) nitrogen heterocyclic compounds. Although a total of 28 peaks were identified in the S-1, S-2 and S-3 fractions, there were quite a few product overlaps among the fractions. With respect to the wt % of hexane solubles, the fraction S-1 (hexane-benzene eluate) was the most concentrated of the nitrogen containing fractions at 3.45% wt; fraction S-2 (benzene eluate) was the next at 1.19% wt and S-3 (benzene ether eluate) was the least at 0.99% wt (Table 12). The fraction from column clean up which accounted for 0.1% wt of hexane soluble was not analyzed. The compounds identified in fraction S-1, S-2 and S-3 are listed in Tables 15, 16 and 17, respectively, and their chromatographic profiles are shown in Figures 21, 22 and 23, respectively.

## 7. Ethanol-THF Eluate (A-4), HPAH

The last fraction, A-4, eluted from neutral alumina using 10% ethanol with tetrahydrofuran (THF) were HPAH. They were the second most concentrated class of chemicals (26.22% wt). Although phenols (the acidic oxygen components) have been analyzed in synthetic fuels<sup>(108,109,110,111)</sup>,

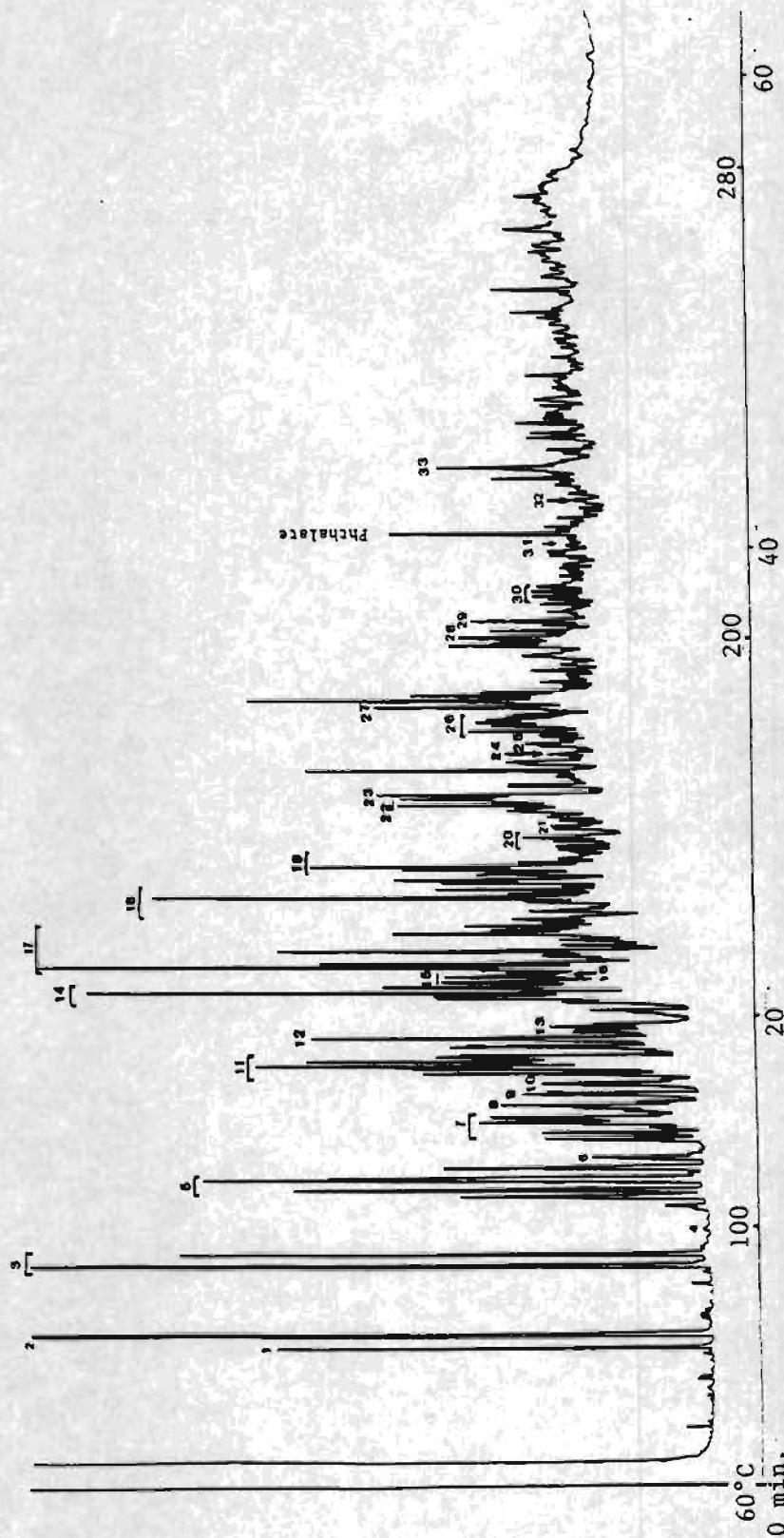


Figure 20. Capillary GC profile of neutral polycyclic aromatic compounds of fraction A-2. Peak numbers correspond with compounds listed in Table 14. The chromatogram was obtained using a 12m x 0.2mm fused silica capillary column SB-Phenyl-5 coated with 33 micron film. The temperature was programmed from 60°C to 280°C at 4°C/min. after a 1 min. isothermal period (FID).

Table 14

Polycyclic aromatic compounds in fraction A-2		
Peak Number	Mol. Wt.	Compound
1	132	tetrahydronaphthalene
2	128	naphthalene
3	142	C <sub>1</sub> -naphthalenes
4	154	diphenyl
5	156	C <sub>2</sub> -naphthalenes
6	168	dibenzofuran
7	170	C <sub>1</sub> -naphthalenes
8	166	fluorene
9	168	C <sub>1</sub> -biphenyl
10	182	C <sub>1</sub> -dibenzofuran
11	182	C <sub>1</sub> -biphenyls
12	180	dihydroanthracene
13	180	C <sub>1</sub> -fluorene
14	180	C <sub>2</sub> -biphenyls
15	196	C <sub>1</sub> -biphenyls
16	178	phenanthrene
17	196	C <sub>1</sub> -biphenyls
18	192	C <sub>1</sub> -phenanthrenes
19	—	not identified
20	206	C <sub>1</sub> -phenanthrenes
21	202	fluoranthene
22	208,222	C <sub>1</sub> ,C <sub>2</sub> -fluorenes
23	202	pyrene
24	216	benzo (a) fluorene
25	216	benzo (b) fluorene
26	216	C <sub>1</sub> -pyrene and/or C <sub>1</sub> -fluoranthene
27	232	tetrahydrobenz (a) anthracene
28	228	benz (a) anthracene
29	228	chrysene
30	242	C <sub>1</sub> -benz (a) anthracene and/or C <sub>1</sub> -chrysene
31	256	C <sub>1</sub> -benz (a) anthracene and/or C <sub>1</sub> -chrysene
32	252	benzofluoranthene
33	252	benzopyrene

Table 15

## Secondary nitrogen polycyclic aromatic heterocycles (2° PANH), in fraction S-1

Peak Number	Mol. Wt.	Compound
1	145	C <sub>2</sub> -indole
2	159	C <sub>3</sub> -indole
3	186	octahydrophenanthrene
4	167	4-azafluorene
5	182	C <sub>2</sub> -biphenyl
6	178	phenanthrene
7	179	benzoquinoline
8	167	carbazole
9	181	C <sub>1</sub> -carbazole
10	195	C <sub>2</sub> -carbazole
11	209	C <sub>3</sub> -carbazole
12	223	C <sub>4</sub> -carbazole

Table 16

## Amino polycyclic aromatic hydrocarbons (APAH) in fraction S-2

Peak Number	Mol. Wt.	Compound
1	179	benzo (h) quinoline*
2	196	xanthone
3	193	C-1 benzoquinoline
4	193	amino anthracene/ amino phenanthrene
5	208	9, 10 phenanthrene-dione
6	207	C-2 benzoquinoline
7	221	C-3 benzoquinoline
8	235	C-4 benzoquinoline
9	233	Tetrahydro- naphthoquinoline
10	229	naphthoquinoline

\* Compound identified by retention time.

Table 17

## Tertiary nitrogen polycyclic aromatic heterocycles (3° PANH), in fraction S-3

Peak Number	Mol. Wt.	Compound
1	197	C <sub>1</sub> -tetrahydroquinoline
2	193	C <sub>1</sub> -benzoquinoline
3	207	C <sub>2</sub> -benzoquinoline
4	221	C <sub>3</sub> -benzoquinoline
5	203	azapyrene
6	217	C <sub>1</sub> -azapyrene and/or C <sub>1</sub> -azafluoranthene

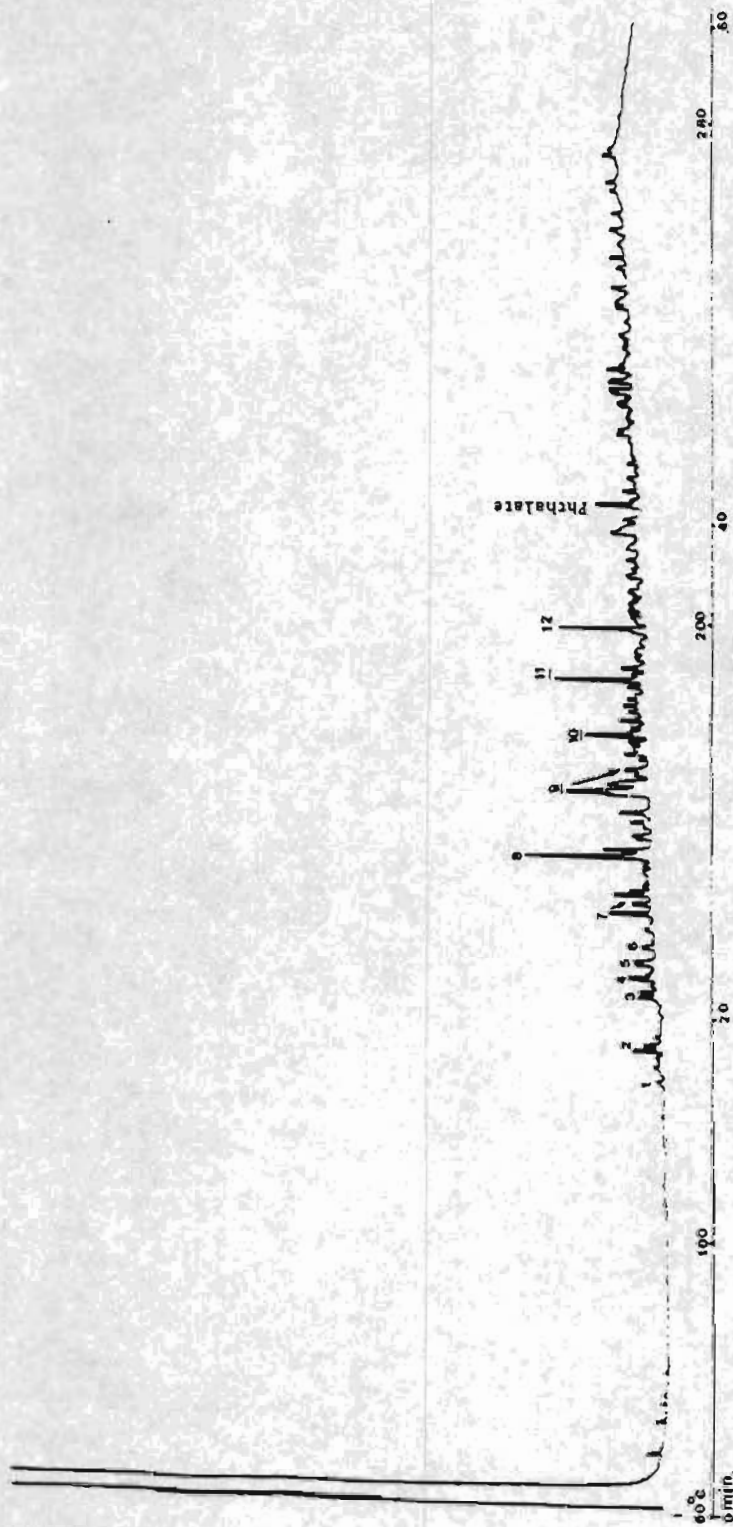


Figure 21. Capillary GC profile of secondary nitrogen polycyclic aromatic heterocycles of fraction S-1. Conditions were as in Figure 20. Compounds identified are listed in Table 15.

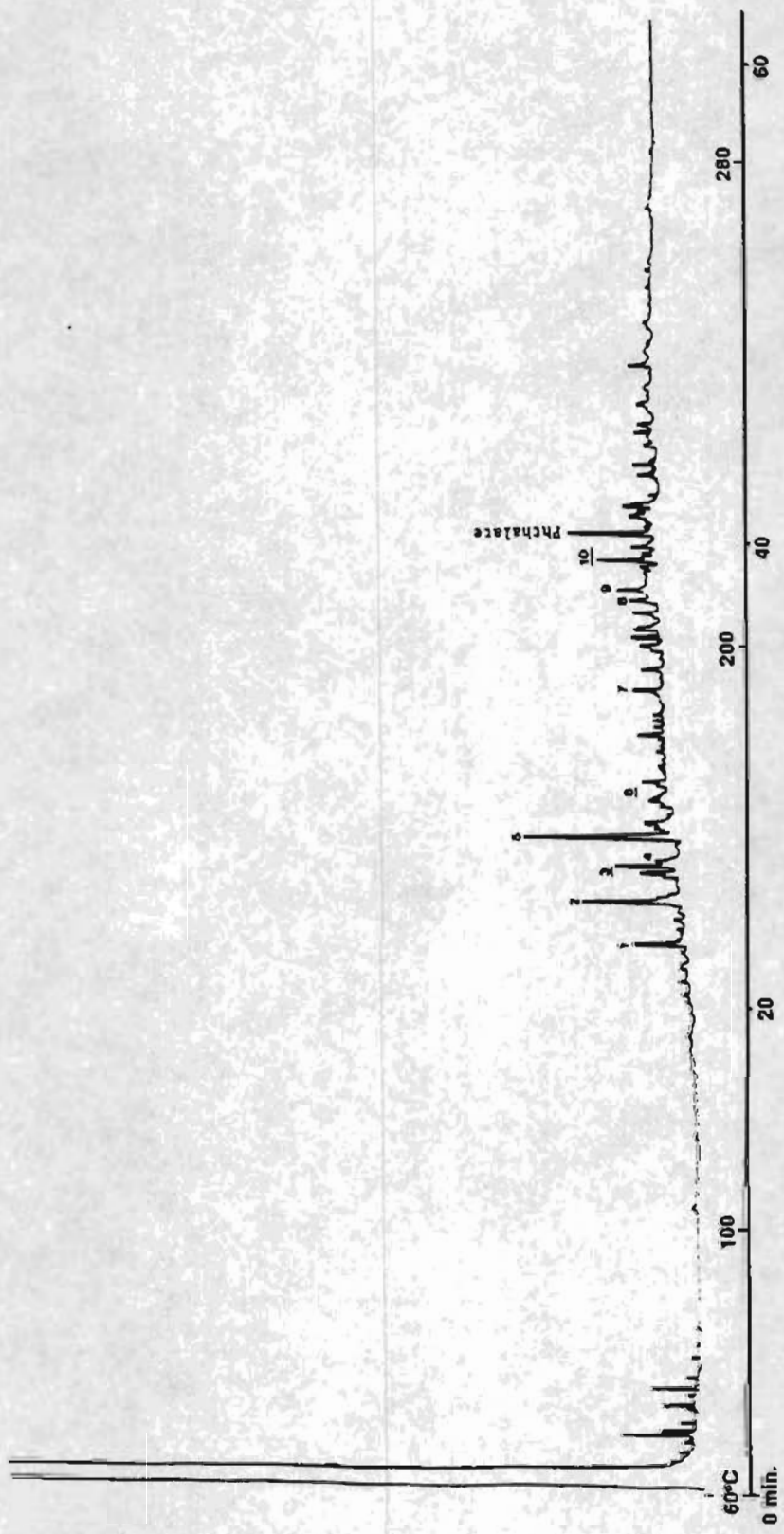


Figure 22. Capillary GC profile of amino polycyclic aromatic hydrocarbons of fraction S-2. Conditions were as in Figure 20. Compounds identified are listed in Table 16.

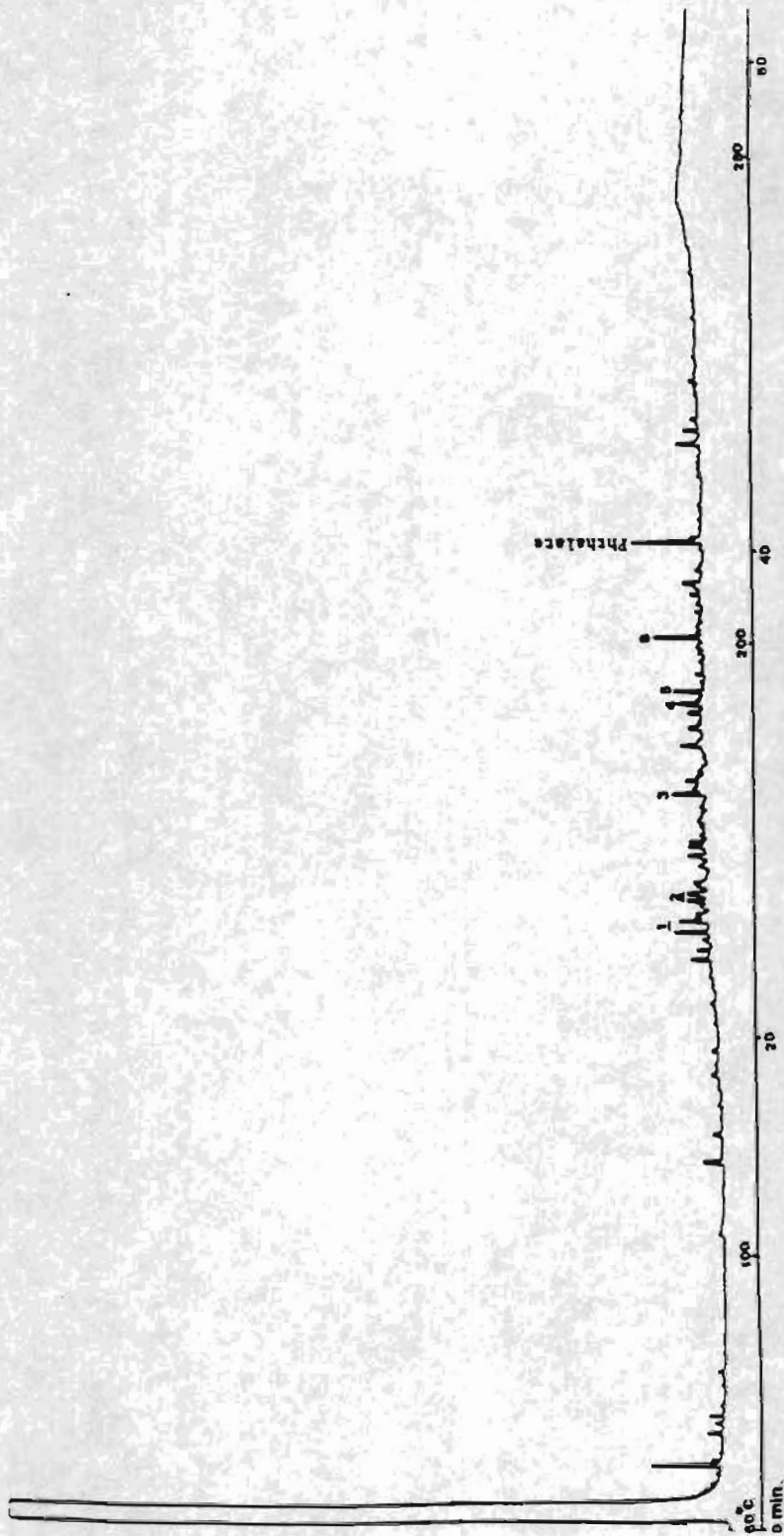


Figure 23. Capillary GC profile of tertiary nitrogen polycyclic aromatic heterocycles of fraction S-3. Conditions were as in Figure 20. Compounds identified are listed in Table 17.



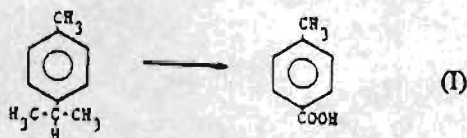
their exact role in direct liquefaction reactions have not been fully understood. They have been used as solvents in the conversion of low rank coals into liquid fuels (ChemCoal Process)<sup>(112,113)</sup>. The adverse effects of phenols and other oxygen containing cyclic aromatic compounds is well known in coal liquefaction for the consumption of hydrogen (eg.  $\phi\text{OH} + \text{H} \rightarrow \phi + \text{H}_2\text{O}$ ). Economically, conversion of phenols into hydrocarbon in coal liquids is not rewarding on two counts: 1) they consume hydrogen, and 2) the price of phenol is about twice that of benzene<sup>(114)</sup>. Removal of phenols and pentadines<sup>(114)</sup> from synfuels is, however, necessary since they have been shown to be the culprits in retrograde reactions leading to aging<sup>(115,116)</sup>. Phenols are toxic and hence it is very desirable to separate them from synfuels to obtain a more environmentally acceptable product. Figure 24 shows the chromatographic profile of fraction A-4 and Table 18 shows the compounds identified in the fraction.

## 8. Nitric Acid Oxidation

Although nitric acid oxidation is not as selective as aqueous  $\text{Na}_2\text{Cr}_2\text{O}_7$  oxidation, it is often used in estimating the degree of condensation in coal and its products<sup>(117,118)</sup>. In this study only the inertinite enriched coal was subjected to  $\text{HNO}_3$  oxidation to determine its degree of condensation.

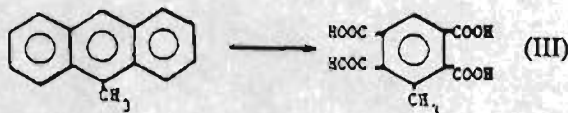
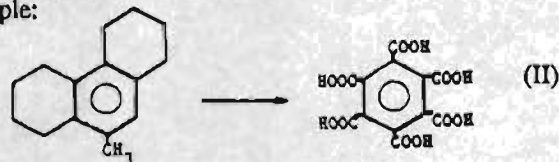
The action of  $\text{HNO}_3$  is rather drastic and produces benzene carboxylic acids from polymers containing aromatic (benzene) units. It has been shown<sup>(119)</sup> that the aliphatic groups larger than methyl are easily converted into carboxylic (COOH) groups.

Example:

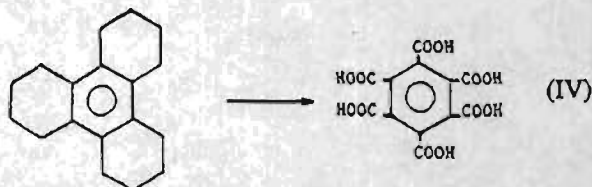


Also, alicyclic groups in hydroaromatic compounds have been found<sup>(120)</sup> to undergo  $\text{HNO}_3$  oxidation to yield carboxylic groups.

Example:



Methyl groups may resist oxidation, but in (II) are found to yield COOH groups. More complex aromatic structures have also been converted into benzene carboxylic acid<sup>(121)</sup>. Example:



Hence, by measuring the yield of the benzene carboxylic acids and the number of carboxylic acid groups on each benzene ring, it is possible to estimate the degree of condensation of the substance undergoing  $\text{HNO}_3$  oxidation.

## 9. $\text{HNO}_3$ Oxidation Procedure

A sample of 0.5 g enriched coal was placed in a 50 ml tared round bottom flask and refluxed for 5 hours at  $60^\circ\text{C}$  with 40%  $\text{HNO}_3$  (aqueous). The mixture was constantly stirred with a magnetic stirrer. After the reaction, the mixture was cooled and the coal mineral matter was filtered off. The filtrate was evaporated to dryness below  $40^\circ\text{C}$  in a rotary evaporator. The dry residue was esterified with 10 ml of 12%  $\text{BF}_3$  in MeOH and heated to reflux for 2 hours. The reaction mixture was cooled and the residue was dissolved in 30 ml of  $\text{CH}_2\text{Cl}_2$ . The solution was extracted with 100 ml of saturated NaCl solution. The aqueous phase was extracted twice with two portions of 30 ml  $\text{CH}_2\text{Cl}_2$ . The combined organic phase was washed with 100 ml of 10%  $\text{Na}_2\text{CO}_3$  and 100 ml of saturated aqueous NaCl respectively. The separated organic phase was dried over anhydrous sodium sulfate, and most of the solvent was removed using a rotary evaporator. The last few ml were evaporated to dryness under a stream of  $\text{N}_2$ . The residue was weighed and dissolved in  $\text{CH}_2\text{Cl}_2$  prior to GC-MS analysis.

The GC-MS analysis of the esterified mixture showed that the benzene carboxylic methyl esters were concentrated in the isomers containing 2- $\text{COOCH}_3$  groups per benzene ring. Therefore the degree of condensation of the inertinite enriched coal was estimated to be 3, which indicates that the major part of the inertinite enriched coal's chemical structure did not exceed clusters of more than 3 rings. This fact suggests that this coal is relatively young and further can, at least partially, account for the higher than expected reactivity. Figure 25 shows the GC-MS total ion profile and the chromatographic conditions.

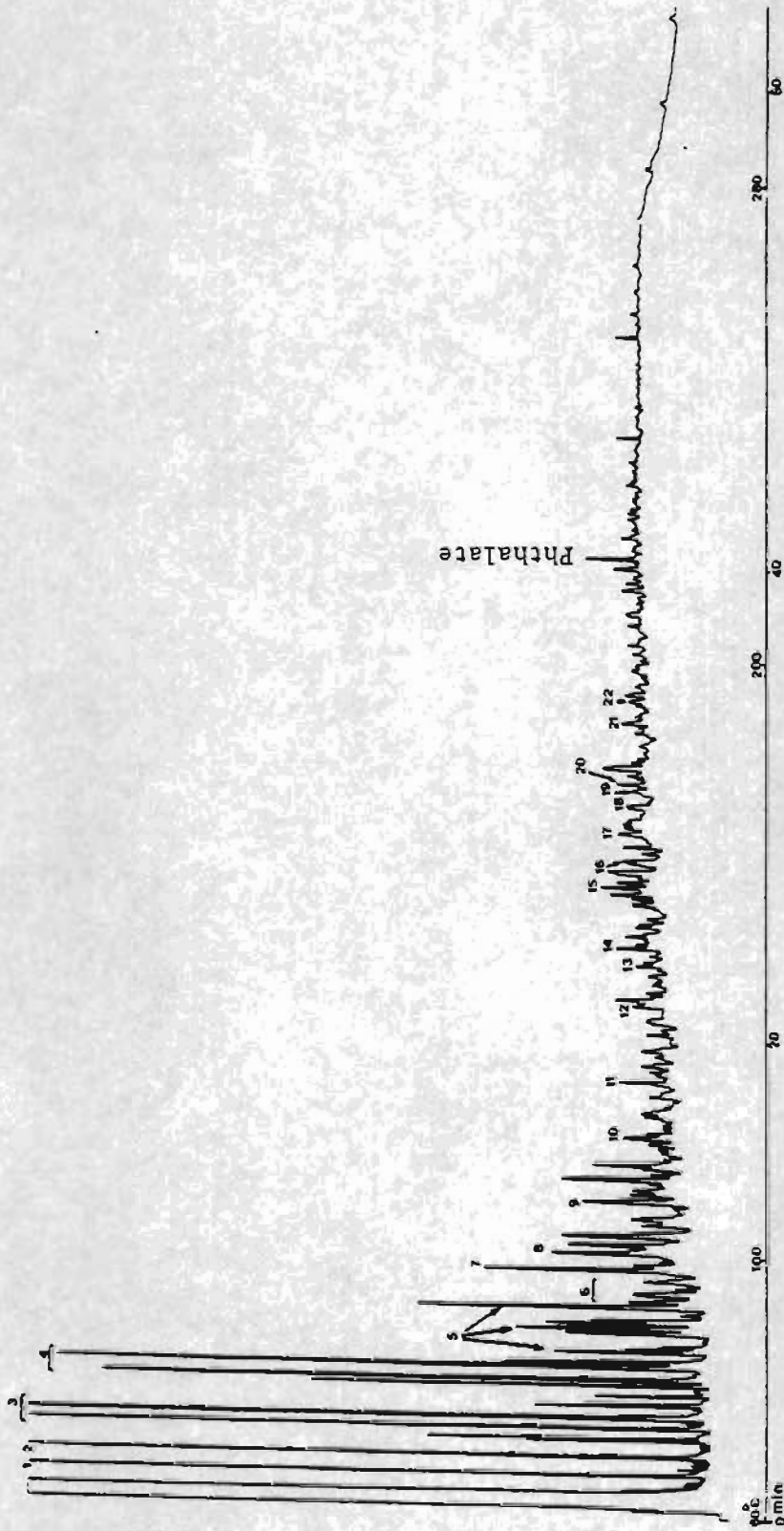


Figure 24. Capillary GC profile of hydroxyl polycyclic aromatic hydrocarbons of fraction A-4. Conditions were as in Figure 20. Compounds identified are listed in Table 18.

**Table 18**  
**Hydroxyl polycyclic aromatic hydrocarbons in fraction A-4**

Peak Number	Mol. Wt.	Compound
1	86	THF artifact ( $\gamma$ -butyrolactone)
2	94	phenol
3	108	o } cresols m } p }
4	122	C <sub>2</sub> -phenols
5	136	C <sub>3</sub> -phenols
6	143	not identified
7	134	dihydro indanol
8	148	C <sub>1</sub> -indanol
9	170	hydroxy biphenyl
10	162	C <sub>2</sub> -indanol
11	184	C <sub>1</sub> -hydroxy biphenyl
12	170	hydroxy biphenyl
13	184	C <sub>1</sub> -hydroxy biphenyl
14	184	C <sub>1</sub> -hydroxy biphenyl
15	182	hydroxy fluorene
16	198	C <sub>2</sub> -hydroxy biphenyl
17	196	C <sub>1</sub> -hydroxy fluorene
18	212	C <sub>3</sub> -hydroxy biphenyl
19	220	naphthyl phenol
20	226	C <sub>4</sub> -hydroxy biphenyl
21	234	C <sub>1</sub> -naphthyl phenol
22	220	naphthyl phenol

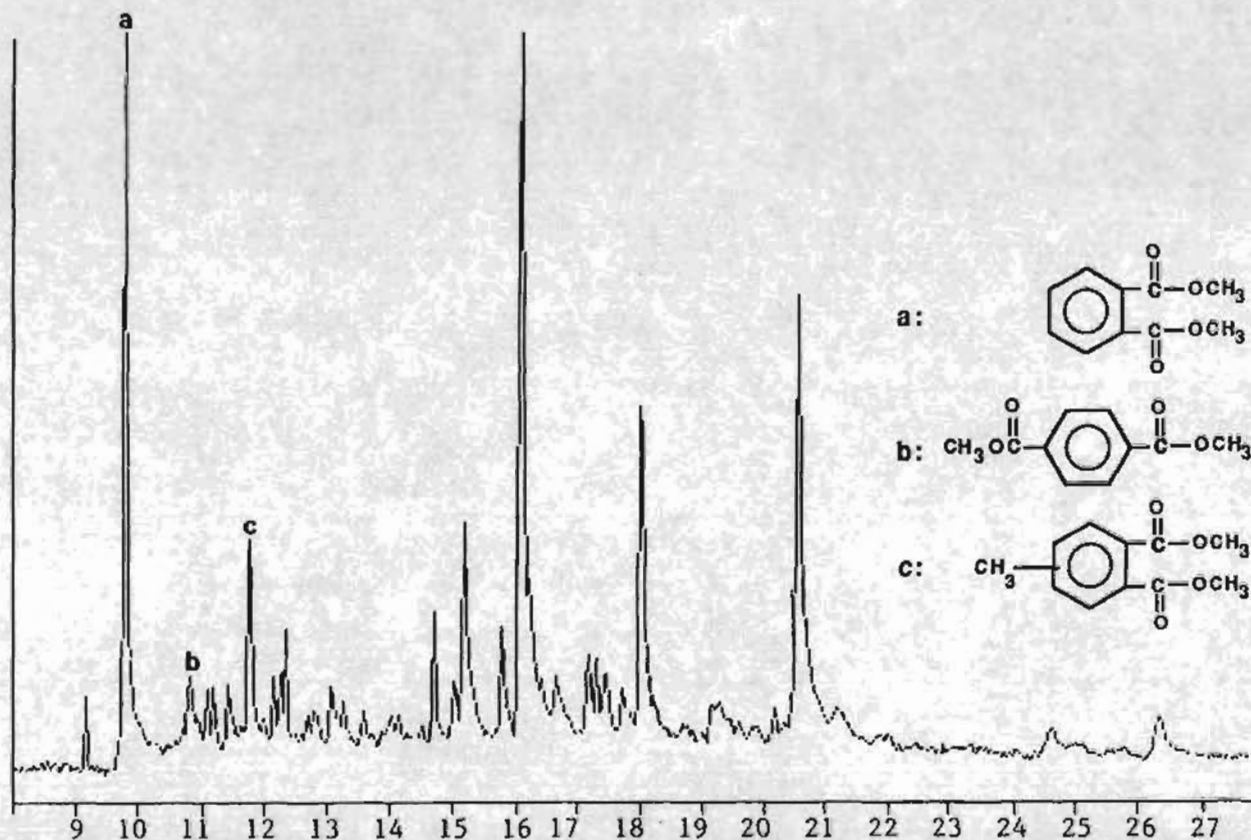


Figure 25. GC-MS total ion chromatogram of the esterified  $\text{HNO}_3$  oxidation product. Peaks a, b and c are compounds with benzene rings containing not more than two  $\text{COOCH}_3$  groups. Since their combined concentrations constitute a major portion of benzene carboxylic esters in the ester mixture, the degree of condensation of the inertinite enriched coal was estimated to be 3 or less. The chromatogram was obtained on the same column, DB-5, as in Figure 19. An HP 5890 GC & HP 5985 MS detector operated at 70 eV electron beam were used. Temperature program:  $0^\circ\text{C}$  for two min. followed by  $6^\circ\text{C}/\text{min.}$  to  $320^\circ\text{C}$ . Injected: 0.02 microliters.

## CHAPTER 5

### 1. Summary and Conclusion

The inertinite maceral concentration in Northern Alaska's coals are found to vary between a few percent to 50% by volume. In this work the feed coal, UA-139, was deliberately enriched to render the coal less reactive so that the product distribution obtained from liquefaction reactions could be used as a baseline reference in projecting the yield of products, when feed coals of the same rank but different inertinite maceral concentrations are used under similar conditions and severity.

The original coal (UA-139) with an inertinite concentration of 31.2% (Table 2) was pulverized, wet sieved and dried to obtain a -65 x 400 mesh coal sample. A 1500g portion of the sample was taken through the inertinite enrichment process by specific gravity separation. A series of perchloroethylene and naphtha solutions were prepared to obtain specific gravities varying from 1.40 to 1.60. The sink-float separations were performed at different specific gravities and the various fractions were petrographically analyzed (Table II, Appendix A). The yields from 1.5 and 1.6 floats were low, each containing less than 10% of the DAF feed coal but almost the same concentration of inertinites. Since they were petrologically very similar, the floats from 1.5 and 1.6 specific gravities were combined to yield a composite sample containing 63.4% inertinites. The efficiency of inertinite separation using perchloroethylene and naphtha mixture was found to level off at 1.5 and 1.6 specific gravities.

The proximate and ultimate analysis of the original coal (UA-139) and the enriched coal (Table 3) were similar. The main differences were that the enriched coal was 9.6 wt % lower in moisture, 462 BTU/lb higher in heating value and, at 0.48 wt %, about 1.3 times more concentrated in sulfur.

The enriched coal was oxidized with  $\text{HNO}_3$  to estimate the degree of condensation. The esterified mixture was analyzed by GC-MS for benzenecarboxylic methyl esters, which were found to be concentrated in the isomers containing two  $\text{COOCH}_3$  groups per benzene ring (Figure 25). Hence the degree of condensation of the inertinite enriched coal was estimated to be 3, which means that the major part of the coal's primary chemical structure did not exceed clusters of more than 3 rings. This is contrary to most structures attributed to bituminous coal, suggesting a younger, high volatile coal, and may at least partially explain the higher than expected conversions.

Extraction of enriched coal with benzene-alcohol azeotrope and tetrahydrofuran (THF) produced very low yields of hexane solubles (oils) and asphaltene and preasphaltenes (tars) (Table 4). This suggests that the alkyl side chains are held more firmly than the weak hydrogen bonds in some lower rank coals.

The inertinite enriched coal was liquefied directly by

two methods to compare the product yields. The reactions were conducted at 425°C and residence times (Rt) of 0 and 30 minutes with a cold  $\text{H}_2$  pressure of 500 psig for hydroliquefaction and 1000 psig for catalytic liquefaction. Catalytic hydrogenation with  $\text{MoS}_2$  yielded a total THF soluble conversion of 60.03%wt (DAF coal) while hydroliquefaction with tetralin yielded 42.22% wt (DAF coal) at 30 minutes Rt. These yields, from Table 9, were corrected for  $\text{H}_2\text{O}$  produced during liquefaction.

The hexane solubles (oils/tar) were separated into different chemical classes with open column chromatography. Neutral alumina and silicic acid were used as solid supports. The hexane fraction (A-1) from the neutral alumina column was analyzed by capillary gas chromatography. Normal alkanes from  $\text{C}_{11}$  to  $\text{C}_{32}$  (Table 13) were identified on the basis of retention times of standard n-alkanes. The hexane fraction containing the n-alkanes was found to be third most concentrated component (10.21% wt) of the hexane solubles (oils/tar) obtained from catalytic liquefaction. The isoprenoids pristane and phytane were identified and their ratio r, was found to be approximately 4.25. Since the concentration of pristane was greater than phytane, the oxidation potential of the coal forming environment must have been predominantly oxidizing<sup>(105)</sup>.

The carbon preference index (CPI) is an indicator of maturity of oils and coals. It was calculated to be 1.04. Whenever the n-alkane distribution in a sample of bitumen or any other naturally occurring oils/tars or waxes approaches a CPI = 1, it will usually yield a GC profile similar to crude oil. Therefore, the hexane solubles (oils/tar) obtained from the catalytic liquefaction are similar to petroleum crude.

The benzene fraction from neutral alumina (A-2) was found to be the major component (32.02% wt) of the hexane solubles (oils/tar). It was analyzed by GC-MS and 33 peaks were identified (Table 14). Similar to solvent refined coal<sup>(62)</sup> the PAH fraction was found to contain a high degree of alkyl substituted compounds.

Fraction A-3, the chloroform-ethanol eluate, was found to constitute 7.03% wt of the hexane solubles (oils/tar), the lowest among the four fractions (Table 11). The fraction (A-3) was further resolved using silicic acid to obtain fractions containing secondary nitrogen polycyclic aromatic heterocycles (S-1), amino polycyclic aromatic hydrocarbons (S-2) and tertiary nitrogen polycyclic aromatic heterocycles (S-3). All these fractions were analyzed by GC-MS and the compounds identified are listed in Tables 15, 16 and 17.

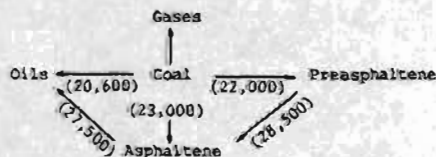
The last fraction, A-4, was the tetrahydrofuran-ethanol eluate and was the second most abundant portion of the hexane solubles (26.22% wt). Twenty two peaks were identified by GC-MS analysis (Table 18) with phenols being the major part of the A-4 fraction.

Although the scheme to separate the chemical classes followed in this work was quick and simple, some product overlaps occurred, including 1) dibenzofuran, a heterocyclic

aromatic compound reported with neutral polyaromatic cyclic compounds of fraction A-2 and 2) some PAC's like phenanthrenes reported with the secondary nitrogen polycyclic aromatic hydrocarbons of fraction S-1. Further, the yields were not as good as reported for SRC<sup>(62)</sup>. The low recovery of about 82% wt was probably due to a large concentration of the more polar compounds binding irreversibly to the solid supports. Column cleanup of the solid supports with MeOH, however, produced only a small recovery, 6.62% wt. Thus, there was a total loss of about 18% by wt. Probably a more polar solvent would have yielded a better recovery in the column cleanups. The polar compounds in the column cleanups were not identified. The analysis of the residues from catalytic liquefaction showed a lower % wt of moisture, hydrogen, oxygen and higher wts % of ash, carbon and sulfur (Table VIII, Appendix A), like a char.

In both catalytic liquefaction (CL) and hydroliquefaction (HL), gas analyses showed that CO<sub>2</sub> was the major component at 7.46% wt CL and 6.25% wt (HL), followed by CO at 0.98% wt CL and 0.53% wt (HL) and C<sub>1</sub>-C<sub>5</sub> hydrocarbons at 0.80% wt CL; 1.55% wt HL respectively. These figures were calculated on dry ash free (DAF) basis and correspond to 30 minutes residence time (Table 5).

The solid products, asphaltenes, preasphaltenes and residues obtained in both 0 and 30 min. Residence time by catalytic liquefaction experiments were analyzed using Fourier transform infrared spectroscopy (FTIR) for organic groups. These were identified on the basis of band intensities which are proportional to the concentration of the aliphatic CH, CH<sub>2</sub> and CH<sub>3</sub> groups at 2920 and 2850 cm<sup>-1</sup> in the preasphaltenes and asphaltenes. These bands were stronger in the 30 min. preasphaltenes than in 0 min. preasphaltene (Figure 14). The intensities of these bands in 30 min. asphaltenes was stronger than the 30 min. preasphaltenes due to a higher concentration of aliphatic CH, CH<sub>2</sub> and CH<sub>3</sub> groups in the former. The data presented in Tables 6 and 7 show that more asphaltenes and oils were produced at longer residence time indicating an increased conversion through cracking of preasphaltenes into asphaltenes and asphaltene to oils according to Cronauer and Ruberto's kinetic model<sup>(63)</sup>:



The numbers in the paranthesis are the activation energies (cal/g.mole) of the reactions involved. Since these energies were attained during the 30 min. residence time, they lead to more cracking.

FTIR and x-ray diffraction analyses were performed on the low temperature ash (LTA) of the enriched coal to identify the mineral matter. Quartz was found to be the predominant mineral.

The high temperature ash of the inertinite enriched coal was analyzed for major oxides and trace elements using directly coupled plasma spectroscopy (DCPS) and inductively coupled plasma spectroscopy (ICPS) respectively. Table VI in Appendix A shows no major changes in the wt % of major oxides between the ashes of the enriched coal and UA-139. Therefore the fusibility properties of the enriched coal should almost be the same as UA-139 which has an initial deformation temperature = 2320°F, softening temperature = 2410°F and fluid temperature = 2520°F. Table VII, Appendix A, shows the trace elements in parts per million (ppm). It does not contain any elements like Hg or U, which are harmful to either health or environment.

In conclusion, the enriched coal produced few toxic polyaromatic hydrocarbons with more than 3 rings. It is a source of phenols since they were a major part of the tetrahydrofuran and ethanol eluate (A-4). A minor drawback in this coal for producing liquid fuels is the presence of small amounts of carbazoles and dibenzofurans, which reduce the stability of liquid fuels through gum formation, discoloration and odor. However, the aforementioned compounds are ubiquitous in coal conversion work. They must be removed or converted from any coal derived liquid fuels.

## 2. Recommendations for Additional Work

The completed work suggests that direct liquefaction is possible under relatively mild conditions even for inertinite rich Alaskan bituminous coals. These data lend encouragement to future use of this enormous resource as liquefaction feed stocks. Research which could lead to lower processing costs would make this economical and possible sooner. Therefore, the following recommendations are suggested that could lead to process improvements:

- 1) With quantities of heavy crudes available in the Northern Basin, coprocessing should be evaluated.
- 2) Coprocessing should focus on well characterized crudes and coals from the immediate vicinity as synergisms are sought.
- 3) Due to the low sulfur content in these coals, other reactive catalysts that are more sensitive to sulfur poisoning than the conventional molybdenum catalysts could be considered.
- 4) Kinetic data for the conversion of inertinite enriched coal should be developed as conservative lower bounds for modelling coal conversion and hydrogen consumption.
- 5) Oxidation and/or other reaction studies leading to the elucidation of the organic matrix of the inertinite enriched coal can provide additional information for better understanding of liquefaction reactions.
- 6) During the chemical class separation process, about 18% wt of the hexane solubles were not recovered. The recovery and identification of the compounds in the unrecovered fraction would be helpful in understanding the chemical nature of liquid coal products.

## BIBLIOGRAPHY

1. Schaff, R.G. Coal Resources of Alaska, Division of Geological and Geophysical Survey, Information Circular 17, 9 (1983).
2. Merritt, R.D. Alaska: Coal Fields and Seams. Public Disclosure File 86-90, Alaska Division of Mining and Geological and Geophysical Surveys, Nov. 1986 (Address: 974 Univ. Ave., Fairbanks, Ak. 99709).
3. Merritt, R.D. Alaska Bituminous Coal and Anthracite. Public Disclosure File 88-15. Alaska Division of Mining and Geological and Geophysical Surveys, April (1988).
4. Heng, S. and Shibaoka, M. "Hydrogenation of the Inertinite Macerals of Bayswater Coal." *Fuel* 62, 610-612 (1983).
5. Durie, R.A. "The characteristics of Australian coals and their implications in coal liquefaction." *Coal Liquefaction Fundamentals*. Ed: D.D. Whitehurst. Amer. Chem. Symp. Series 139, 53-75 (1980).
6. Pearson, D.E. "Trends in utilization of British Columbia coal." in *Coal: Phoenix of the 80's*. Ed: A. Taweel. CIC Coal Symposium, Halifax, Nova Scotia, Canada, Canadian Society for Chemical Engineering, Vol. 1, 21-22 (1982).
7. Rao, P.D. and Smith, J. "Petrology of Cretaceous Coals from Northern Alaska." Final Technical Report. DOE-DEOFG 22-80PC 30237 from the Univ. of Alaska to U.S. Dept. of Energy. 9 (1988).
8. Sexton, R.J. "The Hazards of Health in the Hydrogenation of Coal." *Arch. Environ. Health* 1, 208-231 (1960).
9. Dong, M., Schmeltz, I., Lavole, E., Hoffmann, D. In *Carcinogenesis*, Vol. 3. "Polynuclear Aromatic Hydrocarbons." Eds: Jones, P.W., Fruedenthal, R.I. Raven Press, New York, 98-108 (1978).
10. Koppenhal, D.W., Manahan, S.E. "Hazardous Chemicals from Coal Conversion Processes." *Environ. Sci. Technol.* 10, 1104-1107 (1976).
11. Mapstone, G.E. "Studies in Shale Oil, Part X. Tar Bases and Gum Formation in Shale Gasoline." *The J. Inst. Petrol.* 47, 35 (1961).
12. Durshel, H.V., Sommers, A.L. "Isolation and Identification of Nitrogen Compounds in Petroleum." *Anal. Chem.* Vol. 38, No. 1, 19-28 (1966).
13. Hurtung, G.K., Jewell, D.M. "Carbazoles Phenazines and Dibenzofuran in Petroleum Products; Methods of Isolation, Separation and Determination." *Anal. Chim. Acta.* 26, 514-547 (1962).
14. Dinneen, G.U., Brickel, W.D. "Gum Formation in Shale Oil Naptha." *Ind. Eng. Chem.* 43, No. 7, 1604-1607 (1951).
15. Frankenfeld, J.W., Taylor, W.F. "Effects of Nitrogen Compounds on Deposit Formation During Synfuel Storage." *ACS Div. Fuel Chem. Prepr.* 23, No. 4, 205-214 (1978).
16. Ford, C.D., Holms, S.A., Thomson, L.F., Latham, D.R. "Separation of Nitrogen Compound Types from Hydrotreated Shale Oil Products by Adsorption Chromatography on Basic and Neutral Alumina." *Anal. Chem.* 53, 831-836 (1981).
17. Viland, C.K. "Effects of Nitrogen Compounds on Catalytic Cracking Yields." Symposium on Nitrogen Compounds in Petroleum. 132nd ACS Meeting, New York, N.Y. Abstracts of Papers. 9R. (Sept. 1957).
18. Furimsky, E. "Deactivation and Regeneration of Refinery Catalysts." *Erdo("o)l und Kohle* 32, 383-390 (1979).
19. White, C.M., Schweighardt, F.K., Schultz, J.L. "Combined Gaschromatographic-Mass Spectrometric Analyses of Nitrogen Bases in Light Oil from a Coal Liquefaction Product." *Fuel Processing Technology* 1, 209-215 (1977/78).
20. Rao, P.D. and Wolf, E.N. "Characterization and Evaluation of Washability of Alaskan Coals." Final Technological Report for Phase III. DOE/ET/13350-T6 (1982).
21. Youtcheff, J.S. and Rao, P.D. "Characterization of Alaskan Coals: Evaluation of their Liquefaction Behavior." Report prepared for USDOE under contract DE-FG-22-84PC 70774 (1986).
22. Rutt, G.C. and Youtcheff, J.S. "Catalytic Hydrogenation of an Inertinite Rich Coal." Focus on Alaskan Coal '86, Proceedings of the Conference (1986).
23. Lee, Sang-Ho and Youtcheff, J.S. "The Effect of Calcium on Liquefaction of Alaskan Coals." Focus on Alaska's Coal '86, Proc. of the Conference (1986).

24. Dumm, T.F. and Hogg, R. "Washability of Ultrafine Coal." Society of Mining Engineers. Caller No. D., Littleton, Colorado 80127 (1987).
25. Dyrkacz, G.R., Bloomquist, C.A.A., Horwitz, E.P. "Laboratory Scale Separation of Coal Macerals." Sep. Science Technol. 16 (10), 1571 (1981).
26. Dyrkacz, G.R. and Horwitz, E.P. "Separation of Coal Macerals." Fuel 61, 3 (1982).
27. Berkowitz, N. "An Introduction to Coal Technology." Academic Press, New York (1979).
28. Torch, H.H., "Synthesis of Hydrocarbons from Water Gas." Chemistry of Coal Utilization, Supplementary volume, 1041-1080. Ed: H.H. Lowry, Wiley, New York (1945).
29. Probst, R.F. and Hicks, R.E. "Synthetic Fuels." McGraw-Hill Chemical Engineering Series (1982).
30. Trimm, D.L. "Designing Catalysts." Chemtech, 9, 571-577 (1979).
31. Lee, E.S. "Synfuels from Coal." AIChE Monograph Series No. 14, AIChE, New York, page 42 (1982).
32. Phillips, E.M. et al. "A Comparative Study of Coal Liquefaction and Economics for Solvent Refined Coal Based Processes." Coal Processing Technology, Vol. VI, 193-208, American Institute of Chemical Engineers, New York (1980).
33. Nowacki, P. "Coal Liquefaction Processes." Noyes Data Corp., Park Ridge, N.J. (1979).
34. Stotler, H.H. and Schutter, R.T. "Status and Plans of H-Coal Pilot Plant." Coal Processing Technology, Vol. V, 73-77, American Institute of Chemical Engineers, New York (1979).
35. Mitchell, W.N., Trachte, K.L. and Zaczepinsky, S. "Performance of Low Rank Coals in the Exxon Donor Solvent Process." Ind. Eng. Chem. Product Res. Dev. 18, 311-314 (1979).
36. Epperly, W.R. and Taunton, J. "Exxon Donor Solvent, Coal Liquefaction Process Development." Coal Conversion Technology. Ed: A.H. Pelofsky. ACS Symposium Series No. 110, American Chemical Society, Washington, D.C. (1979).
37. Epperly, W.R. and Wade, D.T. "Exxon Donor Solvent Coal Liquefaction Process: Development Program Status." Permit No. AM-80-39, 1980 National Petroleum Refiners Association, Am. Meeting, New Orleans (Mar. 1980).
38. Spencer, D.F. and Alpert, S.B. "Liquefaction and Gasification: a Promising Outlook." Coal Mining & Processing, 16, 44-49 (Aug. 1979).
39. Wisner, W. "Kinetic Comparison of Coal Pyrolysis and Coal Dissolution." Fuel 47, 575-586 (1968).
40. Hill, G.R., Hariri, H., Reed, R.I., Anderson, L.L. "Kinetics and Mechanism of High Volatile Coal." Coal Science, American Chem. Soc. Adv. Chem. Ser. 55. Ed: P.H. Given. Washington, D.C. (1966).
41. Whitehurst, D.D., Farcasiu, M. and Mitchell, T.O. "The Nature and Origin of Asphaltene in Processed Coals." Annual report from Mobil Research Development Corp. to Electric Power Research Institute Report, EPRI-AF-252 (1976).
42. Maroni, E.C., Burke, F.P., Winschel, R.A. and Wilson, B.W. "Integrated Two-Stage Liquefaction Process: Solvent Quality Effects." ACS Div. Fuel Chem., Preprints 28(1), page 154 (1983).
43. Schiffer, A.N., Peluso, M., Chen, J. and Schindler, H.D. "Integrated Two-Stage Coal Liquefaction." Energy Progress, 2, page 220 (1982).
44. Derbyshire, F.J., Varghese, P. and Whitehurst, D.D. "Two-Stage Liquefaction of a Subbituminous Coal." Fuel 62, 491-497 (1983).
45. Gray, R.H. "Health and Environmental Effects of Coal Liquefaction Processes: Environmentally Acceptable Technology Development." Energy, Vol. 9, No. 4, 315-322 (1984).
46. Gray, R.H. "A Strategy for Environmentally Acceptable Technology Development." Northern Engineer Vol. 15, No. 2, 12-17 (1983).
47. Wise, W.S. "Solvent Treatment of Coal." Mills and Boone, Ltd. London (1971).
48. Burgess, M.J. and Wheeler, R.V. "The Volatile Constituents of Coal." J. of the Chem. Soc. London, 99, 649 (1911).
49. Fisher, F., Broche, H., Stauch, J. "The Coking Properties of Coals." Fuel 5, 466 (1926).



50. Dryden, I.G.C. "Behaviour of Bituminous Coals towards Solvents." *Fuel* 29, 197-222 (1950).
51. Dryden, I.G.C. "Chemical Constitution and Reactions of Coal in Chemistry of Coal Utilization." Supplementary Volume. Ed: H.H. Lowery, John Wiley and Sons, New York, page 232-295 (1963).
52. Kroger, C. "Die Steinkohleextraktion." *Erdöl und Kohle* 9, No. 7, 441-446; No. 8, 516-520 (1956).
53. Davidson, R.M. "Molecular Structure of Coal." *Coal Science* Vol. 1. Eds: M. Gobarty, J.W. Larsen and I. Wender, Academic Press, New York (1982).
54. Merzec, A., Juzws, M., Betles, K. and Sobkowiak, M. "Bituminous Coal Extraction in Terms of Electron Donor and Acceptor Interactions in the Solvent/Coal System." *Fuel Proc. Tech.* 2, 35 (1979).
55. Oele, A.P., Waterman, H.I., Goedkoop, M.L. and vanKrevelen, D.W. "Extractive Disintegration of Bituminous Coals." *Fuel* 30, 169 (1951).
56. Gillet, A. and Pirlot, A. "A Complete Solution in Benzene of the Fundamental Matter of Coal." *Fuel* 15, 124 (1936).
57. Pott, A. and Broche, H. "Die Auflo(,)sung von Kohle auf dem Wege der Druckextraktion unter besonderer Bero(,)cksichtigung der Spaltenden Hydrierung der Extrakte." *Gluckauf* 69, 903 (1933).
58. Szladow, A.J. "Some aspects of the Mechanism and Kinetics of Coal Liquefaction." Ph.D. Thesis, Pennsylvania State University (1979).
59. Yarzab, R.F., Given, P.H., Spackman, W. and Davis, A. "Dependence of Coal Liquefaction Behavior on Coal Characteristics: IV Cluster Analysis for Characteristics of 104 Coals." *Fuel* 59, 81 (1980).
60. Neill, P.H. and Given, P.H. "The Dependence of Liquefaction Behavior on Coal Characteristics." Final Technical Report, March 81 - Feb 84, Part IV. Dept. of Material Science and Coal Research Section, Pennsylvania State University, page 43-47 (1984).
61. Mudamburi, Z. and Given, P.H. "The Dependence of Liquefaction Behavior on Coal Characteristics." Final Report, March 81 - Feb 84 Part III: A Study of the Products of Liquefaction of Some American and British Coals. Coal Research Section, Pennsylvania State University, page 48-50 (1983).
62. Later, D.W., Lee, M.L., Bartle, K.D., Kong, R.C. and Vassilaros, D.L. "Chemical Class Separation and Characterization of Organic Compounds in Synthetic Fuels." *Anal. Chem.* 53, 1612-1620 (1981).
63. Given, P.H. and Derbyshire, F.J. "The Mobile Phase in Coals: its Nature and Modes of Release." Quarterly Progress Reports. DOE-PC-60811-3, 4, 5 from Pennsylvania State University to USDOE (1984).
64. Weller, S. "Coal Liquefaction with Molybdenum Catalysts." Proceedings of the 4th International Conference on the Chemistry and Uses of Molybdenum (eds. H.F. Barry and P.C.H. Mitchell) page 179-186, Climax Molybdenum Co., Ann Arbor (1982).
65. Whitehurst, D.D., Farcasiu, M. and Mitchell, T.O. "The Nature and Origin of Asphaltenes in Processed Coals." Report prepared for Electric Power Research Institute, Report No. EPRI-AF-480 (1977).
66. Cronauer, D.C. and Ruberto, R.G. "Investigation of Mechanism of Reactions Involving Oxygen Containing Compounds in Coal." Report prepared for Electric Power Research Institute, Report No. EPRI-AF-422 (1977).
67. Thomas, M.G., Padrick, T.D., Stohl, F.V. and Stephens, H.P. "Decomposition of Pyrite Under Coal Liquefaction Conditions." *Fuel* 61, 761-764 (1982).
68. Baldwin, R.M. and Vinciguerra, S. "Coal Liquefaction Catalysis: Iron Pyrite and Hydrogen Sulfide." *Fuel* 62, 498-501 (1983).
69. Scatterfield, C.N. "Heterogeneous Catalysis in Practice." McGraw-Hill, New York (1980).
70. Attar, A. and Hendrikson, G.G. "Functional Groups and Heteroatoms in Coal." *Coal Structure*. Ed: Robert A. Meyers. Academic Press, New York, page 131-198 (1982).
71. Searle, A.B. and Grimshaw, R.W. "The Chemistry and Physics of Clays and Ceramic Materials." III edition. Interscience Publishers, Inc., New York, page 253 (1959).
72. Fridel, R.A. "Infrared Spectroscopy in Coal Structure Research." *Applied Spectroscopy*. Ed: O.N. Kendall. Reinhold, N. Y., pages 312-343 (1966).
73. Speight, J.B. "Assessment of Structures in Coal by Spectroscopic Techniques." in *Analytical Methods*

- of Coal and Coal Products. Ed: C. Karr, Jr. Vol. 2, Academic Press, New York, pages 75-101 (1978).
74. Painter, P.C., Snyder, R.W., Starsinic, M., Coleman, M.M., Kuehn, D.W. and Davis, A. "Fourier Transform IR Spectroscopy: Application to Quantitative Determination of Functional Groups in Coal." Coal Products: Analytical Characterization Techniques. Ed: E.L. Fuller, Jr. ACS Symposium Series No. 205, pages 47-76 (1982).
  75. Solomon, P.R., Hamblin, D.G. and Cavangelo, R.M. "Applications of FTIR Spectroscopy in Fuel Science." Coal and Coal Products: Analytical Characterization Techniques. Ed: E.L. Fuller, Jr. ACS Symposium Series No. 205, pages 77-131 (1982).
  76. Solomon, P.R. "Relation Between Coal Structure and Thermal Decomposition Products." Div. Fuel Chem., ACS Prepr. 24(2), pages 184-195 (1979).
  77. Solomon, P.R. "Relation Between Coal Structure and Thermal Decomposition Products." Eds: M.L. Gorbaty and K. Ouchi. Adv. in Chem. Ser. No. 192, ACS, Washington, D.C., pages 95-112 (1981).
  78. Painter, P.C., Coleman, M.M., Jenkins, R.G., Whang, P.W., and Walker, P.L. Jr. "Fourier Transform Infrared Study of Mineral Matter in Coal. A Novel Method for Quantitative Mineralogical Analysis." Fuel 57, 337-344 (1978).
  79. Painter, P.C., Coleman, M.M., Jenkins, R.G. and Walker, P.L. Jr. "Fourier Transform Infrared Study of Acid Demineralized Coal." Fuel 57, 125-126 (1978).
  80. Given, P.H. and Yarzab, R.F. "Analysis of Organic Substance of Coals: Problems Posed by the Presence of Mineral Matter." Analytical Methods for Coal and Coal Products Vol. 2. Ed: C. Karr, Jr., Academic Press, New York, pages 3-39 (1978).
  81. Miller, R.N. "A Geochemical Study of the Inorganic Constituents in Some Low Rank Coals." Ph.D. thesis, Pennsylvania State University (1977).
  82. Fujii, S., Osawa, Y. and Sugimara, H. "Infrared Spectra of Japanese Coal: The Absorption Bands at 3030, 2930 and 1600  $\text{cm}^{-1}$ ." Fuel 49, 68 (1970).
  83. Wen, C.S. "Solvent Refined Coal (SRC) Process: Coking of SRC-II Process Streams." Topical report submitted to USDOE Report No. DOE/ET/10104-21 (1981).
  84. Walker, P.L. Jr. "Pyrolysis of Coal." Prepared for seminar on Modern Developments in Combustion Technology, Pennsylvania State University, July 23-25 (1979).
  85. Szladow, A.J. and Given, P.H. "Some Aspects of Mechanism and Kinetics of Coal Liquefaction." Technical Report 3, prepared for USDOE. Report No. FE-2494-TR-3 (1979).
  86. Youtcheff, J.S. and Given, P.H. "Dependence of Coal Liquefaction Behavior on Coal Characteristics. Eight Aspects of Phenomenology of Liquefaction of Some Coals", Fuel 61, 980-987 (1982).
  87. Rao, H.S., Murty, G.S. and Lahiri, A. "The Infrared and High Resolution Nuclear Magnetic Resonance Spectrum of Coal Tar Pitch." Fuel 39, 236 (1960).
  88. Elofson, R.M., Shultz, K.F. "The Electron Spin Resonance Spectra of Cellulose Chars Treated with Halogens." ACS Div. Fuel Chem., Prepr. Vol. 11, No. 2, Part 2, 513 (1967).
  89. Sharkey, A.G. Jr. and McCartney, J.T. "Physical Properties of Coal and its Products." Chemistry of Coal Utilization. Ed: Martin A. Elliot. Wiley Interscience, page 257 (1981).
  90. Czuchajowski, L. "Infrared Spectra of Carbonized Coals and Coal like Materials and some Absorption Changes During Subsequent Oxidation." Fuel 40, 361 (1961).
  91. Mukherjee, D.K. and Choudhury, B.P. "Catalytic Effect of Mineral Matter in North Assam Coal on Hydrogenation." Fuel 55, 4-8 (1976).
  92. Hertz, H.S., Brown, J.M., Chester, S.N., Guenther, F.R., Hilpert, L.W., May, W.E., Parris, R.M., Wise, S.A. "Determination of Individual Organic Compounds in Shale Oil." Anal. Chem. 52, 1650-1657 (1980).
  93. Rubin, I.B., Guerin, M.R., Hardigree, A.A., Epler, J.L. "Fractionation of Synthetic Crude Oils from Coal for Biol. Testing." Environ. Res. 12, 358-365 (1976).
  94. Ho, C.H., Clark, B.R., Guerin, M.R., Ma, C.Y., Rao, T.K. "Aromatic Nitrogen Compounds in Fossil Fuels-A Potential Hazard?" Prepr. Pap. ACS Div. Fuel Chem., Vol. 24, No. 1, 281 (1979).
  95. Jones, A.R., Guerin, M.R., Clark, B.R. "Preparative-Scale Liquid Chromatographic Fractionation of

- Crude oil Derived from Coal and Shale." *Anal. Chem.* 49, 1766-1771 (1977).
96. Wilson, B.W., Peterson, M.R., Pelroy, R.A., Cresto, J.T. "In-vitro Assay for Mutagenic Activity and Gas Chromatographic-Mass Spectral Analysis of Coal Liquefaction Material and the Products resulting from its Hydrogenation." *Fuel* 60, 289-294 (1981).
  97. Farcasiu, M. "Fractionation and Structural Characterization of Coal Liquids." *Fuel* 56, 9-14 (1977).
  98. Schiller, J.E., Mathison, D.R. "Separation Method for Coal Derived Solids and Heavy Liquids." *Anal. Chem.* 49, 1225-1228 (1977).
  99. Jewell, D.M., Weber, J.H., Bunger, J.W., Plancher, H., Latham, D.R. "Ion-exchange, Coordination and Adsorption Chromatographic Separation of Heavy-end Petroleum Distillates." *Anal. Chem.* 44, 1391-1395 (1972).
  100. Clark, B.R., Ho, C.H., Jones, A.R. "Chemical Class Fractionation of Fossil Derived Materials for Biological Testing." *Adv. Chem. Ser. No. 170*, 282-294 (1976).
  101. Maxwell, J.R., Pillinger, C.T. and Ellington, G. Q. "Organic Geochemistry." *The Chem. Soc. London. Qtr. Rev.* 25, 571 (1971).
  102. Bray, E.E. and Evans, E.D. "Distribution of n-Paraffins as a Clue to Recognition of Source Beds." *Geochim. Cosmochim. Acta* 22, 2 (1961).
  103. Brooks, J.D. and Smith, J.W. "The Diagenesis of Plant Lipids During the Formation of Coal, Petroleum and Natural Gas-II. Coalification and the Formation of Oil and Gas in the Gippsland Basin." *Geochim. Cosmochim. Acta* 33, 1183 (1969).
  104. Kvenvolden, K.A. "Molecular Distribution of Normal Fatty Acids and Paraffins in Some Lower Cretaceous Sediments." *Nature (London)* 209, 573 (1966).
  105. Tissot, B.P. and Welte, D.H. "Petroleum Formation and Occurrence." Springer-Verlag, Berlin (1978).
  106. Parees, D.M. and Kamzelski, A.Z. "Characterization of Coal Derived Liquids Using Fused Silica Capillary Column GC-MS." *J. Chromatogr. Sci.*, 20, 441 (1982).
  107. Chang, H.C.K., Masaharu Nishioka, Bartle, K.D., Wise, S.A., Bayona, J.M., Markides, K.E. and Lee, M.L. "Identification and comparison of low molecular weight neutral constituents in two different coal extracts." *Fuel* 67, 45 (1988).
  108. Hertz, H.S., Brown, J.M., Chester, S.N., Gunther, F.R., Hilpert, L.W., May, W.E., Parris, R.M., Wise, S.A. "Determination of Individual Organic Compounds in Shale Oil." *Anal. Chem.* 52, 1650-1657 (1980).
  109. Schweighart, F.K., White, C.M., Friedman, S., Shultz, J.L. "Organic Chemistry of Coal." A.C.S. Washington, D.C., p. 240-257 (1978).
  110. Uden, P.C., Carpenter, A.P., Hackett, H.M., Henderson, D.E., Siggia, S. "Qualitative Analysis of Shale Oil Acids and Bases by Porous Layer Open Tubular Gas Chromatography and Interfaced Vapour Phase Infrared Spectrophotometry." *Anal. Chem.* 51, 38-43 (1979).
  111. Schabron, J.F., Hurtubise, R.J., Silver, H.F. "Chromatographic and Spectrometric Methods for the Separation, Characterization, and Identification of Alkyl Phenols in Coal Derived Solvents." *Anal. Chem.*, 51, 1426-1433 (1979).
  112. Knudson, C.L., Rindt, J.R., Willson, W.G. "Low Severity Coal Processing: the ChemCoal Process." IVth Korea/USA Joint Workshop on Coal Utilization. Organized by Korea Institute of Energy and Resources & Pittsburgh Energy Technology Center (1987).
  113. Willson, W.G., Knudson, C.L., Farnum, S.A., Cisney, S., Ness, R., Rindt, J.R., Porter, C.R. and Brolick, H.J. "ChemCoal Process Development Program with Indian Head Lignite." Final report, DOE/FE/60181-2087 (DE86014270) (June 1986).
  114. Knudson, C.L. "Production of Jet Fuels from Coal Derived Liquids." Vol. II Characterization of Liquid by Products from the Great Plains Gasification Plant. AFWAL-TR-87-2042. AERO Propulsion Lab., AF Wright Aeronautical Laboratories, Wright-Patterson Air Force Base, Ohio 45433-6563 (May 1988).
  115. Browden, J.N. and Brinkman, D.W. "Stability Characteristics of Some Shale and Coal Liquids." DOE report DOE/BETC/4162-10 (1980).

116. Hara, T., Jones, L., Li, N.C., Tervari, K.C. "Ageing of SRC Liquids." *Fuel* 60, 1143 (1981).
117. Anders, E., Hayatsu, R. and Studier, M.H. "Organic Compounds in Meteorites." *Science* 182, 781 (1973).
118. Hayatsu, R., Matsuoka, S., Scott, R.G., Studier, M.H. and Anders, E. "Origin of Organic Matter in the Early Solar System-VII. The Organic Polymer in Carbonaceous Chondrites." *Geochim. Cosmochim. Acta* 41, 1325 (1977).
119. Tuley, W.F. and Marvel, C.S. "Organic Synthesis." *Collect. Vol. 3*, p. 822 (1955).
120. Nes, W.R. and Mosetting, E. J. "The Anthrasteroid Rearrangement. II. The Structural Proof of 1-methyl-2,3,5,6-tetracarboxybenzene." *J. Am. Chem. Soc.* 76, 3186 (1954).
121. vanKrevelen, D.W. "Coal" page 220, Elsevier, Amsterdam (1961).

## APPENDIX A: TABLES

**Table I: Weight fractions obtained at different specific gravities.**

Specific Gravity	Weight Fraction (grams)
Float 1.40	501.63
1.40-1.45	325.73
1.45-1.50	219.60
1.50-1.55	91.50
1.55-1.60	41.11
Sink 1.60	261.29
Total	1440.86

Note: 1.5 kg (1500 g) was the initial weight of the -65 x 400 mesh coal. The major loss was mainly due to the removal of near gravity material that appeared as a layer between the floats and sinks. Additional loss was due to the fine particles sticking to the filter paper and other utensils used in the separation process.

**Table II  
Petrographic Analysis of Original Coal and Enriched Fractions**

% Macerals	Original Coal (UA-139)	1.5 Float	1.6 Float	Composite (1.5+1.6 Floats)
Vitrinite	57.8	38.8	36.4	36.6
Fusinite*	0.2	2	0.6	2
Semi Fusinite*	24	50.4	55.2	50
Macrinite*	4.6	7	4.4	8
Globular Mac.*	0.6	1.2	2.8	2.8
Inertodetinite*	1.8	0.6	0.6	0.6
Pseudo Vit.	8.8	0	0	0
Spornite	1	0	0	0
Resinite	0.4	0	0	0
Lipinite	0.4	0	0	0
Alginite	0.2	0	0	0
Cutinite	0.2	0	0	0
% Total Inertinites	31.2	61.2	63.6	63.4

\*Inertinites

**TABLE III**  
**A SUMMARY OF THE MAJOR CHARACTERISTICS OF THE THREE MACERAL GROUPS IN HARD COAL**

Maceral group	Plant origin	Reflectance			Chemical properties		Technological characteristics
		Description	Rank	Reflected light, %	Characteristic element	Typical products on heating	
VITRINITE	Woody trunks, branches, twigs, stems, stalks, bark, leaf tissue, shoots	Dark to medium grey	High vol. to medium volatile	0,5 to 1,1	Oxygen-rich	Light hydrocarbons Decreasing amounts of volatiles	<ul style="list-style-type: none"> <li>• Combusts rapidly</li> <li>• Pyrolysis</li> <li>• Hydrogenation/liquefaction</li> <li>• Coking</li> <li>• Combusts with little smoke</li> <li>• Combusts with no smoke</li> </ul>
		Pale grey	Low volatile Bituminous	1,1 to 1,6			
		White	Bituminous	1,6 to 2,0			
		White	Anthracite	2,0 to 10,0			
EXINITE	Cuticles, spores, resin bodies, algae	Black-brown	High vol.	-0,0 to 0,5	Hydrogen-rich	Early methane gas Oil Condensates Wet gases (decreasing)	<ul style="list-style-type: none"> <li>• Combusts very rapidly</li> <li>• Pyrolysis</li> <li>• Hydrogenation/liquefaction</li> <li>• For bitumen production</li> </ul>
		Dark grey	Bituminous	-0,5 to 1,1			
		Pale grey	Med. vol. Bituminous	-1,1 to 1,6			
		Pale grey (= vitrinite) to white shadows	Low vol. Bituminous to anthracite	-1,6 to 10,0			
INERTINITE	As for vitrinite, and oxidized detrital organic humus	Medium grey	High vol. Bituminous	0,7 to 1,6	Carbon-rich		<ul style="list-style-type: none"> <li>• Combusts slowly</li> <li>• Maintains flame</li> <li>• Relatively inert in coking</li> <li>• hydrogenation</li> <li>• liquefaction</li> <li>• pyrolysis</li> </ul>
		Pale grey	All bituminous coals and anthracite	1,6 to 10,0			
		White					
		Yellow white					

**Table IV**  
**Parametric conditions of the Gas Chromatograph**  
**during gas analysis**

<b>CH<sub>4</sub>, CO<sub>2</sub>, CO Gases:</b>	
Column	Carbosieve S (10' 1/8")
Detector	TCD (210°C)
Carrier	He (20 ml/min.)
Injector Temp.	210°C
<b>Temperature Program:</b>	
Initial Temp.	40°C
Rate	15°C/min. after 10 min. isothermal
Final Temp	200°C
Total Time	25 min.
<b>C<sub>1</sub> - C<sub>3</sub> Gases:</b>	
Column	Chromosorb 102 (12' 1/8")
Detector	FID (300°C)
Carrier	He (20 ml/min.)
Injector Temp.	210°C
<b>Temperature Program:</b>	
Initial Temp.	40°C
Rate	15°C/min. after 10 min. isothermal
Final Temp.	200°C
Total Time	25 min.

**Table V**  
**Concentration of cations in the combined washings of ammonium acetate**  
**and HCl (% wt in enriched DAF coal )**

Si	Fe	Cu	Mg	Mn	Ti	Al	Na	K
0.00019	0.00066	0.0041	0.00053	0.00002	—	—	0.0064	0.00012

**Table VI**  
% wt concentration of major elements in the ash of enriched coal

	SiO <sub>2</sub>	Fe <sub>2</sub> O <sub>3</sub>	Al <sub>2</sub> O <sub>3</sub>	MgO	CaO	Na <sub>2</sub> O	K <sub>2</sub> O	TiO <sub>2</sub>	MnO	P <sub>2</sub> O <sub>5</sub>
*	54.54	2.12	29.82	1.71	5.72	2.15	0.92	1.13	0.03	0.22
**	59.00	2.40	21.80	2.20	4.90	3.05	1.10	0.80	0.03	—

\* enriched coal  
\*\* UA-139

**Table VII**  
Concentration of trace elements, ppm in the ash of enriched coal

Ba	Sr	Cr	Ni	Co	V	Cu	Zr	Be
3,737	581	1.4	18.5	16.9	72.6	206	397	6.4

**Table VIII**  
Analysis of residues\*\*

	% wt						
	Ash	Moisture	C	H	N	O*	S
0 min.	24.32	1.44	77.18	4.36	1.30	15.74	1.42
30 min.	39.91	0.49	82.19	3.92	1.36	8.70	3.83

\*\* DAF basis  
\* By difference



## APPENDIX B

### Calculation involving the impregnation of coal with the catalyst

40 g of coal taken for catalyst treatment to obtain 1% loading of Mo by wt of coal, the Mo required is expressed in moles.

=  $0.4/95.94$ g/mole where 95.94 - At Wt of Mo

=  $4.17 \times 10^{-3}$  moles of Mo

Volume of 0.1 mole catalyst solution is equal to  $4.17 \times 10^{-3} + 0.1 = 4.17 \times 10^{-2}$  L = 41.7 ml

therefore the amount of ammonium hepta molybdate (AHM) required

=  $4.17 \times 10^{-3}$  moles of Mo x 1 mole AHM/7 moles of Mo

=  $5.96 \times 10^{-4}$  moles

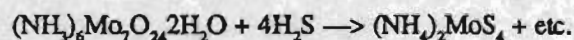
therefore wt of AHM required to obtain 1% loading of 40g of coal

=  $5.96 \times 10^{-4}$  moles of AHM x 1193.58g/moles AHM

where, 1193.58 is the molecular wt of AHM

= 0.7190g AHM

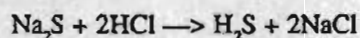
Amount of  $\text{Na}_2\text{S}$  required:



i.e.,  $4.17 \times 10^{-3}$  moles Mo x 4 moles of  $\text{H}_2\text{S}$ /moles of Mo

= 0.0167 moles of  $\text{H}_2\text{S}$

$\text{H}_2\text{S}$  is generated from  $\text{Na}_2\text{S}$



0.0167 moles of  $\text{H}_2\text{S}$  x 1 mole of  $\text{Na}_2\text{S}$ /mole of  $\text{H}_2\text{S}$

=  $0.0167 \times 78$  where 78 = molecular wt of  $\text{Na}_2\text{S}$

= 1.3010 g

3 fold excess of  $\text{Na}_2\text{S}$  was taken to generate the  $\text{H}_2\text{S}$ .

$1.3010 \times 3 = 3.9031$  g  $\approx$  4g

## APPENDIX C

### A. CPI Calculation:

Odd carbon number	peak ht(mm)	Even carbon number	peak ht(mm)
C <sub>17</sub>	34.0	C <sub>16</sub>	33.0
C <sub>19</sub>	33.0	C <sub>18</sub>	34.0
C <sub>21</sub>	29.5	C <sub>20</sub>	30.5
C <sub>23</sub>	27.0	C <sub>22</sub>	28.5
C <sub>25</sub>	20.0	C <sub>24</sub>	22.5
C <sub>27</sub>	12.5	C <sub>26</sub>	16.0
C <sub>29</sub>	8.0	C <sub>28</sub>	10.0
C <sub>31</sub>	4.0	C <sub>30</sub>	4.0
		C <sub>32</sub>	2.0

$$\Sigma(C_{17} \text{ to } C_{31}) = 168 \text{ mm}$$

$$\Sigma(C_{16} \text{ to } C_{30}) = 147.5 \text{ mm}$$

$$\Sigma(C_{18} \text{ to } C_{32}) = 178.5 \text{ mm}$$

$$CPI = \frac{1}{2} \left( \frac{168}{147.5} + \frac{168}{178.5} \right)$$

$$= \frac{1}{2} (2.079) = 1.0395$$

$$= 1.04$$

Note: Peak height measurements were taken from the original chromatogram before size reduction.

CPI of crude oils vary from  $\approx 5$  to  $\approx 1$ , depending upon the extent of cracking. When it is  $\approx 1$ , the amount of odd and even number of carbon chains (alkanes) in the crude are approximately equal. Such a crude is considered to be premium grade.

### B. Calculation of r (pristane/phytane):

$$r = \frac{\text{pristane}}{\text{phytane}} = \frac{1.7\text{mm}}{0.4\text{mm}} = 4.25$$